Study on Anti-inflammatory Activity of *Curcuma mangga* Rhizomes

Kanidta Kaewkroek

A Thesis Submitted in Partial Fulfillment of the Requirements for the Degree of

Master of Pharmacy in Pharmaceutical Sciences

Prince of Songkla University

2009

Thesis	Study on Anti-inflammatory Activity of *Curcuma mangga* Rhizomes
Author	Miss Kanidta Kaewkroek
Major Program	Pharmaceutical Sciences

Major Advisor

...……..……..
(Assoc. Prof. Dr. Supinya Tewtrakul)

Co-advisor

…….….....
(Asst. Prof. Dr. Chatchai Wattanapiromsakul)

Examining Committee:

...…….……Chairperson
(Assoc. Prof. Dr. Sunibhond Pummangura)

....……..……...
(Assoc. Prof. Dr. Supinya Tewtrakul)

..…….……..
(Asst. Prof. Dr. Chatchai Wattanapiromsakul)

. …….…….....
(Asst. Prof. Dr. Sirima Mahattanadul)

The Graduate School, Prince of Songkla University, has approved this thesis as partial fulfillment of the requirements for the Master of Pharmacy Degree in Pharmaceutical Sciences

……....
(Assoc. Prof. Dr. Krerkchai Thongnoo)
Dean of Graduate School

ชื่อวิทยานิพนธ์ การศึกษาฤทธิ์ต้านการอักเสบของเหง้าขมิ้นขาว

ผู้เขียน นางสาวกนิษฐา แก้วเกริก

สาขา เภสัชศาสตร์

ปีการศึกษา 2552

บทคัดย่อ

งานวิจัยนี้ได้ศึกษาฤทธิ์ต้านการอักเสบของสารสกัดหยาบและสารบริสุทธิ์จากเหง้าขมิ้นขาว โดยใช้ lipopolysaccharide (LPS) เป็นตัวเหนี่ยวนำการสร้างสารไนตริกออกไซด์ (NO) และพรอสตาแกลนดินอี 2 (PGE_2) ใน RAW 264.7 cell line จากการประเมินฤทธิ์ทางชีวภาพเบื้องต้นของสารสกัดในชั้นต่างๆ (bioassay-guided) พบว่าสารสกัดชั้นคลอโรฟอร์มมีฤทธิ์ยับยั้งการสร้าง NO ได้ดีที่สุดโดยมีค่า IC_{50} เท่ากับ 2.1 µg/ml ตามด้วยสารสกัดชั้นเฮกเซน เอทิลอะซีเตท และชั้นน้ำ ซึ่งมีค่า IC_{50} เท่ากับ 3.8 µg/ml, 23.5 µg/ml และ >100 µg/ml ตามลำดับ สารบริสุทธิ์ที่แยกได้ ได้แก่ demethoxycurcumin (**1**) ซึ่งแยกได้จากสารสกัดชั้นคลอโรฟอร์ม 15,16 bisnorlabda-8(17), 11 dien-13-one (**2**) และ diterpene diethyl acetal [(*E*)-15,15-diethoxylabda-8(17),12-dien-16-al] (**3**) ซึ่งแยกได้จากสารสกัดชั้นเฮกเซน โดยสาร **2** และ **3** เป็นสารที่แยกได้เป็นครั้งแรกในเหง้าขมิ้นขาว ในการศึกษาฤทธิ์ต้านการอักเสบได้นำ bisdemethoxycurcumin (**4**) ซึ่งเป็นสารที่มีโครงสร้างคล้ายกับ demethoxycurcumin มาร่วมทดสอบฤทธิ์ด้วย ผลการทดสอบพบว่าสาร **3** มีฤทธิ์ยับยั้งการสร้าง NO ดีที่สุด โดยมีค่า IC_{50} เท่ากับ 9.4 µM ตามด้วยสาร **1**, **4** และสาร **2** ซึ่งมีค่า IC_{50} เท่ากับ 12.1, 16.9 และ 30.3 µM ตามลำดับ ผลการทดสอบฤทธิ์ยับยั้งการสร้าง PGE_2 พบว่าสาร **1** มีฤทธิ์ยับยั้งดีที่สุด โดยมีค่า IC_{50} เท่ากับ 4.5 µM, ตามด้วยสาร **4** (IC_{50} = 5.6 µM), **3** (IC_{50} = 35.3 µM) และ **2** (IC_{50} = 42.5 µM) ตามลำดับ สาร **1**, **3** และ **4** มีประสิทธิภาพในการยับยั้งการสร้างเอนไซม์ iNOS และ COX-2 ในระดับ transcription เนื่องจากมีฤทธิ์ยับยั้ง mRNA expression ของเอนไซม์ทั้งสองชนิด โดยขึ้นกับความเข้มข้นที่ให้ ในขณะที่สาร **2** มีฤทธิ์ยับยั้งเฉพาะการแสดงออกของ iNOS mRNA จากผลการศึกษาดังกล่าวสรุปได้ว่าขมิ้นขาวและสารบริสุทธิ์ที่แยกได้มีฤทธิ์ต้านการอักเสบ และมีศักยภาพสูงที่จะนำมาพัฒนาเป็นยาเพื่อใช้รักษาโรคที่เกี่ยวกับการอักเสบ

Thesis Title Study on Anti-inflammatory Activity of *Curcuma mangga* Rhizomes

Author Miss Kanidta Kaewkroek

Major Program Pharmaceutical Sciences

Academic Year 2009

Abstract

In the present study, we investigated the anti-inflammatory effect of the extract and pure compounds from *C. mangga* rhizomes against lipopolysaccharide (LPS)-induced nitric oxide (NO) and prostaglandin E_2 (PGE_2) production in RAW 264.7 cell line. From bioassay-guided fractionation, the result showed that the chloroform fraction exhibited the most potent inhibitory activity with an IC_{50} value of 2.1 μg/ml, followed by the hexane fraction (IC_{50} = 3.8 μg/ml), EtOAc fraction (IC_{50} = 23.5 μg/ml) and water fraction (IC_{50} >100 μg/ml), respectively. Demethoxycurcumin (**1**) was isolated from the chloroform fraction, 15,16 bisnorlabda-8(17), 11 dien-13-one (**2**) and diterpene diethyl acetal [(*E*)-15,15-diethoxylabda-8(17),12-dien-16-al] (**3**) were isolated from the hexane fraction. Compounds **2** and **3** were first isolated from the rhizomes of *C. mangga*. For anti-inflammatory investigation, bisdemethoxycurcumin (**4**) whose structure is similar to that of **1** was also tested. Of the tested compounds, compound **3** exhibited the highest activity against NO production with an IC_{50} value of 9.4 μM, followed by **1** (IC_{50} = 12.1 μM), **4** (IC_{50} = 16.9 μM) and **2** (IC_{50} = 30.3 μM). For the effect on PGE_2 production, demethoxycurcumin (**1**) possessed the highest activity with an IC_{50} value of 4.5 μM, followed by **4** (IC_{50} = 5.6 μM), **3** (IC_{50} = 35.3 μM) and **2** (IC_{50} = 42.5 μM), respectively. The mechanism in transcriptional level revealed that compounds **1**, **3** and **4** down-regulated the mRNA expressions of iNOS and COX-2 genes in dose-dependent manners, whereas compound **2** down-regulated only the expression of iNOS mRNA. These results suggest that *C. mangga* and its compounds exert anti-inflammatory activity and have a high potential to be developed as a pharmaceutical preparation for treatment of inflammatory-related diseases.

ACKNOWLEDGMENTS

First I would like to express my deepest grateful thank to my advisor, Associate Professor Dr. Supinya Tewtrakul for her helpful advice, guidance, encouragement and support throughout my study.

My special thanks goes to my co-advisor, Assistant Professor Dr. Chatchai Wattanapiromsakul, for his helpful guidance, encouragement and suggestion throughout my thesis.

I also would like to express my great thanks to the Graduate school of Prince of Songkla University for scholarship supporting this research.

I would like to thanks the Department of Pharmacognosy and Pharmaceutical Botany and the Pharmaceutical Laboratory Service Center, Faculty of Pharmaceutical Sciences, Prince of Songkla University for their support in scientific equipment.

Many thanks go to all staffs of the Faculty of Pharmaceutical Sciences, Prince of Songkla University for their kindness and help.

Finally, I would like to thank my family and friends for their love and encouragement. Most importantly, I would like to thank my beloved parents, my sister and everyone in my family for their understanding, encouragement, love and support.

Kanidta Keawkroek

CONTENTS

CONTENTS (continued)

LIST OF TABLES

LIST OF FIGURES

LIST OF FIGURES (continued)

LIST OF SCHEMES

LIST OF ABBREVIATIONS AND SYMBOLS

br	broad (for NMR signals)
etc.	et cetera
COSY	correlation spectroscopy
d	doublet (for NMR signals)
DEPT	distortionless enhancement by polarization transfer
EIMS	electron-impact mass spectroscopy
et al.	et alibi
g	gram
h	hour
HMBC	heteronuclear multiple bond correlation
HMQC	heteronuclear multiple-quantum coherence
IC_{50}	inhibitory concentration at 50% of tested subject
IR	infrared
J	coupling constant
kg	kilogram
L	liter
m	multiplet (for NMR signals)
mg	milligram
min	minute
ml	milliliter
mM	millimolar
MS	mass spectroscopy
m/z	mass-over-charge ratio
NMR	nuclear magnetic resonance
P	*P*-value
pH	potential of hydrogen
s	singlet (for NMR signals)

LIST OF ABBREVIATIONS AND SYMBOLS (continued)

t	triplet (for NMR signals)
UV-VIS	ultraviolet-visible
δ	chemical shift in ppm
ε	molar absorptivity
λ_{max}	maximum wavelength
ν_{max}	wave number
$^{\circ}$ C	degree of Celsius
/	per
μL	microliter
μM	micromolar
%	percentage
®	trade name

CHAPTER 1

INTRODUCTION

1.1 General introduction

1.1.1 Inflammation

Inflammation is a protective response intended to eliminate the initial cause of cell injury as well as the necrotic cell and tissues resulting from the original insult. Inflammation accomplishes its protective mission by diluting, destroying or otherwise neutralizing harmful agents (e.g., microbes and toxins) and then sets into motion the events that eventually heal and repair the sites of injury. Without inflammation, infections would go unchecked and wounds would never heal. In the context of infections, inflammation is part of a broader protective response that immunologists refer to as innate immunity (Kumar et al., 2007).

Although inflammation helps clear infections and other noxious stimuli and initiates repair, the inflammatory reaction and the subsequent repair process can cause considerable harm. The components of the inflammatory reaction that destroy and eliminate microbes and dead tissues are also capable of injuring normal tissues. The pathology may even become the dominant feature if the reaction is very strong (e.g., when the infection is severe), prolonged (e.g., when the eliciting agent resists eradication) or inappropriate (e.g., when it is directed against self-antigens in autoimmune diseases or against usually harmless environmental antigens in allergic disorders). This is why the process of inflammation is fundamental to virtually all of clinical medicine (Kumar et al., 2007).

The inflammatory response consists of two main components, a vascular reaction and a cellular reaction. Many tissues and cells are involved in these reactions, including the fluid and proteins of plasma, circulating cells, blood vessels, and cellular and extracellular constituents of connective tissue. The circulating cells include neutrophils, monocytes that mature into inflammatory macrophages that subsequently proliferate and thereby affect the functions of resident tissue macrophages, eosinophils, lymphocytes, basophils and platelets. The extracellular

matrix consists of the structural fibrous proteins (collagen, elastin), adhesive glycoproteins (fibronectin, laminin, nonfibrillar collagen, tenascin, and others) and proteoglycans. The basement membrane is a specialized component of the extracellular matrix consisting of adhesive glycoproteins and proteoglycans (Kumar et al, 2005; Serhan and Savill, 2005).

1.1.2 Acute inflammation

The acute inflammatory response begins after lethal or non-lethal cellular injury. Cellular injury may be caused by trauma, oxygen or nutrient deprivation, genetic or immune defects, chemical agents, microorganisms, temperature extremes or ionizing radiation. Unlike the immune response, which takes days to develop, the vascular effect of inflammation are immediate, occurring in seconds. First, arterioles near the site of injury constrict briefly. Vasoconstriction is followed by vasodilation, which increases blood flow to the inflamed site. Arteriolar dilation increases pressure in the microcirculation, which may increase the exudation of plasma and blood cells into the tissues. Exudation causes edema and swelling. As plasma moves outward, blood remaining in the microcirculation flows more slowly and becomes more viscous (thick and sticky). Leukocytes (white blood cells) migrate to vessel walls and adhere there. At the same time, biochemical mediators stimulate the endothelial cells that line capillaries and venules to retract, creating spaces at junctions between the cells. The leukocyte, which otherwise could not penetrate vessel walls, are able to squeeze out through the spaces created by endothelial retraction (Rote, 2002).

This state of vascular permeability continues throughout acute inflammation, permitting blood cells and plasma proteins to exude continuously into inflamed tissues. Once in the tissues, these cells and proteins act in concert to (1) stimulate and control subsequent inflammatory processes and (2) interact with components of the immune response.

Neutrophils are the first phagocytic leukocytes to arrive at the inflamed site. They phagocytose (ingest) bacterial, dead cells and cellular debris and then they die and are removed as pus through the epithelium or the lymphatic system. The next phagocytes on the scene are monocytes and macrophages, which perform many of the same functions as neutrophils but for a longer time and later in the inflammatory response. Other cells found in inflamed tissues

are eosinophils, which help control the inflammatory response and act directly against parasites; basophils, which have a function similar to that of mast cell; and platelets, which are cytoplasmic fragments that stop bleeding if vascular injury has occurred. All these cells, along with the substances they produce, act at the site of tissue injury to kill microorganisms and remove the debris of "battle," including exudate and dead cells. This prepares the lesion for tissue regeneration or repair, the process known as resolution (Rote, 2002).

Macrophages are the main cells responsible for the innate immunity, and their activation by LPS and IFN-γ from host immune cell is important for controlling infections. However, the overwhelming activation of macrophages can cause a severe inflammatory state (Cho et al., 2008). Inappropriate or prolonged macrophage activation is largely responsible for the pathology of acute (e.g. septic shock) and chronic (e.g. rheumatoid arthritis, inflammatory bowel disease and chronic obstructive pulmonary disease) inflammatory conditions (Schroder et al., 2006). LPS is one of the major constituents of the outer membrane of gram-negative bacteria and the immune system is constantly exposed to low levels of LPS through infections. LPS recognition and signal transmission are the key events aimed at eliminating an invading pathogen. LPS induces an acute phase stress response characterized by translocation of nuclear factor-kappa B (NF-κB) into the nucleus of cells, subsequently inducing the expression of a variety of proteins, including inflammatory mediators (Cobb et al., 2000).

The LPS-induced activation of macrophages results in the production of bioactive lipids, reactive oxygen species and in particular, inflammatory cytokines to fight and clear the bacterial infection (Figure 1). However, LPS mediates both the beneficial and deleterious reaction to the host. The excessive and uncontrolled production of inflammatory mediators triggered by LPS is harmful and can lead to potentially lethal systemic disorders such as septic shock. This antigen can activate macrophages to release some inflammatory mediators such as NO, TNF-α, PGE_2 and so on through NF-κB activation. Therefore, the inhibition of NF-κB activation and the production of the proinflammatory mediators (NO, PGE_2) and proinflammatory cytokine (TNF-α, IL-1) is an important therapeutic consideration in development of anti-inflammatory agents (Cho et al., 2008).

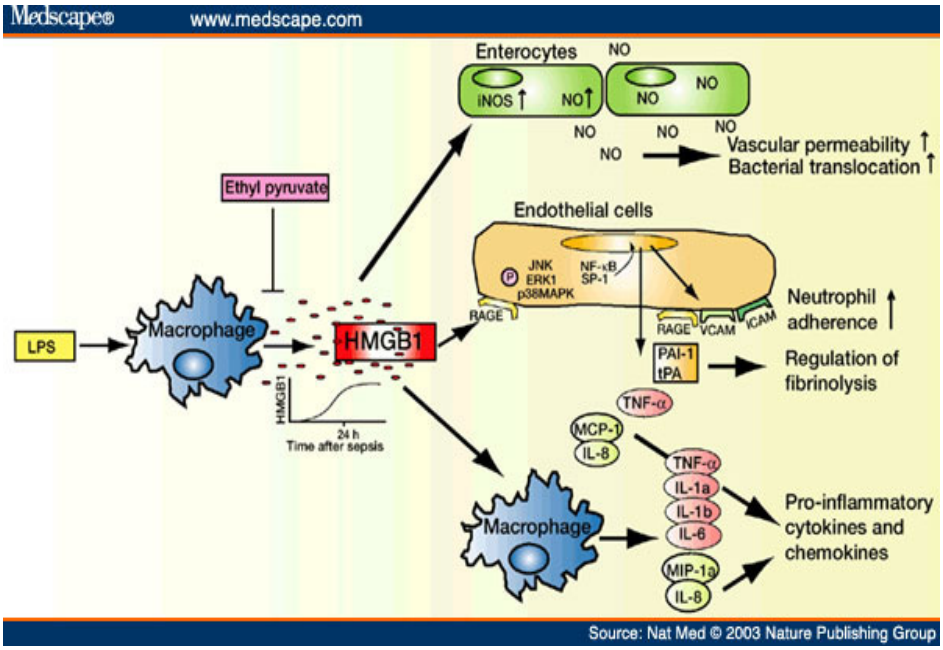

Figure 1 The LPS-induced activation of macrophages results in production of inflammatory cytokines (Riedemann et al., 2003).

1.1.3 Chemical mediators of inflammation

Chemical mediators may be produced locally by cells at the site of inflammation or they may be circulating in the plasma (typically synthesized by the liver) as inactive precursors that are activated at the site of inflammation. Cell-derived mediators are normally sequestered in intracellular granules and are rapidly secreted upon cellular activation (e.g., histamine in mast cells) or are synthesized de novo in response to a stimulus (e.g., prostaglandins and cytokine). Plasma-protein-derived mediators (complement proteins, kinins) typically undergo proteolytic cleavage to acquire their biologic activities.

Most mediators induce their effects by binding to specific receptors on target cells. Mediators may act on only one or a very few targets or they may have widespread action, with differing outcomes depending on which cell type they affect. Some mediators have direct enzymatic and/or toxic activities (e.g., lysosomal proteases and ROS). Mediators may stimulate

target cells to release secondary effector molecules. Different mediators may have similar actions, in which case they may amplify a particular response or they may have opposing effects, thus serving to control the response (Kumar et al., 2007).

Cytokines

Cytokines are key modulators of inflammation. They participate in acute and chronic inflammation in a complex network of interactions. Several cytokines exhibit some redundancy in function and share overlapping properties as well as subunits of their cell surface receptors (Feghali et al., 1997).

Cytokines are regulatory polypeptides that are produced by virtually all cells. In general, cytokines are not constitutively produced. However, in the presence of appropriate stimuli, for example LPS from gram negative bacteria, increased gene expression and production of the cytokines will occur, leading to the initiation of an inflammatory response. Major cytokine involved in the initiation of inflammation are tumor necrosis factor-alpha (TNF-α) and interleukin-1 (IL-1). Regulation of their gene expression inflammatory cytokines is in part controlled by activation of transcription factors such as NF-κB (Lantz et al., 2005).

NF-κB is a transcription factor (a complex of proteins) that binds to DNA and activates gene transcription not only of proinflammatory cytokines but also that of chemokines and enzymes of the arachidonic acid cascade (Baldwin, 1996; Pahl, 1999). The most predominantly characterised NF-κB complex is a p50/p65 heterodimer, which is constitutively present in an inactive cytoplasmic complex by binding to inhibitor κB-α, (IκB-α) and other IκB proteins. Stimulation results in phosphorylation of inhibitory proteins by IκB kinases followed by their degradation, which allows the translocation of NF-κB to the nucleus and binding to a NF-κB motif to act as transcriptional regulator (Rioja et al., 2002; Song et al., 2009; Li and Nabel, 1997; Naumann, 2000).

Inflammatory mediators and enzymes

Nitric oxide (NO)

NO is a highly diffusible stable gas composed of one atom each of nitrogen and oxygen. It is synthesized by a family of enzymes that are collectively called nitric oxide synthase, NOS (Thomas and Ramwell, 1998; Crawford, 2006).

There are three isoforms of NOS, with different tissue distribution. Neuronal nitric oxide synthase or nNOS is a constitutively expressed neuronal NOS, which does not play a significant role in inflammation. Inducible NOS or iNOS is an inducible enzyme present in macrophages and endothelial cell. It is induced by a number of inflammatory cytokines and mediators, most notably by IL-1, TNF and IFN-γ and by bacterial endotoxin and is responsible for production of NO in inflammatory reaction. iNOS is also present in many other cell types, including hepatocytes, cardiac myocytes and respiratory epithelium. Endothelial NOS or eNOS is a constitutively synthesized NOS found primarily (but not exclusively) within endothelium (Figure 2) (Kumar et al., 2007; Cummings and Tarleton, 2004; Wattanapitayakul et al., 2007; Kone et al., 2003). NO has a significant effect on vascular smooth muscle tone and blood pressure. The vasodilator action of NO in vascular smooth muscle is mediated by its activation of guanylyl cylase. Apart from being a vasodilator, NO is also a potent inhibitor of neutrophil adhesion to the vascular endothelium. This is due to the inhibitory effect of NO on the expression of adhesion molecules on the endothelial surface (Thomas and Ramwell, 1998; Lowenstein et al., 1992).

Formation of NO from L-arginine is shown in the Figure 3. The activation of iNOS by cytokine, results in the metabolism of L-arginine to L-citrulline and NO (Thomas and Ramwell, 1998; Bredt and Snyder, 1990; Salvemini et al., 1994). Bacterial products and various inflammatory cytokines, such as LPS, IL-1, TNF-α, and IFN-γ, were shown to induce NO from various cells. Combinations of two or three of TNF-α, IL- 1, IFN-γ, and LPS synergistically stimulated rodent macrophage and hepatocyte NO production. These findings suggest that inflammatory cytokines contribute to the upregulation of NO production in inflamed joints (Sakurai et al., 1995 and Pan et al., 2008).

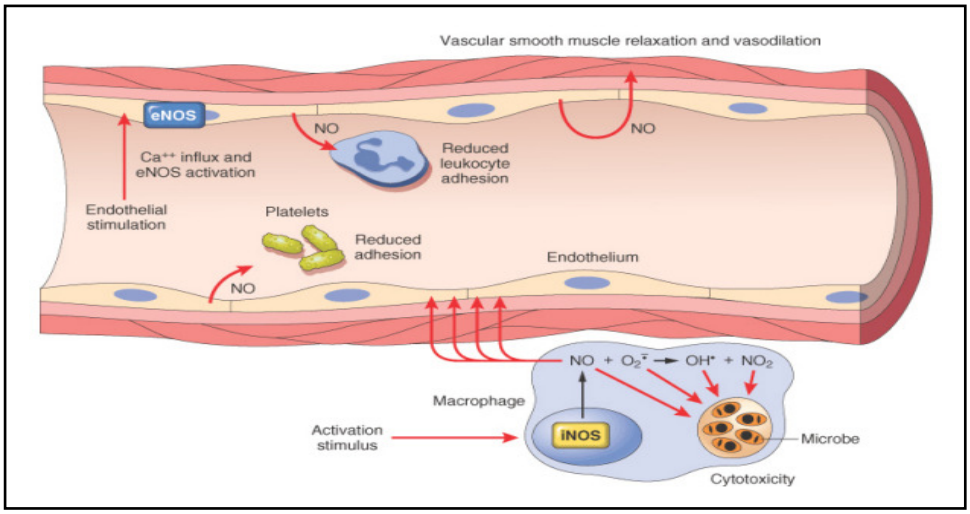

Figure 2 Functions of nitric oxide (NO) in blood vessels and macrophages, produced by two NO synthase enzymes. NO derived eNOS causes vasodilation and NO derived iNOS produced free radicals that are toxic to microbial and mammalian cells. NOS, nitric oxide synthase (Kumar et al, 2005).

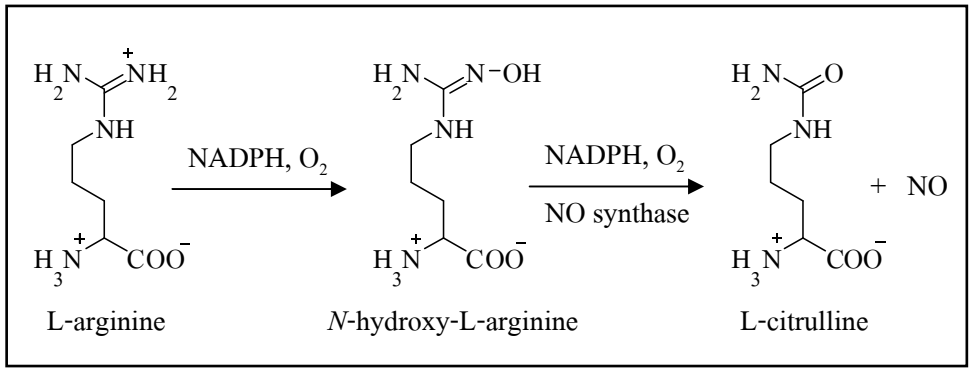

Figure 3 NO generation from L-arginine (Thomas and Ramwell, 1998; Stuehr, 2004; Newton et al., 2003)

NO generated, largely by iNOS exerts complex regulatory activity on the function, growth and death of many immune and inflammatory cell types both *in vitro* and *in vivo*. The signalling processes through which NO acts to regulate these cells are extremely complex and are only just beginning to be unraveled, but are largely indirect through generation

of reactive nitrogen oxide species that chemically modify enzymes, signaling proteins and transcription factors (Figure 2) (Coleman, 2001).

Prostaglandin E_2 (PGE_2)

The eicosanoids are oxygenation products of polyunsaturated long chain fatty acids. Arachidonic acid is a 20-carbon (C20) fatty acid that contains four double bonds beginning at the omega-6 position to yield a 5,8,11,14-ecosatetraenoic acid. For eicosaniod synthesis to occur, arachidonic acid must first be released or mobilized from membrane phospholipids by one or more lipases of the phospholipase A_2 (PLA_2). Two unique but related cyclooxygenase isozymes have been discovered that convert arachidonic acid into prostaglandin endoperoxide. Prostaglandin endoperoxide H synthase-1 (PGH synthase-1) or cyclooxygenase-1 (COX-1) is constitutively expressed, ie, it is always present. In contrast, PGH synthase-2 or cyclooxygenase -2 (COX-2) is inducible, ie, its expression varies markedly depending on the stimulus. The two isozymes also differ in function in that COX-1 is widely distributed and has housekeeping function, eg, gastric cytoprotection. Two to fourfold increases occur following humoral stimulation. In contrast, COX-2 is an immediate early response gene product in inflammatory and immune cells and is prominently expressed (tenfold to eighteenfold) by proinflammatory cytokines, growth factors, oncogenes, carcinogens and tumor promoters implying a role for COX-2 in both inflammation and control of cell growth (Foegh, M.L et al., 1998; Sugiatno et al., 2006; Vane et al., 1994).

Products produced by the arachidonic acid metabolism include both cyclooxygenase products (prostaglandins, thromboxanes) and lipooxygenase products (leukotrienes, LTs) (Figure 4). Products such as LTB_4 and PGE_2, which are representative of these two pathways, can initiate polymorphonuclear neutrophil (PMN) recruitment and changes in vascular tone and blood flow (Lantz et al., 2007; Nakao et al., 2002). Increased production of prostaglandins during an inflammatory response is achieved by induction of COX-2 via NF-κB activation (Lantz et al., 2005; Shishodia et al., 2003).

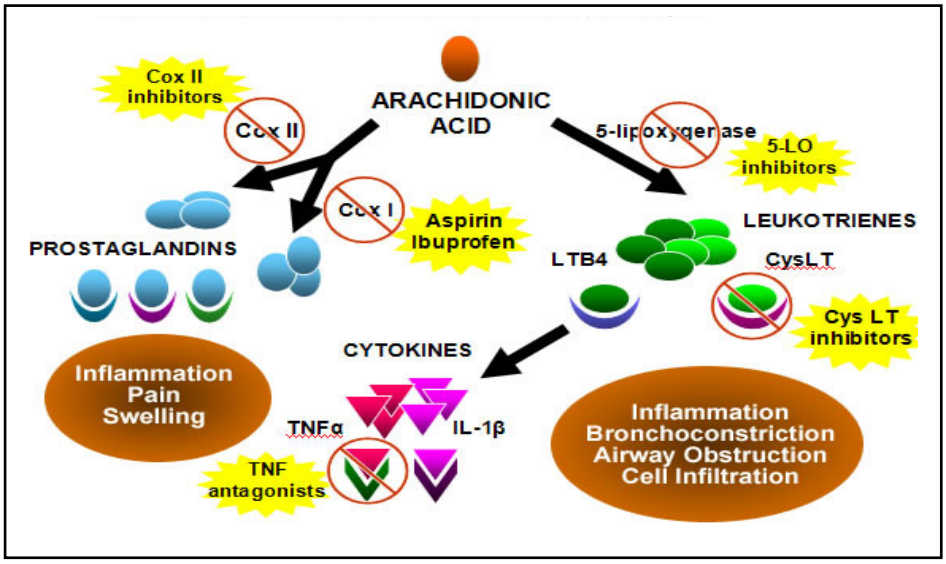

Figure 4 Arachidonic acid is metabolized to produce inflammatory mediators. Many current anti-inflammatory and pain medicines can inhibit some portion of the arachidonic acid pathways (Wake Forest University Health Sciences, 2009)

Leukotrienes, prostaglandins and thromboxanes have been implicated in diverse physiological processes, including asthma, inflammation, carcinogenesis, hemostasis, parturition, maintenance of renal function, pain and fever. Given of the central importance of this pathway to health and disease, over $10 billion per year is spent by consumers to block various inflammatory mediators in the pathway and their resulting effects on signs and symptoms of disease. Most inhibitors provide some relief, but side effects may be problematic (aspirin and ibuprofen irritate the stomach, some COX-2 inhibitors appear to have adverse vascular effects). Consequently, there is significant interest in finding other approaches to managing these diseases and symptoms (Kim et al., 2003).

Drugs for treatment of inflammation

Non-steroidal anti-inflammatory drugs (NSAIDs), such as aspirin, sulindac and indomethacin are widely believed to have anti-inflammatory effects due to their ability to inhibit prostanoid production and relieve inflammation by inhibiting cyclooxygenase (COX) (Chung et al., 2008; Yamamoto and Gaynor, 2001). As well, Aspirin (acetylsalicylic acid, ASA) reduces

pain (analgesic) and fever (antipyretic), which may be helpful in many cases. However, ASA causes side effects such as gastric haemorrhage, hypersentivity and thrombocytopenia. It is also not recommended for children with viral infection because the combination of ASA and a viral infection is believed to contribute to the development of Reye's syndrome, a serious complication involving the brain and liver. The side effects caused by other NSAIDs are similar to those of aspirin, but they are less severe.

Glucocorticoids or steroidal anti-inflammatory drugs, are synthetic chemicals that are related to the naturally occurring glucocorticoids, such as hydrocortisone, produced by the adrenal cortex gland in the body. These drugs are extremely valuable in the treatment of many disorders, but also have significant undesirable effects such as immunosuppression, hyperglycemia, adrenal insufficiency and anovulation that may affect health care.

Other drugs, such as analgesics for treatment of pain, antihistamines and antibiotics for prevention of secondary infection may be required, depending on the cause of the inflammation (Gould, 2002).

1.1.4 Plant

Curcuma mangga Val.&Zijp. is a perennial herb in a Zingiberaceae family commonly grown in Thailand, Peninsular Malaysia and Java. It is locally known as "mango turmeric" because of its mango-like smell when the fresh rhizome is cut (Thai name is Kha-Min-Khao) (Abas et al., 2005). The Zingiberaceae consists of about 1200 species of which 1000 are found in tropical Asia. Zingiberaceae rhizomes are widely used in Asia as both traditional medicine and spices (Kiat et al., 2006).

C. mangga is common in the tropical and equatorial region easily grown from bulbs roots. Topsoil and planted at a depth of 4 inches in a good size pot or ground, with plenty of water and a good exposure of sun would see it blooms in 4 months. The plant would grow to a height of 3 to 4 feet with long broad deep green coloured leaves. The tuber is bright yellow in colour and it gives out a fragrance of a mango. The taste of the tuber is similar to the mango. The flower would last for about 3 months and the plant would wither. Due to this characteristic and its palatable taste, *C. mangga* is then become a popular vegetable, of which the tips of young

rhizomes and shoots are consumed raw with rice. Medicinally, the rhizomes are used in Asian folk medicine to treat gastritis, chest pains, fever and general debility, as well as to aid postpartum healing. It has been reported that the ethanolic extract of this plant showed antifungal activity against three plant pathogens (Abas et al., 2005; Abas et al., 2006).

1.2 Literature review

The investigation of chemical constituents of *C. mangga* was performed on both non-volatile and volatile parts. Chromatographic separation led to the isolation of 3 compounds from non volatile part. The structure determination was accomplished by the aids of spectroscopic means and the previous data of related compounds. A structure of new labdane type diterpene, 15-ethoxy-8(17), 12-labdadien-15, 16-olide was deduced through extensive 1D and 2D NMR studies. Moreover, β-sitosterol and stigmasterol was detected as a mixture of steroidal compounds. The volatile constituents hydrodistilled from the fresh rhizome was analysed by GC/MS and at least 30 components were determined. The major compound was monoterpene group (97.46%), myrcene (84.61%), β-phellandrene (6.63%) and trans-ocimene (3.85%). From antimicrobial activity examination, the essential oil exhibited broad spectrum against microorganism with strong bactericidal effect on *Staphylococus aureus* and *Microsporum gypseum* (Makboon et al., 2000). Moreover, the ethanol and water extracts from *C. mangga* also possessed anti-allergic activity (Tewtrakul and Subhadhirasakul, 2007).

The previous studies showed that *C. mangga* contains protein that resembles *Ribosome-inactivating proteins* (RIPS), which have activity to cleave supercoiled DNA. *In vitro* study indicated that the addition of crude extract of *C. mangga* on cancer cell-lines (B-LCL, EBV cells and Raji cell-lines) and normal lymphocytes, showed cytotoxic effect higher than that of normal cells (Lestariana et al., 2003). The methanol and hexane fractions of *C. mangga* were the most potent against Den2 virus NS2B/NS3 protease activity and may provide potential leads towards the development of anti-viral agents (Kiat et al., 2006). Recently, a more important medicinal characteristic was discovered when (+)-zerumin B was also found to possess potent cytotoxicity (IC_{50} value of 0.59 μM) against the MCF-7 (breast cancer) cell line (Margaros and Vassilikogiannakis, 2008; Chan et al., 2008).

A new labdane diterpene glucoside, curcumanggoside (**1**), together with nine known compounds, including labda-8(17),12-diene15,16-dial (**2**), calcaratarin A (**3**), scopoletin (**4**), zerumin B (**5**) , 1,7-bis(4-hydroxyphenyl)-1,4,6-heptatrien-3-one (**6**), *p*-hydroxycinnamic acid (**7**), curcumin (**8**), demethoxycurcumin (**9**) and bisdemethoxycurcumin (**10**) have been isolated from the rhizomes of *C. mangga* (Figure 5)(Abas et al., 2005).

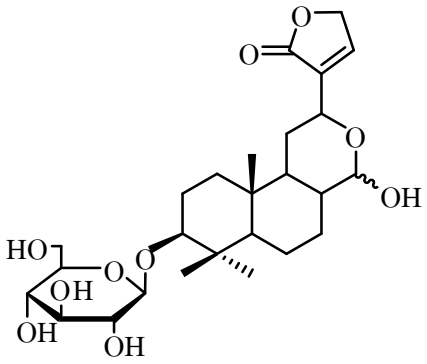

(**1**)

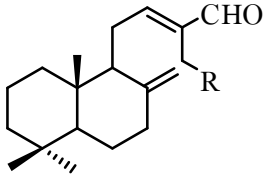

(**2**) R = CHO

(**3**) R = $CH(OCH_3)_2$

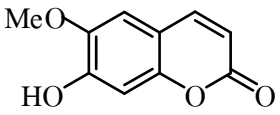

(**4**)

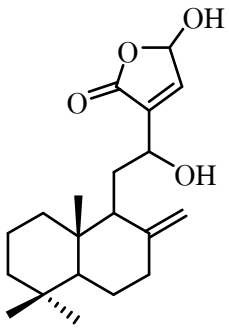

(**5**)

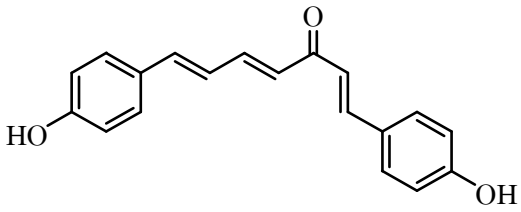

(**6**)

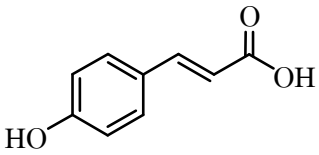

(**7**)

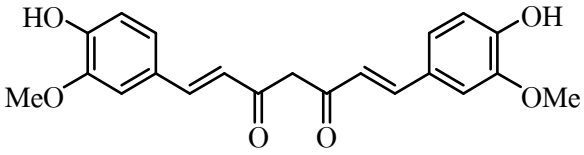

(**8**)

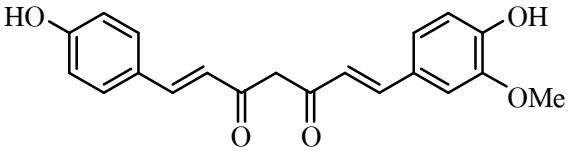

(**9**)

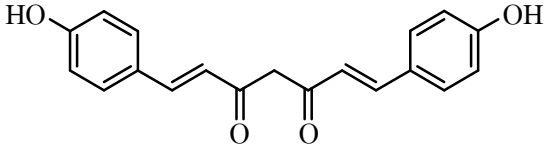

(**10**)

Figure 5 Chemical constituents isolated from *C. mangga* rhizomes

Table 1 Percentage inhibition of lipid peroxidation by compounds isolated from *C. mangga* using $Fe_3(CN)_6$ method (Abas et al., 2005).

Compound[a]	% Inhibition
Curcumanggoside	0
Labda-8(17),12-diene-15,16-dial	5.7±0.1
Calcaratarin A	11.5±0.3
Zerumin B	16.5± 0.6
Scopoletin	94.9±0.5
Demethoxycurcumin	93.8±0.1
Bisdemethoxycurcumin	93.3± 02
1,7-Bis(4-hydroxyphenyl)-1,4,6-heptatrien-3-one	92.9±0.1
Curcumin	96.5±0.1
α-Tocopherol	45.2±0.4
Quercetin	51.3±0.6
Butylated hydroxytoluene (BHT)	99.9±0.3

[a] Concentration of 300 μM.

Demethoxycurcumin, bisdemethoxycurcumin, 1,7-bis(4-hydroxyphenyl)-1,4,6-heptatrien-3-one, curcumin and scopoletin showed antioxidant activity with percentage inhibition of more than 90% (Table 1). Zerumin B, demethoxycurcumin, bisdemethoxycurcumin and curcumin also showed high cytotoxic activity against a panel of human tumor cell lines (Table 2). Zerumin B was found to be the most active toward MCF-7 cells with an IC_{50} value of 0.59 μM and showed moderate activity toward HL-60, HepG2, and DU-145 cells with IC_{50} values of 7.21, 25.33 and 11.21 μM, respectively (Abas et al., 2005).

Table 2 Cytotoxic activity of zerumin B, demethoxycurcumin, bisdemethoxycurcumin and curcumin against various cancer cell lines [a-d] (Abas et al., 2005).

Compound	HE-60	HepG2	MCF- 7	DU-145	NCI-H460
Zerumin B	7.21	25.33	0.59	11.21	-
Curcumin	34.22	35.53	10.44	20.6	27.6
Demethoxycurcumin	24.21	>50	18.51	21.7	25.7
Bisdemethoxycurcumi	25.12	>50	33.78	30.1	88.1

[a]Results are expressed as IC_{50} values (μM). SD of three experiments performed in triplicate. [b]Compounds **1**, **2**, **3**, and 1,7-bis(4-hydroxyphenyl)-1,4,6-heptatrien-3-one could not be evaluated because of their insufficient amount. [c]Scopoletin is inactive against all cell lines tested (IC_{50} > 50 μM). [d] Key to cell lines used: HL-60 = human leukemia, HepG2 = liver cancer, MCF-7 = breast cancer, DU-145 = human prostate cancer, NCI-H460 = lung cancer cells.

Curcumin, Demethoxycurcumin and Bisdemethoxycurcumin

Curcuminoids which are natural phenolic coloring compounds found in the rhizomes of *Curcuma longa* Linn, are commonly known as turmeric. Three main curcuminoids have been isolated from turmeric: curcumin, demethoxycurcumin, bisdemethoxycurcumin. Several studies demonstrated that curcuminoids modulated mutidrug-resistance gene and protein function and displayed anticarcinogenic, antioxidant, anti-inflammation and antiangiogenic properties. Whether analogs of curcumin, such as demethoxycurcumin and bisdemethoxycurcumin, modulate cancer cell invasion and metastasis to the same extent as curcumin did. Among three forms of curcuminoids, bisdemethoxycurcumin and demethoxy-curcumin showed higher potency than curcumin, suggesting that loosing a methoxy group on each side of curcumin might promote antimetastasis activity (Yodkeeree et al., 2008).

In vitro studies demonstrated that curcumin inhibited the production of inflammatory mediators including, phospholipase, lipooxygenase (LOX), COX-2, LTs,

thromboxane (TXAs), prostaglandins (PGs), NO, monocyte chemoattractant protein (MCP)-1, interferon-inducible protein, TNF-α, IL-1 and IL-12 (Chainani-wu, 2003). Curcumin inhibited NO production and expression of iNOS protein and mRNA in RAW 264.7 cells stimulated with LPS or IFN-γ (Surh et al., 2001; Brouet and Ohshima, 1995).

In addition, curcumin was reported to inhibit superoxide and PGE_2 production through COX-2. The wide range of action of curcumin is most likely due to its interaction and inhibition of transcription factor activation, specifically NF-κB (Lantz et al., 2005; Singh and Aggarwal, 1995; Natarajan et al., 1996; Singh and Singh, 2009). Curcumin was found to inhibit NF-κB activation by blocking IκB-α degradation in the cytoplasm and translocation of p65 to the nucleus. Alternatively, curcumin could suppress NF-κB activation by directly interfering with the DNA binding of the functionally active subunit of NF-κB (Han et al., 2002).

Demethoxycurcumin and bisdemethoxycurcumin are natural compounds abundant in several *Curcuma* species. As a component of turmeric and curry, they are widely found in the human diet (Gafner et al., 2004). These two compounds have shown antioxidant and free radical scavenging properties (Eun-Kyoung et al., 2001). The anti-angiogenic activity of demethoxycurcumin was finally evaluated in a cDNA microarray (Kim et al., 2002).

Demethoxycurcumin and bisdemethoxycurcumin inhibited NO production, COX-2 and iNOS expression and suppressed LPS-induced IκB-α prosphorylation and degradation in a dose-dependent manner. All of these anti-inflammation effects could be attributed at least in part to the inhibition of LPS induced NF-κB activation. The effects and concentrations of these two compounds on the cytotoxicity were observed in the macrophages as well as their IC_{50} values for inhibition of NO, NF-κB, iNOS and COX-2. The anti-inflammatory and the cytotoxicity activity of demethoxycurcumin were found to be better than those of bisdemethoxycurcumin at the same concentration. It appears that the presence of the methoxy groups in the curcumin molecules is essential to anti-inflammatory activity. In the similar manner, the methoxy groups enhance cytotoxicity in macrophages. The safe concentration of demethoxycurcumin is lower than 43.7 μM and that of bisdemethoxycurcumin is lower than 61.3 μM (Guo et al., 2008)

Scopoletin

Scopoletin (7-hydroxy-6-methoxycoumarin, SCT) is a coumarin derivative. This coumarin widely occurs as secondary plant metabolites, especially in a member of the Solanaceae family. SCT has previously been described as an anti-inflammatory and antiproliferative agent that exhibits various activities such as the inhibition of inducible nitric oxide synthase and prostaglandin synthase (Rollinger et al., 2004). Moreover, scopoletin has been more extensively investigated with respect to several pharmacological properties. Besides, SCT also inhibited prostaglandin synthetase *in vitro* studies in ovalbumin-induced acute arthritic swelling in rat, as well as in formaldehyde-induce subacute arthritic swellings in rats. The topical application of this compound also showed a remarkable high potency in inhibition of ethyl phenylpropiolate (EPP)-induced edema of the rat ear with 100-200 times more potent than the reference compounds, mepyramine and oxyphenbutazone (Farah and Samuelsson, 1991).

1.3 Background and objectives

Since *C. mangga* rhizomes have long been used for treatment of inflammation and possessed marked anti-NO and PGE_2 activity, we thus investigated the inhibitory activity of compounds isolated from this plant against NO and PGE_2 production using RAW264.7 macrophage-like cells, as well as the anti-inflammatory mechanism in transcriptional level on mRNA expression.

The objectives of this investigation are therefore as the following;

1. To study on anti-inflammatory activity of *C. mangga* crude extract
2. To isolate and elucidate the structures of pure compounds from *C. mangga* extract
3. To study on anti-inflammatory activity of pure compounds from *C. mangga* extract as well as their anti-inflammatory mechanisms against mRNA expression of iNOS and COX-2 genes at transcriptional level

CHAPTER 2

EXPERIMENTAL

2.1 General

All solvents for general purposes and chromatography were analytical grade. Thin layer chromatography (TLC) was performed on Merck® pre-coated silica gel 60 F_{254} plates (0.20 mm thickness). Chromatographic separations performed over the columns of C18 (10 mm, 250 mm) (Alltech Associates, Inc). Visualization was done with observation under UV light (254 nm). The optical density was measured with a microplate reader (Bio-Tek instruments, Inc). PCR kits (Rever Tra Dash) from TOYOBO Co., Ltd., Japan were used. Takara PCR Thermal Cycler Dice TP600 (Takara, Japan) and UV light box (Gel Doc model 1000, Bio-Rad, USA) were used.

2.2 Chemicals and reagents used for cell culture

Murine macrophage-like RAW264.7 cell line (purchased from Cell Lines Services), lipopolysaccharide (LPS, from *Escherichia coli*), RPMI-1640 medium, 3-(4,5-dimethyl-2-thiazolyl)-2,5-diphenyl-2*H*-tetrazolium bromide (MTT), L-nitroarginine (L-NA), caffeic acid phenethylester (CAPE), indomethacin and phosphate buffer saline (PBS) were purchased from Sigma Aldrich (Sigma Aldrich, Missouri, USA). Fetal calf serum (FCS) was bought from Gibco (Invitrogen, California,USA). Penicillin-streptomycin was purchased from Invitrogen (Invitrogen, California, USA). 96-Well microplates were obtained from Nunc (Nunc, Birkrød, Denmark). ELISA test kits of PGE_2 were purchased from R&D systems (R&D systems, Minnesota, USA). RNeasy Mini Kit was bought from Qiagen Operon Co., Ltd., USA. First strand cDNA synthesis kit and RT-PCR were purchased from TOYOBO Co., Ltd., Japan. Other chemicals were purchased from Sigma Aldrich (Sigma–Aldrich, Missouri, USA).

2.3 Plant material

The fresh rhizomes of *Curcuma mangga* Val.&Zijp. were collected in Songkhla province, Thailand in 2006. The voucher specimens are SKP No. 206 03 13 01. The plant material was identified by Assoc. Prof. Dr. Sanan Subhadhirasakul and the voucher specimens are kept at the herbarium of the Faculty of Pharmaceutical Sciences, Prince of Songkla University, Songkhla, Thailand (Figure 6).

Figure 6 The *Curcuma mangga* rhizomes

2.4 Isolation and structure elucidation

Twenty kilogram of the fresh rhizomes were cleaned, cut into small pieces, dried in the shade and ground to powder. The powder (1.8 kg) was extracted three times (6 l, each) with EtOH at room temperature. The solvent were removed under reduced pressure to give 309.4 g of crude extract and then partitioned between 90% MeOH and hexane, removed of MeOH,

added of water and partitioned with chloroform. After that the water layer was partitioned with ethyl acetate (EtOAc). Each partition was evaporated to dryness *in vacuo* to give residues of hexane (176.5 g), chloroform (39.1 g), EtOAc (2.5 g) and water fractions (91.1g) (Figure 7), respectively.

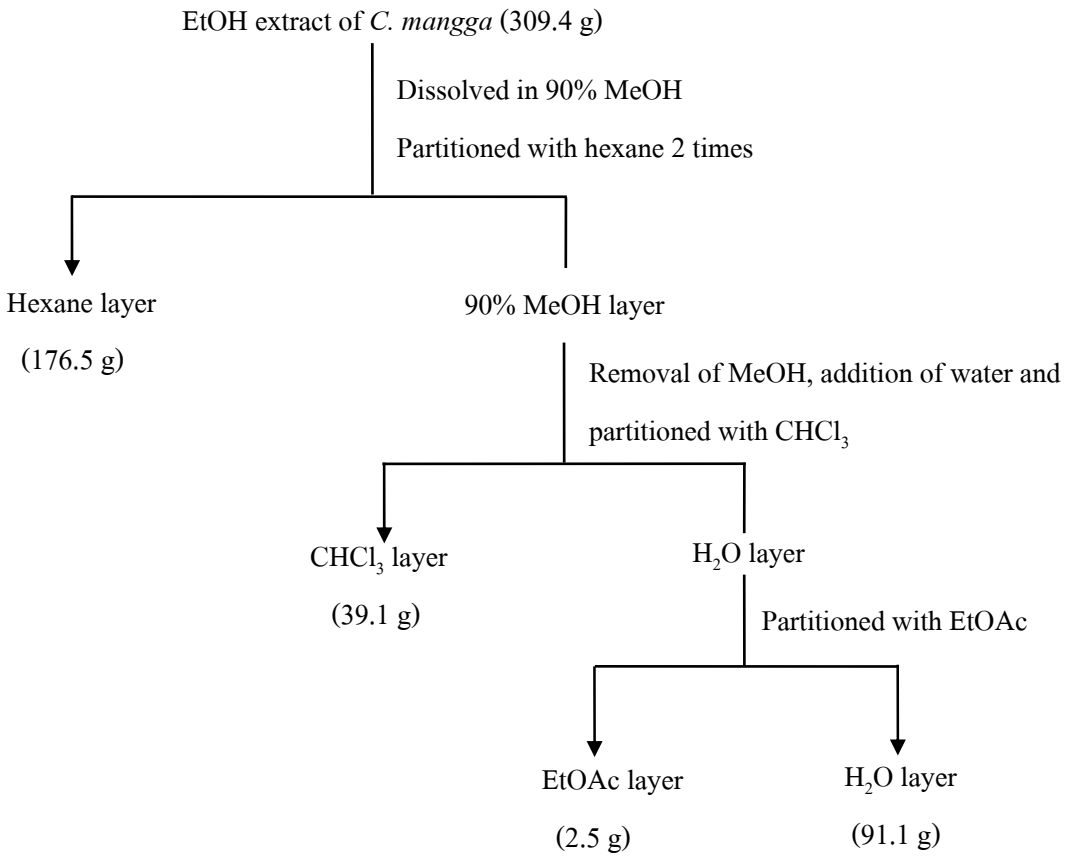

Figure 7 The procedure of *C. mangga* rhizome extraction

The chloroform fraction (12 g) was then adsorbed on 200 g of silica gel by vacuum liquid chromatography (VLC). The column was eluted in ascending polarity manner with hexane, hexane/chloroform, followed by chloroform/methanol mixture to afford ten fractions (C1-C10). Fraction C7 (50 mg) was separated by reversed-phase HPLC, using isocratic method with a flow rate of 2 ml/min. The mobile phase consisted of 70% methanol in water

accomplished using a C18 column (∅10 mm, 250 mm). The eluent was monitored at 254 nm, to afford six subfractions (C1-C6). Repeated column chromatography of the subfraction C6 (10 mg) by gel permeation chromatography on Sephadex LH-20 (10% chloroform in methanol) afforded demethoxycurcumin (**1**) (yellow needles, 2 mg) (Figure 8).

Figure 8 The vacuum liquid chromatography of the chloroform fraction

The hexane fraction (80 g) was chromatographed on 1,500 g of silica gel. The column was eluted in ascending polarity with hexane/EtOAc (98:2 to EtOAc 100%; 15 l) to afford eleven fractions (H1-H11). Fraction H4 (1.75 g) was subjected to column chromatography on 100 g of silica gel eluted with hexane/EtOAc (98:2 to EtOAc 100%; 2 l) to give ten subfractions (H1-H10). Further column chromatography of the subfraction H5 (160 mg) was on 140 g of silica gel using hexane/dichloromethane (1:1, 800 ml) which afforded seven fractions (H1-H7). Fraction H6 (45 mg) was separated by HPLC, using isocratic method with a flow rate of 3 ml/min. The mobile phase consisted of 90% methanol in water, using a C18 column (∅10 mm, 250 mm). The eluent was monitored at 254 nm, to afford 15,16 bisnorlabda-8(17), 11 dien-13-one (**2**) (white needles, 21 mg).

Fraction H5 from the first column (1.3 g) was then adsorbed on 80 g of silica gel by vacuum liquid chromatography. The column was eluted in ascending polarity manner with hexane, hexane/EtOAc, followed by EtOAc/methanol mixture to afford eight fractions (H1-H8). Fraction H2 (50 mg) was separated by reversed-phase HPLC, using isocratic method with a flow rate of 2 ml/min. The mobile phase consisted of 100% methanol; was accomplished using a C18 column (∅10 mm, 250 mm). The eluent was monitored at 254 nm, to afford six subfractions (H1-H6). Repeated column chromatography of the subfraction H4 (19 mg) by gel permeation chromatography on Sephadex LH-20 (10% chloroform in methanol) afforded (*E*)-15,15-diethoxylabda-8(17),12-dien-16-al (**3**) (amorphous powder, 13 mg) (Figure 9).

Since bisdemethoxycurcumin could not be isolated from the rhizomes of *C. mangga* in the present study, the ethanol extract of *Curcuma longa* (500 mg) was then chromatographed on 120 g of silica gel. The column was eluted with chloroform to afford bisdemethoxycurcumin (**4**) (yellow needles, 6 mg).

The structures of compounds **1-4** were elucidated using the spectroscopic techniques and compared with the reported spectral data (Itokawa et al., 1980; Weyerstahl et al., 1995; Duker-Eshun et al., 2002; Paramasivam et al., 2009).

Figure 9 The vacuum liquid chromatography of fraction H5 (hexane)

2.5 Physical properties of isolated compounds

Demethoxycurcumin (**1**): yellow needles; UV ($CHCl_3$) λ_{max} (log ε) 415 (3.6) nm; IR (KBr) ν_{max} 3414 , 2926, 1625 cm^{-1}; ^1H NMR (500 MHz), see table 3.

15,16 bisnorlabda-8(17), 11 dien-13-one (**2**): white needles; UV ($CHCl_3$) λ_{max} (log ε) 244 (3.7) nm; IR (KBr) ν_{max} 1662 cm^{-1}; EIMS m/z 260.2148 (calcd for $C_{18}H_{28}0$, 260.2140); ^{1}H and ^{13}C NMR (500 MHz for ^{1}H and 125 MHz for ^{13}C), see table 4.

(*E*)-15,15-diethoxylabda-8(17),12-dien-16-al (**3**): amorphous powder; UV ($CHCl_3$) λ_{max} (log ε) 244 (3.7) nm; IR (KBr) ν_{max} 2928, 2711, 1683 cm^{-1}; EIMS m/z 376.3 (calcd for $C_{24}H_{40}0_3$, 376.2640); ^{1}H and ^{13}C NMR (500 MHz for ^{1}H and 125 MHz for ^{13}C), see table 5.

Bisdemethoxycurcumin (**4**): yellow needles; UV (CH_3OH) λ_{max} (log ε) 415 (4.8) nm; IR (KBr) ν_{max} 3445, 1629 cm^{-1}; ^{1}H NMR (500 MHz), see table 6.

2.6 Anti-inflammatory activity test

2.6.1 Determination of nitric oxide production

Inhibitory effect on NO production by murine macrophage-like RAW264.7 cells was evaluated using a modified method from that previously reported (Tewtrakul and Subhadhirasakul, 2008). RAW264.7 cell line was cultured in RPMI medium supplemented with 0.1% sodium bicarbonate and 2 mM glutamine, penicillin G (100 units/ml), streptomycin (100 µg/ml) and 10% FCS. The cells were harvested with 0.25% trypsin-EDTA and diluted to a suspension in a fresh medium. Cell counts were measured using a standard trypan blue cell counting technique. The cell concentration was adjusted to 1×10^{6} cells/ml in the same medium. 100 µl of cells suspension were seeded in 96-well culture and incubated for 1 h at 37 ºC in a 5 % CO_2 incubator to promote adherence to the bottom of the well. After that, the medium was replaced with a fresh medium containing 100 µg/ml of LPS together with the test samples at various concentrations (3–100 µg/ml for crude extracts and 3–100 µM for pure compounds) and was then incubated for 48 h. NO production was determined by measuring the accumulation of

nitrite in the culture supernatant using the Griess reagent (Figure 10A). The optical density was measured with a microplate reader at 570 nm.

Griess reaction is first described in 1879 and is the most frequently used analytical approach to quantitate the major metabolites of NO because of the simplicity of the Griess reaction, its easy and inexpensive analytical feasibility. The overall reaction is described in the scheme 1 (Sun et al., 2003; Cother, 1987; Guevara et al., 1998).

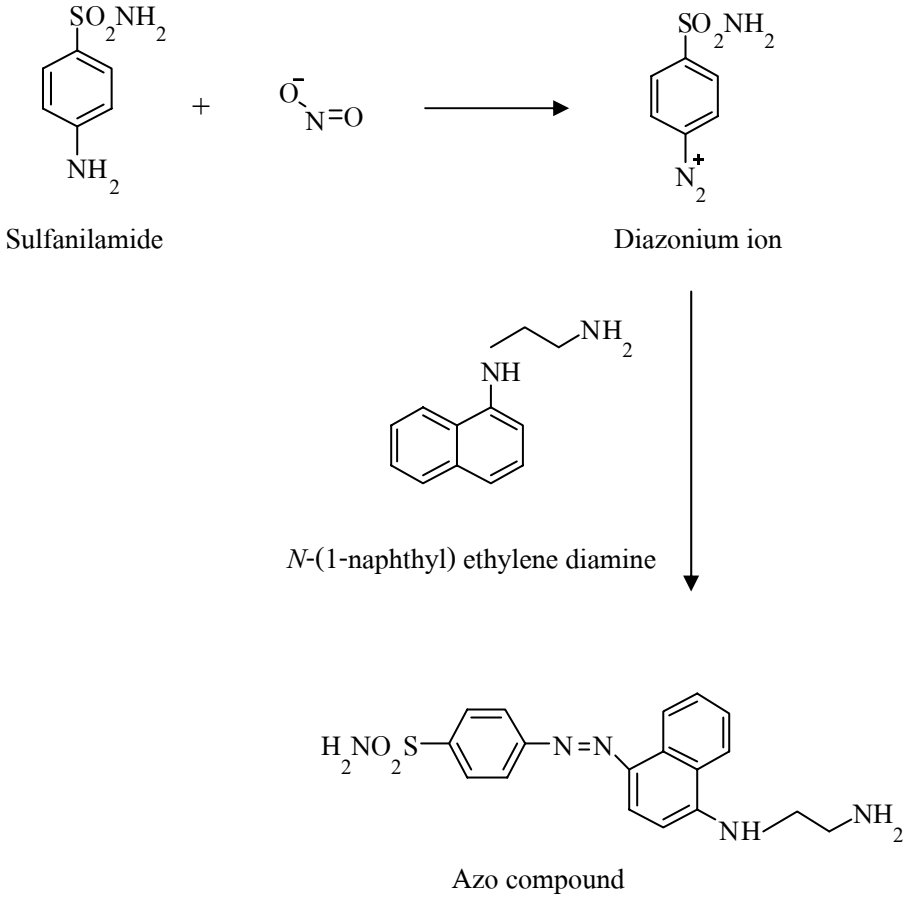

The scheme 1 The Griess reaction, under acidic conditions, nitrite reacts with the amino group of sulfanilamide to form the diazonium cation, which couples to *N*-(1-naphthyl) ethylenediamine in *para*-position to form the corresponding azo dye (Tsikas, 2007).

L-NA (NO synthase inhibitor), CAPE (NF-κB inhibitor) and indomethacin (non-steroidal anti-inflammatory drug, NSAID, iNOS and COX inhibitor) were used as positive controls. The stock solution of each test sample was dissolved in DMSO and the solution was added to the medium RPMI (final DMSO is 1%). Inhibition (%) was calculated using the following equation and IC_{50} values were determined graphically ($n = 4$):

Inhibition (%) = $[(A - B) / (A - C)] \times 100$

A-*C*: NO_2^- concentration (μM) [*A*: LPS (+), sample (-); *B*: LPS (+), sample (+); *C*: LPS (-), sample (-)].

2.6.2 Cytotoxicity test

Cytotoxicity was determined using the MTT (3-(4,5-dimethylthiazol-2-yl)-2,5-diphenyltetrazolium bromide, a tetrazole) colorimetric method. MTT assay, first described by Mosmann in 1983, is based on the ability of a mitochondrial dehydrogenase enzyme from viable cells to cleave the tetrazolium rings of the pale yellow MTT and form a dark blue formazan crystals which is largely impermeable to cell membranes, thus resulting in its accumulation within healthy cells (The scheme 2). Formazans are produced when tetrazolium salts are reduced by naturally occurring enzymes. A solubilization solution (usually either dimethyl sulfoxide, an acidified ethanol solution, or a solution of the detergent sodium dodecyl sulfate in dilute hydrochloric acid) is added to dissolve the insoluble purple formazan product into a colored solution. The absorbance of this colored solution can be quantified by measuring at a certain wavelength (usually between 500 and 600 nm) by a spectrophotometer. The absorption maxima is dependent on the solvent employed. This reduction takes place only when mitochondrial reductase enzymes are active and therefore conversion can be directly related to the number of viable (living) cells. When the amount of purple formazan produced by cells treated with an agent is compared with the amount of formazan produced by untreated control cells, the effectiveness of the agent in causing death of cells can be deduced, through the production of a dose-response

curve. These formazan dyes are commonly used in cell proliferation and toxicity assays (Scudiere et al., 1988).

After 48 h incubation with the test samples, MTT solution (10 µl, 5 mg/ml in PBS) was added to the wells. After 4 h incubation, the medium was removed and isopropanol containing 0.04 M HCl was then added to dissolve the formazan production in the cells (Figure 10B). The optical density of the formazan solution was measured with a microplate reader at 570 nm. The test compounds were considered to be cytotoxic when the optical density of the sample-treated group was less than 80% of that in the control (vehicle-treated) group.

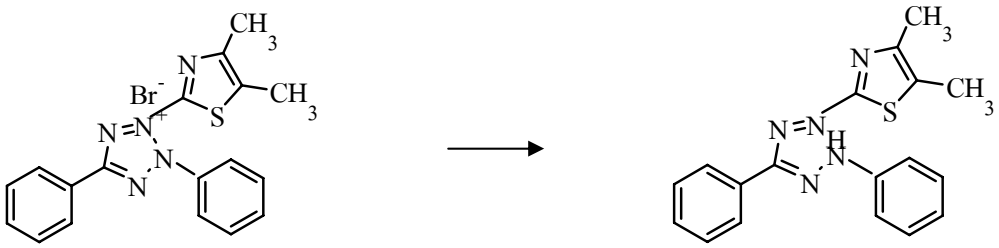

MTT (yellow) MTT formazan (dark blue)

570 nm

The scheme 2 Structures of MTT and formazan.

2.6.3 Determination of prostaglandin E_2 production

The murine macrophage-like RAW264.7 cells were grown and maintained in RPMI-1640 medium supplemented with 0.1% sodium bicarbonate and 2 mM glutamine, penicillin G (100 units/ml), streptomycin (100 µg/ml) and 10% Fetal bovine serum (FBS) in plastic culture flasks at 37 ºC, 5% CO_2, in a fully humidified incubator. The cells were harvested with 0.25% trypsin-EDTA and re-suspended in a fresh medium. Cell counts were measured using a standard trypan blue cell counting technique. The cell concentration was adjusted to 1×10^6 cells/ml in the same medium. 100 µl of cells suspension were seeded in 96-well culture and incubated for 1 h at 37 ºC in a 5 % CO_2 incubator to promote adherence to the bottom of the well. After that, the medium was replaced with LPS in RPMI-1640 (75 µg/ml) which is the triggering agent for PGE_2 production. After that, the samples in various concentrations (3-100 µg/ml for

crude extracts and 3-100 μM for pure compounds) were dispensed into the wells. The cells were incubated for 48 h at the same condition. The supernatant was transferred into 96-well ELISA plate and then PGE_2 concentrations were determined according to a manufacturer's instruction. Absorbance at 450 nm was recorded using a microplate reader (Figure 10C).

2.6.4 Determination of iNOS and COX-2 mRNA expression

2.6.4.1 Total RNA isolation from RAW264.7 cells

RAW 264.7 cells 1.5 ml (1×10^6 cells/ml) were added to 6-well culture plate and allowed to adhere for 1 h at 37 ºC in a humidified atmosphere containing 5% CO_2. After that, cells were harvested after 20 h incubation with various concentrations of samples (3, 10, 30 and 100 μM for pure compounds). The cells were removed from the culture flask by scrapping and were then isolated to obtain RNA using RNeasy Mini Kit. The cells were centrifuged at 4,000 rpm for 5 min. The supernatant were removed and 350 μl of buffer RLT supplemented with 3.5 μl of β-mercaptoethanol was added to the cells and mixed well by pipetting. Then, 350 μl of 70% ethanol was added and mixed by pipetting. After that, 700 μl of the lysate was loaded into the RNeasy mini column in a 2 ml collection tube and centrifuged at 10,000 rpm for 30 s. The flow-through was discarded and 700 μl of buffer RW1 was added to the RNeasy column and centrifuged at 10,000 rpm for 30 s. The RNeasy mini column was transferred to a new collection tube. Buffer RPE 500 μl was added to RNeasy mini column and centrifuged at 10,000 rpm for 30 s. The flow-through was discarded. The 500 μl of buffer RPE was again added to RNeasy mini column and centrifuged at 10,000 rpm for 2 min 30 s. After that, the RNeasy mini column was placed in a 1.5 ml microcentrifuge tube. The 55 μl of RNase free water was added into a mini column and centrifuged at 10,000 rpm for 30 s to obtain total RNA. The isolated RNA was stored at -20 ºC until use.

A

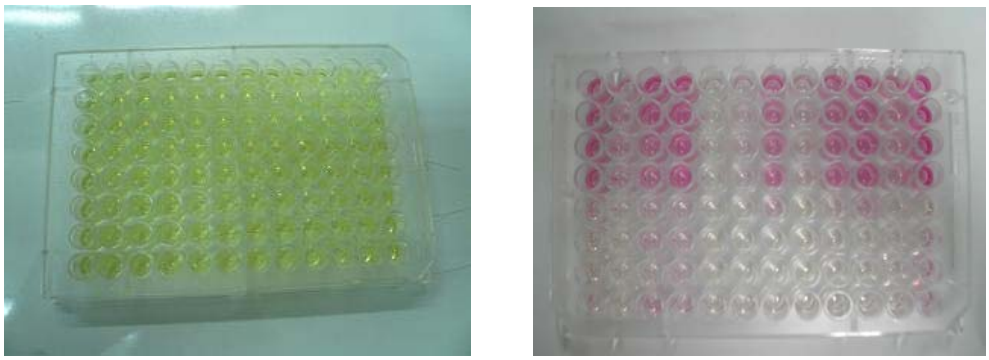

B

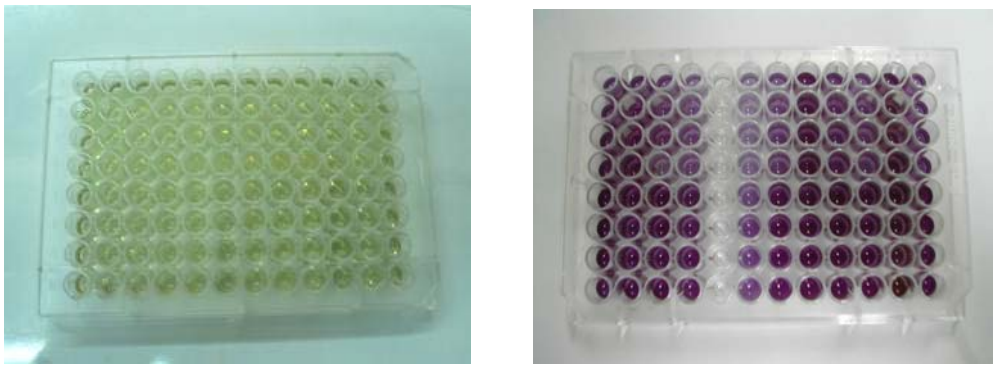

C

Figure 10 The anti-inflammatory activity tests. NO production test (A), cytotoxic activity test (B) and prostaglandin E_2 production test (C).

2.6.4.2 Detection of iNOS and COX-2 mRNA by reverse transcription polymerase chain reaction (RT-PCR).

In order to investigate the mechanisms in transcriptional level of pure compounds from the rhizomes of *C. mangga*, the suppression on mRNA expression of iNOS and COX-2 genes was carried out. Single-stranded complementary DNA (cDNA) was generated using cDNA synthesis kit consisting of RNA solution 11 µl, 5×RT buffer 4 µl, dNTP mixture (10 mM) 2 µl, RNase inhibitor (10 U/µl) 1 µl, Oligo (dT) 20 1 µl and Rever Tra Ace (reverse transcriptase enzyme) 1 µl for a 20 µl reaction. Reverse-transcription was performed at 42 °C for 20 min, 99 °C for 5 min and 4 °C for 5 min. The resulting cDNA was used as a template for subsequent PCR.

The iNOS, COX-2 and β-actin genes were amplified by PCR kit. The β-actin, a constitutively expressed gene, was analyzed as an internal standard. The primers for each gene were as follow; forward primer for iNOS: 5′-ATCTGGATCAGGAACCTGAA-3′ and its reverse primer: 5′-CCTTTTTTGCCCCATAGGAA-3′; forward primer for COX-2: 5′-GGAGAGAC TATCAAGATAGTGATC-3′ and its reverse primer: 5′-ATGGTCAGTAGACTTTTACAGC TC-3′; forward primer for β-actin: 5′-TGTGATGGTGGGAATGGGTCAG-3′ and its reverse primer: 5′-TTTGATGTCACGCACGATTTCC-3.

The PCR mixture is consisted of cDNA 2 µl, dH_2O (RNase free water) 85 µl, 10×PCR buffer 10 µl, forward primer 1 µl, reverse primer 1 µl (10 pmol/µl each) and KOD Dash DNA polymerase (2.5 units) 1µl, to give a final volume of 100 µl. Amplification was performed for 30 cycles using Takara PCR Thermal Cycler Dice TP600 with a following programme: denaturation at 98 ºC for 30 s, annealing at 60 ºC for 30 s and extension at 74 ºC for 1 min. The 580 base pairs (bp) of iNOS, 860 bp of COX-2 and 514 bp of β-actin DNA fragments were obtained and separated on 1.2 % w/v agarose gel electrophoresis. The bands of DNA were detected by staining with SYBR® Safe DNA staining solution for 30 min and were observed under a UV light box at wavelength 312 nm (Figure 11).

A B C

Figure 11 Takara PCR thermal cycler dice TP600 (Takara, Japan) (A), running gel eletrophoresis (B) and UV light box (Gel Doc model 1000, Bio-Rad, USA) (C).

2.7 Statistical analysis

The results were expressed as mean ± S.E.M of four determinations at each concentration for each sample. The IC_{50} values were calculated using the Microsoft Excel program. Statistical significance was calculated by one-way analysis of variance (ANOVA), followed by Dunnett's test.

CHAPTER 3

RESULTS AND DISCUSSION

3.1 Isolation and structure elucidation

3.1.1 Isolation

The fresh rhizomes of *Curcuma mangga* Val.&Zijp. were collected in Songkhla Province, Thailand, in 2006. The powder (1.8 kg) was extracted three times (6 l, each) with EtOH at room temperature. The solvent was removed under reduced pressure to give 309.4 g of crude extract and then partitioned between 90% MeOH and hexane, removed of MeOH, added of water and partitioned with chloroform. After that the water layer was partitioned with EtOAc. Each partition was evaporated to dryness *in vacuo* to give residues of hexane (176.5 g), chloroform (39.1 g), EtOAc (2.5 g) and water fractions (91.1g), respectively.

The chloroform fraction of *Curcuma mangga* and the ethanol extract of *Curcuma longa* were subjected to the chromatographic isolation to obtain demethoxycurcumin (**1**) and bisdemethoxycurcumin (**4**), respectively. The hexane fraction was separated using the chromatographic technique to afford 15,16 bisnorlabda-8(17), 11 dien-13-one (**2**) and (*E*)-15,15-diethoxylabda-8(17),12-dien-16-al (**3**) as the major components.

3.1.2 Structure elucidation

3.1.2.1 Demethoxycurcumin [1-(4-hydroxy-3-methoxyphenyl)-7-(4-hydroxy-phenyl)-1,6-heptadiene-3,5 dione, compound 1]

Compound **1** was obtained as yellow needles (2 mg) from the chloroform fraction using the chromatographic technique (VLC; hexane, hexane/chloroform, followed by chloroform/methanol mixture, reversed-phase HPLC; 70% methanol in water and gel permeation chromatography on Sephadex LH-20; 10% chloroform in methanol).

Compound **1** has a molecular formula of $C_{20}H_{18}O_5$, MW 338. ^{1}H NMR ($CDCl_3$, 500 MHz) δ (ppm): the ^{1}H NMR spectrum of **1** (Figure 12 , Table 3) showed two trans olefins (H7-H8 and H12-H13; d, J = 15.7 Hz), three substituted benzene protons at 7.03 (1H, s), 6.91 (1H, d, J = 8.1 Hz), 7.13 (1H, d, J = 8.1 Hz) and one phenolic methoxyl group signal at 3.93, two protons at 5.77 (s), 5.84 (s) and four substituted benzene protons at 7.45 (2H, d, J = 8.42 Hz) and 6.83 (2H, d, J = 8.42 Hz). These data indicated that **1** was demethoxycurcumin. The data was confirmed by comparison with spectral analysis data reported in the literatures (Péret-Almeida et al., 2005; Kosuge et al., 1985; Kiuchi et al., 1993; Gupta et al., 1999; Jayaprakasha et al., 2002, Du et al., 2006; Zeng et al., 2007; Inoue et al., 2008 and Paramasivam et al., 2009).

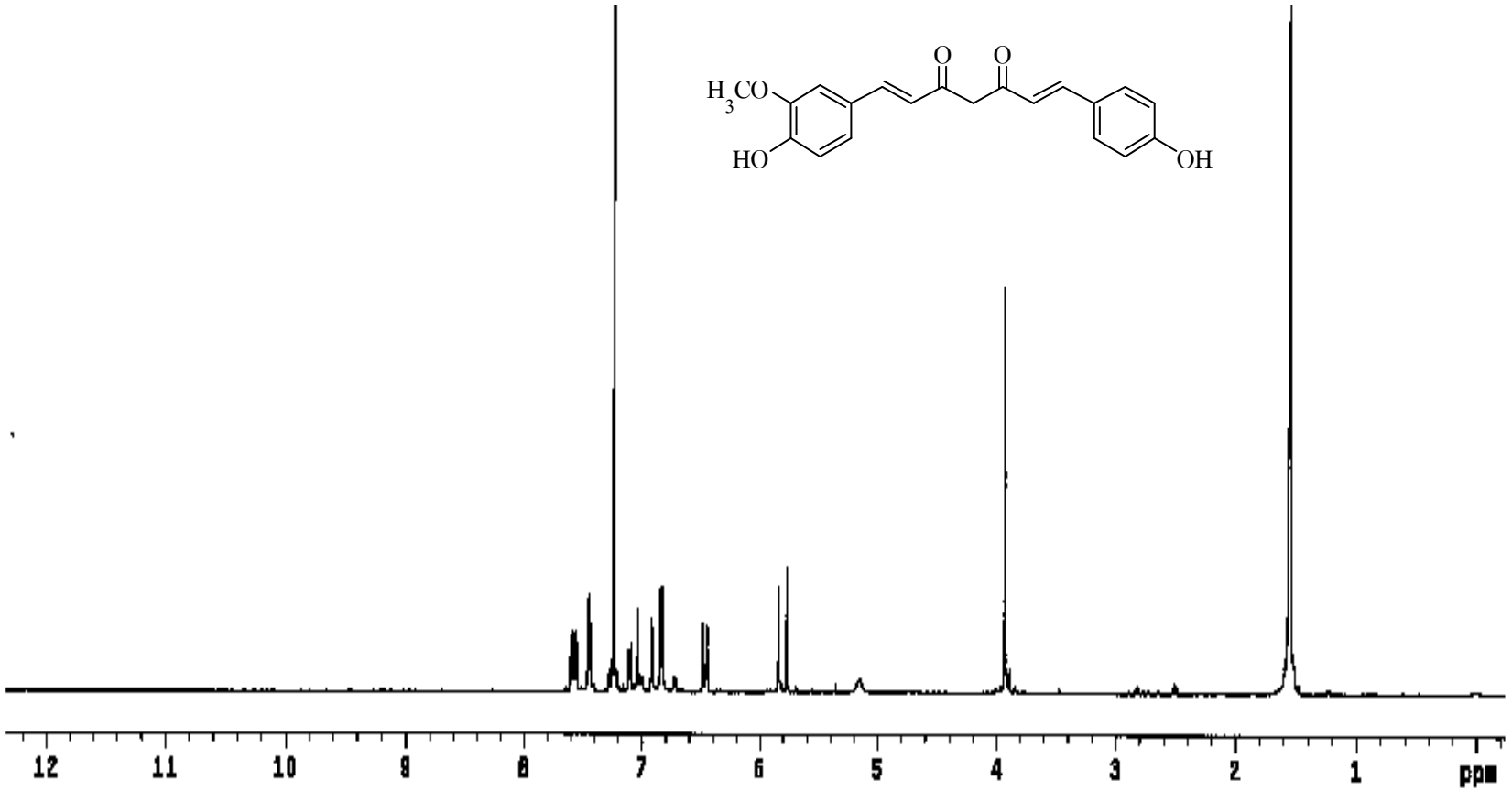

Figure 12 ^{1}H NMR spectrum of compound **1** ($CDCl_3$; 500 MHz)

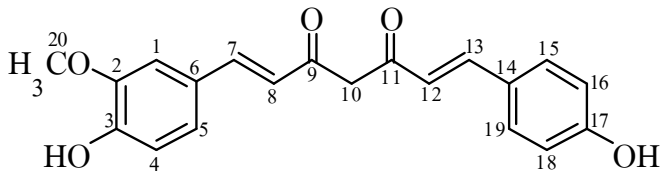

Table 3 ^{1}H spectral data of compound **1** ($CDCl_3$; 500 MHz for ^{1}H) and reference

positions	^{1}H (mutl.; *J* in Hz)	^{1}H (mutl.; *J* in Hz, Péret-Almeida et al., 2005)*
1	7.03 (s)	7.31 (d; 1.6)
2	-	-
3, 17	-	-
4	6.91 (d; 8.1)	6.81 (d; 8.3)
5	7.13 (d; 8.1)	7.13 (dd; 8.3, 1.6)
6	-	-
7	7.57 (d; 15.7)	7.53(d; 15.8)
8	6.46 (d; 15.7)	6.67 (d; 15.8)
9	-	
10	5.77 (s), 5.8 (s)	6.02 (s)
11	-	-
12	6.47 (d; 15.7)	6.67 (d; 15.8)
13	7.58 (d; 15.7)	7.53(d; 15.8)
14	-	-
15,19	7.45 (d; 8.4)	7.13 (d; 8.3)
16,18	6.83 (d; 8.4)	6.81 (d; 8.3)
20	3.93 (s)	3.82 (s)

* ^{1}H NMR in reference was run in DMSO-d_6

3.1.2.2 15,16 bisnorlabda-8(17), 11 dien-13-one (compound 2)

Compound **2** was obtained as white needles (21 mg) from the hexane fraction using the chromatographic technique (CC, reversed-phase HPLC; 90% methanol in water).

The molecular formula of compound **2** was assigned as $C_{18}H_{28}O$ on the basis of the molecular ion peak (M^+) in the high resolution electron capture mass spectrometry at *m/z* 260.2148 (Calcd: 260.2140), indicating that this should be an unusual bisnorditerpene. The ^{1}H-NMR spectrum of **2** (Figure 13 , Table 4) exhibited three methyl signals; δ 0.87, s, 3H; H-18, 0.86, s, 3H; H-19, 0.82, s, 3H; H-20, exo-methylene signals; δ 4.38 (d, *J* = 1.42 Hz, H-17ax) and 4.76 (d, *J* = 1.42 Hz , H-17eq) which are characteristic of a labdane-type diterpenoid and assigned to the methyl groups at C-18, C-19 and C-20 as well as to the methylene group at C-17, respectively. It is further confirmed by the fragment peak at *m/z* 137 in the EIMS. The labdane-type skeleton was supported by the presence of a characteristic base peak at *m/z* 137 in the mass spectrum.

Interpretation of ^{1}H-^{1}H COSY cross peaks in the aliphatic methylene region led to three partial structures, including fragment A [δ 1.15 (m, H-1ax), 1.40 (m, H-1eq), 1.36 (m, H-2ax), 1.46 (m, H-2eq), 1.17 (m, H-3ax) and 1.34 (m, H-3eq)]; fragment B [δ 1.09 (dd, J = 12.69, 2.68 Hz, H-5), 1.38 (m, H-6ax), 1.69 (m, H-6eq), 2.06 (m, H-7ax) and 2.42 (m, H-7eq); fragment C [δ 2.45 (m, H-9), 6.83 (dd, J = 15.0, 10.2 Hz, H-11), 6.0 (d, J = 15.0 Hz, H-12), 4.3 (d, J = 1.46 Hz, H-17ax) and 4.7 (dd, J = 1.46 Hz, H-17eq).

The ^{1}H-NMR spectra [δ 2.24 (3H, s), 6.04 (1H, d, *J* = 15.86 Hz), 6.88 (1H, dd, *J* = 15.86, 10.25 Hz) and ^{1}H-NMR decoupling experiment provided conclusive proof of the side chain (Figure D).

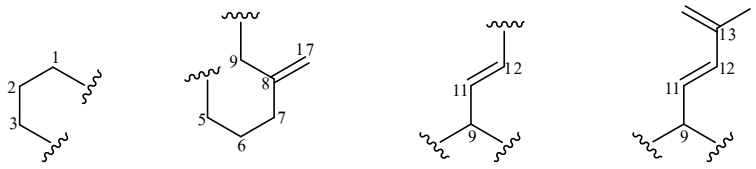

A B C D

The ^{13}C-NMR spectrum (Figure 14, Table 4) and DEPT experiment for **2** confirmed the existence of 18 carbons including four methyls, six methylenes, four methines,

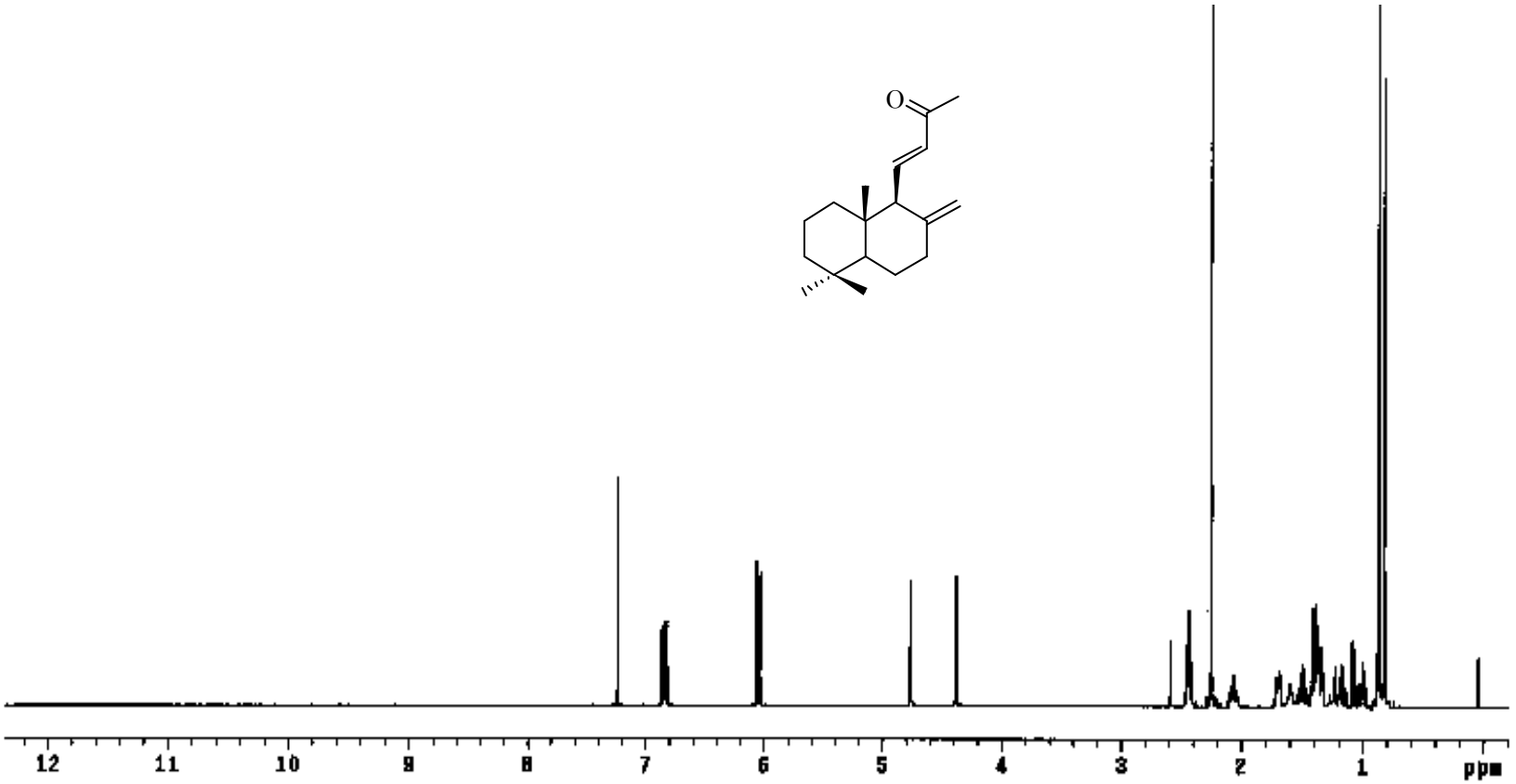

Figure 13 ^{1}H NMR spectrum of compound **2** ($CDCl_3$; 500 MHz)

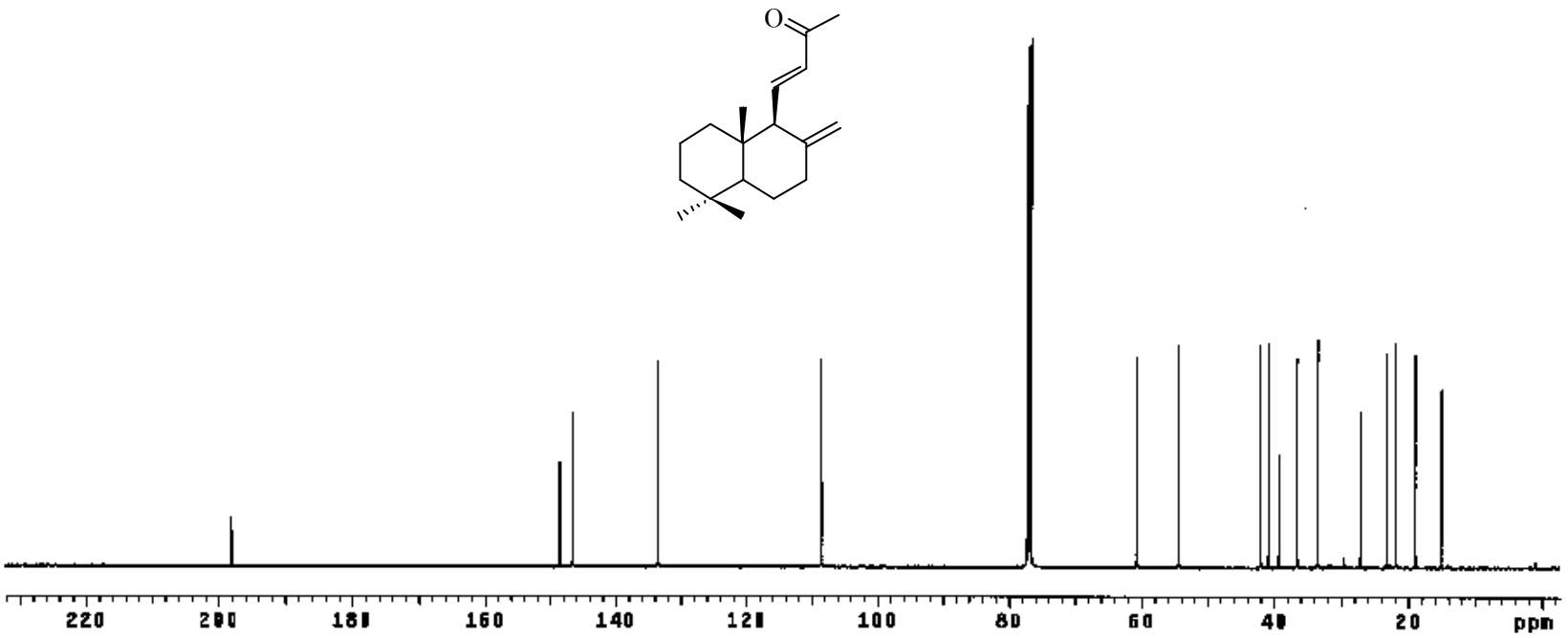

Figure 14 ^{13}C NMR spectrum of compound **2** ($CDCl_3$; 125 MHz)

four quaternary carbons which contain one ketone carbonyl signal at δ 198.14 (C-13), four olefinic carbon signals at δ 148.5 (C-8) and 108.5 (C-17), 146.6 (C-11) and 133.5 (C-12), and four methyl carbon signals at δ 27.1 (C-14), 33.5 (C-18), 21.8 (C-19) and 15.0 (C-20). The structure of side chain (C-11 to C-14) of **2** was deduced from its HMBC spectrum. In the HMBC spectrum (Figure B), the olefinic signal at δ 6.0 (1 H, d, H-12) and methyl signal at δ 2.24 (3H, s, H-14) are correlated with the signal on the ketone group at δ 198.1 (C-13).

The crucial HMBC correlations (Figure 15) included those from C-3, C-4 and C-5 to H-18 and H-19; from C-1, C-5, C-9 and C-10 to H-20; from C-7 and C-9 to H-17; from C-9 to H-12; from C-12 to H-14; from C-13 to H-11, H-12 and H-14. The structure of **2** was therefore proposed as 15,16 bisnorlabda-8(17), 11 dien-13-one, a labdane-type diterpenoid, as shown and was confirmed by comparison with the published data. Compound **2** was first isolated from the rhizomes of *Alpinia speciosa* K. Schum., the seeds of *Alpinia zerumbet* and the rhizomes of *Hedychium acuminatum* (Itokawa et al., 1980; Xu et al., 1996; Weyerstahl et al., 1995). From the present study, this compound was first isolated from the rhizomes of *C. mangga*.

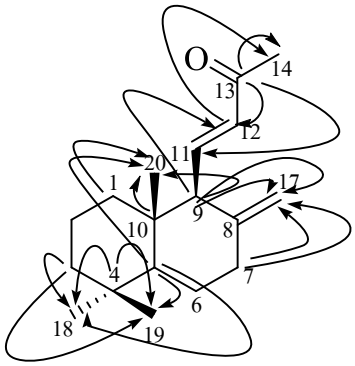

Figure 15 Chemical structure of **2** with crucial HMBC correlation (C → H).

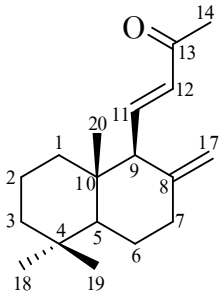

Table 4 ^{1}H and ^{13}C NMR spectral data of compound **2** ($CDCl_3$; 500 MHz for ^{1}H)

positions	^{1}H (mult.; *J* in Hz)	^{13}C (mult.)	^{13}C (mult.; Itokawa et al., 1980)
1ax	2.06 (m)	36.5 (CH_2)	36.6
1eq	2.45 (m)		
2ax	1.38 (m)	18.9 (CH_2)	19.0
2eq	1.49 (m)		
3ax	1.17 (m)	42.0 (CH_2)	42.0
3eq	1.34 (m)		
4	-	33.5 (C)	33.6
5	1.08 (m)	54.4 (CH)	54.4
6ax	1.38 (m)	23.1 (CH_2)	23.2
6eq	1.69 (m)		
7ax	1.0 (m)	40.8 (CH_2)	40.9
7eq	1.15 (m)		
8	-	148.5 (C)	148.5
9	2.41 (d; 10.2)	60.7 (CH)	60.8
10	-	39.3 (C)	39.3
11	6.88 (dd; 15.8, 10.2)	146.6 (CH)	146.5
12	6.0 (d; 15.8)	133.5 (CH)	133.5
13	-	198.1 (C)	197.9
14	2.24 (s)	27.1 (CH_3)	27.2
17ax	4.38 (d; 1.4)	108.5 (CH_2)	108.6
17eq	4.76 (d; 1.4)		

Table 4 (cont.)

positions	^{1}H (mult.; *J* in Hz)	^{13}C (mult.)	^{13}C (mult.; Itokawa et al., 1980)
18	0.87 (s)	33.5 (CH_3)	33.6
19	0.86 (s)	21.8 (CH_3)	21.9
20	0.82 (s)	15.0 (CH_3)	15.1

3.1.2.3 (*E*)-15,15-diethoxylabda-8(17),12-dien-16-al (compound 3)

Compound **3** was obtained as amorphous powder (13 mg) from the hexane fraction using the chromatographic technique (VLC; hexane, hexane/EtOAc, followed by EtOAc/methanol mixture, reversed-phase HPLC; 100% methanol). The molecular formula of **3** was proposed to be $C_{24}H_{40}O_3$ as observable in the EI mass spectrum, which showed a molecular peak at *m/z* 376.3 $[M]^+$, along with 40 protons and 24 carbons observed in the NMR spectra (Table 5). Accordingly, the resulting degree of unsaturation of 5 was determined as one carbonyl, two olefins and two ring systems.

The ^{1}H NMR spectrum of **3** (Figure 16, Table 5) displayed three methyl groups at δ 0.86 (H-18), 0.79 (H-19) and 0.71 (H-20) and two methyl of ethoxy group at δ 1.15 and 1.16 (H-2 and H-2'). The ^{13}C NMR spectrum (Figure 17, Table 5) displayed 24 carbons including those of one aldehyde carbonyl signal at δ 195.0 (C-16) and a olefin composed of four carbons at δ 148.20 (C-8), 108.0 (C-17), 160.2 (C-12) and 138.3 (C-13).

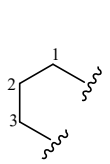

A

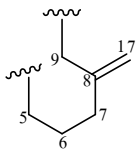

B

The ^{1}H-^{1}H COSY spectrum of **3** indicated that the fragment is similar to A and B of compound **2** which were constructed. Fragment C, C-12 – C-16, differed from that of **2** in that a methylene carbon (δ 24.6, C-11) replaced the olefinic one formerly seen in **2**. HMBC correlations, i.e., from C-3, C-4 and C-5 to H-18 and H-19; from C-1, C-5, C-9 and C-10 to H-20;

from C-7 and C-9 to H-17, helped connecting partial A-B of **3**. The structure of **3** was proposed to be (*E*)-15,15-diethoxylabda-8(17),12-dien-16-al, but is presumably an artifact resulting from a reaction of ethanol used for extraction by comparison of the ^{1}H and ^{13}C spectral of **3** with the previously reported data. Compound **3** was first isolated from the rhizomes of *Aframomum sceptrum* which is also the plant in Zingiberaceae family (Duker-Eshun et al., 2002). However, this is the first report of compound **3** that was isolated from *C. mangga* rhizomes.

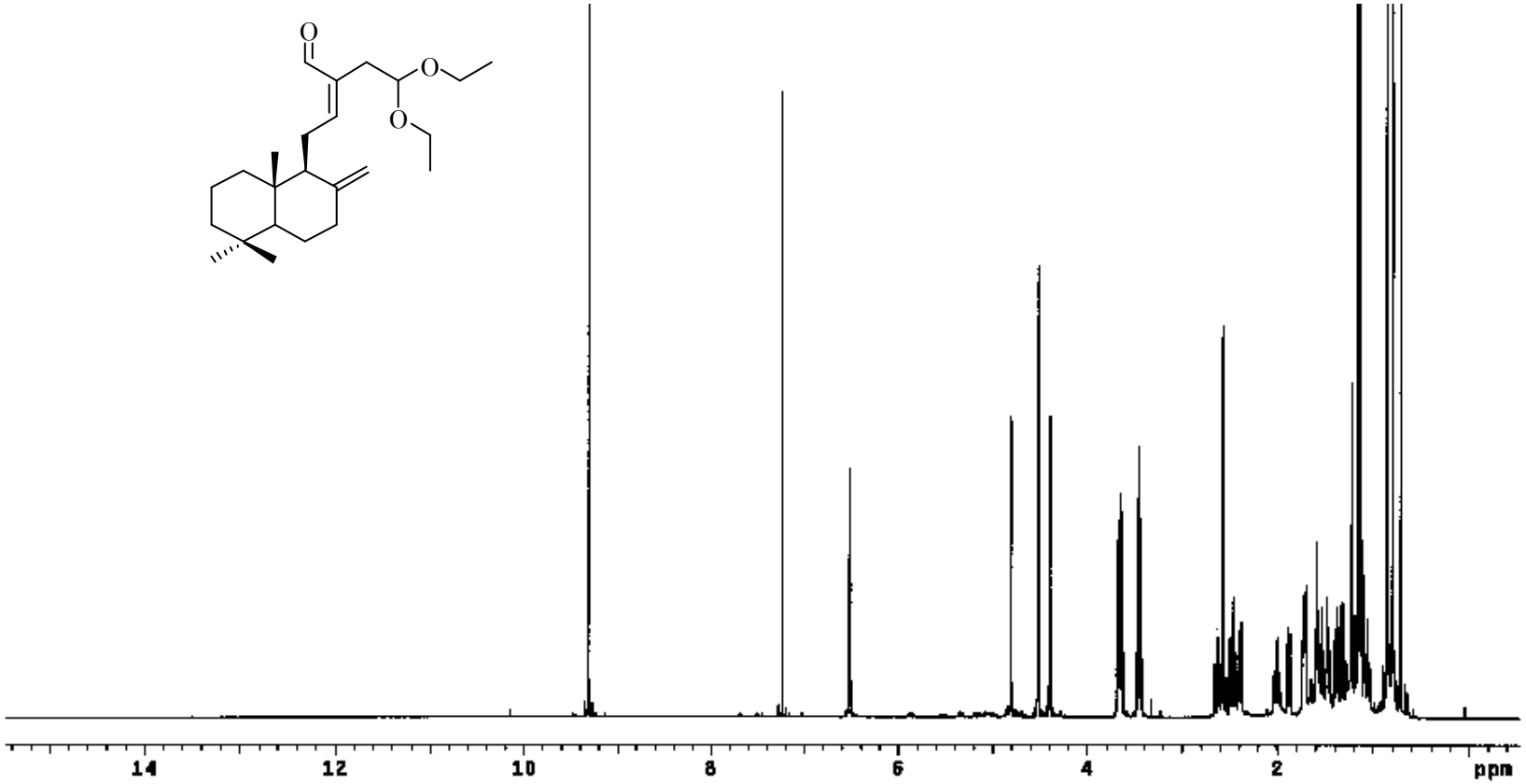

Figure 16 ^{1}H NMR spectrum of compound **3** ($CDCl_3$; 500 MHz)

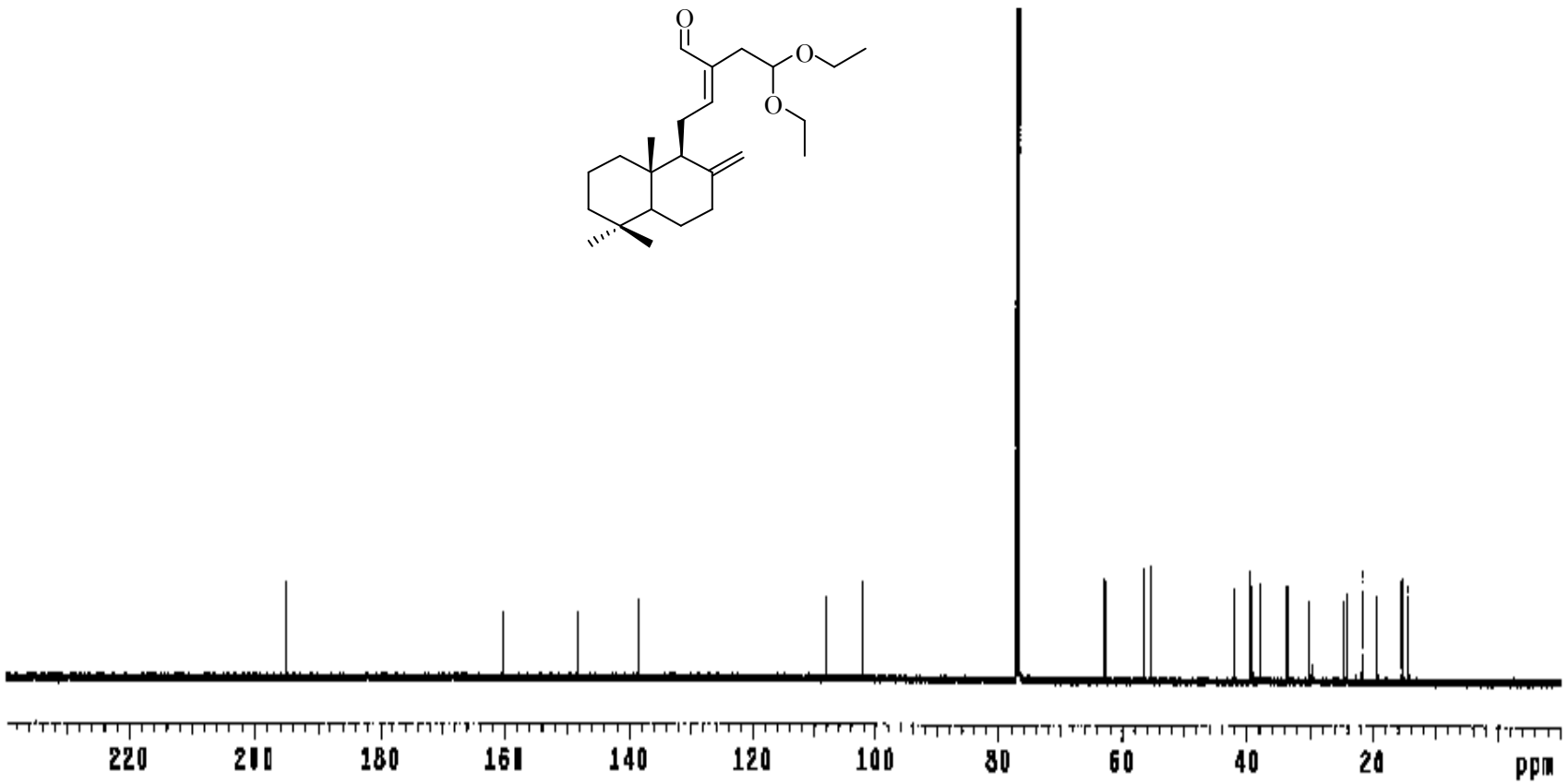

Figure 17 ^{13}C NMR spectrum of compound **3** ($CDCl_3$; 125 MHz)

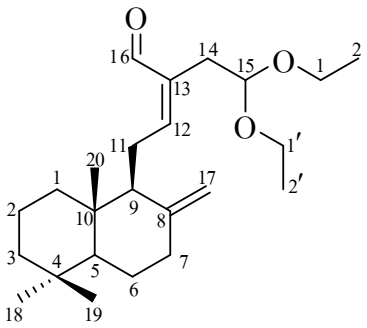

Table 5 ^{1}H and ^{13}C NMR spectral data of compound **3** ($CDCl_3$; 500 MHz for ^{1}H)

positions	^{1}H (mult.; *J* in Hz)	^{13}C (mult.)	^{13}C (mult.; Duker-Eshun et al., 2002)
1ax	1.11 (m)	39.10 (CH_2)	39.1 (CH_2)
1eq	1.70 (m)		
2	1.51 (m)	19.20 (CH_2)	19.10 (CH_2)
3	1.39 (m)	42.00 (CH_2)	41.10 (CH_2)
4	-	33.50 (C)	33.40 (C)
5	1.15 (m)	55.30 (CH)	55.30 (CH)
6ax	1.33 (m)	24.10 (CH_2)	24.0 (CH_2)
6eq	1.73 (m)		
7ax	2.0 (m)	37.80 (CH_2)	37.7 (CH_2)
7eq	2.4 (m)		
8	-	148.2 (C)	148.3 (C)
9	1.87 (d; 10.3)	56.5 (CH)	56.4 (CH)
10	-	39.5 (C)	39.4 (C)
11	2.57 (dd;10.3, 5.8)	24.6 (CH_2)	24.5 (CH_2)
12	6.52 (t; 5.8)	160.2 (CH)	160.3 (CH)
13	-	138.30 (C)	138.40 (C)
14	2.54 (m)	30.2 (CH_2)	30.1 (CH_2)
15	4.52 (t; 5.6)	102.1 (CH)	102.1 (CH)
16	9.31 (s)	195.0 (C)	195.2 (C)
17ax	4.39 (d; 1.4)	108.0 (CH_2)	108.1 (CH_2)

Table 5 (cont.)

positions	^{1}H (mult.; *J* in Hz)	^{13}C (mult.)	^{13}C (mult.; Duker-Eshun et al., 2002)
17eq	4.81 (d; 1.4)		
18	0.86 (s)	33.5 (CH_3)	33.4 (CH_3)
19	0.79 (s)	21.7 (CH_3)	21.5 (CH_3)
20	0.71 (s)	14.3 (CH_3)	14.2 (CH_3)
1, 1'	3.67, 3.45 (m)	62.7, 62.8 (CH_2)	62.7, 62.8 (CH_2)
2, 2'	1.15, 1.16 (t; 6.9)	15.2, 15.3 (CH_3)	15.1, 15.2 (CH_3)

3.1.2.4 Bisdemethoxycurcumin (1,7-bis (4-Hydroxyphenyl)-1,6-heptadiene-3,5-dione, compound 4)

Compound **4** was obtained as yellow needles (6 mg) from the ethanol extract of *Curcumar longa* rhizomes using the chromatographic technique (CC; 100% chloroform). This compound was further used to test for anti-inflammatory effect against NO, PGE_2 production as well as iNOS and COX-2 gene expressions.

Compound **4** has a molecular formula of $C_{19}H_{16}O_4$, molecular weight is 308. ^{1}H NMR (CD_3OD, 500 MHz) δ (ppm): the ^{1}H NMR spectrum of **4** (Figure 18, Table 6) showed four substituted benzene protons, signal at 6.81 (2H, d, J = 8.46 Hz) and 7.48 (2H, d, J = 8.46 Hz), two trans olefins at 7.56 and 6.58 (H7-H8 and H12-H13; d, J = 15.7 Hz) and two protons at 5.77 (s), 5.84 (s). These data indicated that **4** was bisdemethoxycurcumin and was further confirmed by comparison with spectral analysis data reported in the literatures (Gupta et al., 1999; Kosuge et al., 1985; Inoue et al., 2008; Péret-Almeida et al., 2005; Scotter, 2009).

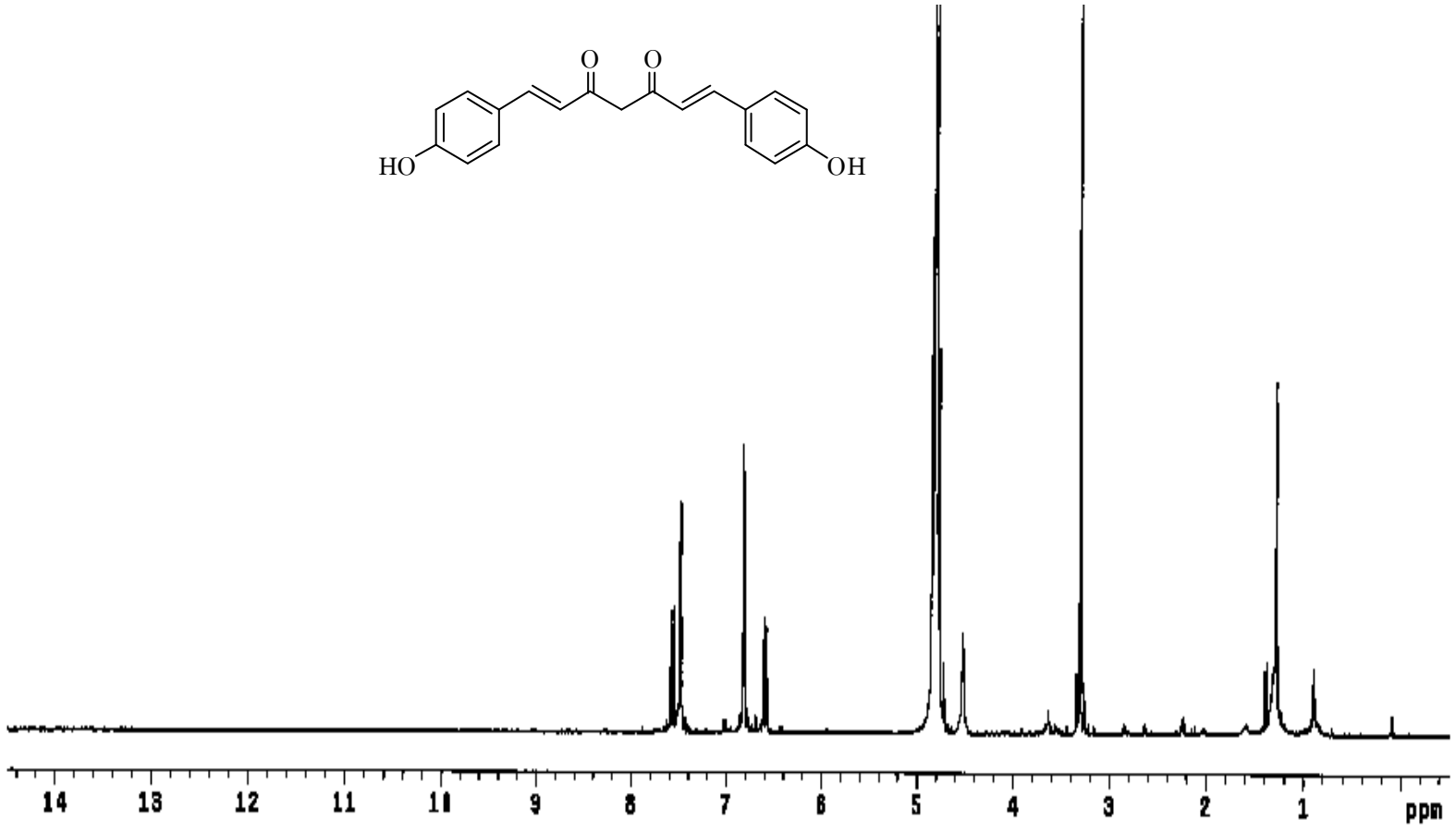

Figure 18 ^{1}H NMR spectrum of compound **4** (CD_3OD; 500 MHz)

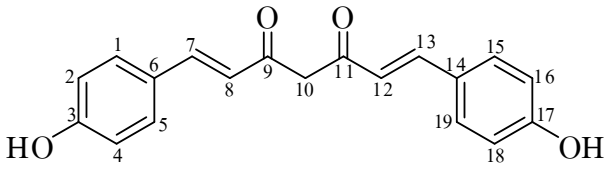

Table 6 ^{1}H spectral data of compound **4** (CD_3OD; 500 MHz for ^{1}H) and reference

positions	^{1}H (mult.; *J* in Hz)	^{1}H (mult.; *J* in Hz, Jayaprakasha, 2002)
1, 5	6.81 (d; 8.4)	6.84 (d; 8.2)
2, 4	7.48 (d; 8.4)	7.56 (d; 8.2)
3, 17	-	-
16, 18	7.48 (d; 8.4)	7.56 (d; 8.2)
15, 19	6.81 (d; 8.4)	6.84 (d; 8.2)
6, 14	-	-
7, 13	7.56 (d; 15.7)	7.56 (d; 15.9)
8, 12	6.58 (d; 15.7)	7.56 (d; 15.9)
9	-	16.4 (bs)
10	4.51 (s)	6.03 (s)
11	-	-

3.2 Anti-inflammatory activity tests

3.2.1 Effect of fractions from *C. mangga* rhizomes and isolated compounds on nitric oxide production

The accumulated nitrite was determined by the Griess reaction in culture medium. NO production was detected in RAW 264.7 cells stimulated by LPS in the presence or absence of samples for 48 h. LPS (100 μg/ml) significantly increased the concentration of nitrite as compared to basal level without LPS.

Ethanol extract, hexane-, chloroform-, ethyl acetate- and water fractions from *C. mangga* rhizomes were investigated for their inhibitory activities against LPS induced NO

production in RAW 264.7 cell lines. Among these species, the chloroform fraction exhibited the most potent inhibitory activity with an IC_{50} value of 2.1 μg/ml, followed by the hexane fraction (IC_{50} = 3.8 μg/ml), EtOAc fraction (IC_{50} = 23.5 μg/ml) and water fraction (IC_{50} > 100 μg/ml), respectively (Table 7).

The chloroform fraction was chromatographed further to obtain demethoxy-curcumin (**1**), the hexane fraction were obtained 15,16 bisnorlabda-8(17), 11 dien-13-one (**2**) and (*E*)-15,15-diethoxylabda-8(17),12-dien-16-al (**3**). Bisdemethoxycurcumin (**4**), derivative of **1**, isolated from the rhizomes of *C. longa*, was also tested for anti-inflammatory effect against NO production. The result indicated that compound **3** ((*E*)-15,15-diethoxylabda-8(17),12-dien-16-al) exhibited the highest activity against NO production with an IC_{50} value of 9.4 μM, followed by **1** (IC_{50} = 12.1 μM) and **2** (IC_{50} = 30.3 μM), respectively (Table 8). It was found that **4** also possessed marked activity with an IC_{50} value of 16.9 μM. Compounds **1** (IC_{50} = 12.1 μM) and **3** (IC_{50} = 9.4 μM) exhibited higher effect than indomethacin (IC_{50} = 14.5 μM) and L-NA, a positive control (NO synthase inhibitor, IC_{50} = 62.7 μM), whereas compound **4** (IC_{50} = 16.9 μM) possessed comparable activity to that of indomethacin (IC_{50} = 14.5 μM) and higher effect than that of L-NA (IC_{50} = 62.7 μM) but lower than that of CAPE, NF-ΚB inhibitor (IC_{50} = 5.2 μM). Therefore, it is possible that compounds **1**-**4** may inhibit NO production through the inhibition of NO synthase and NF-ΚB transcription factor.

The previous study reported that demethoxycurcumin and bisdemethoxycurcumin inhibited LPS-stimulated NO production in a dose-dependent manner, the IC_{50} values were 6.9 and 8.4 μM, respectively (Guo et al., 2008). This result is concurrent with our study that demethoxycurcumin (**1**, IC_{50} = 12.1 μM) exhibited higher inhibitor effect against NO production than bisdemethoxycurcumin **4** (IC_{50} = 16.9 μM).

Compound **2** was first isolated from the rhizomes of *Alpinia speciosa* K. Schum., the seeds of *Alpinia zerumbet* and the rhizomes of *Hedychium acuminatum* which are the plants in Zingiberaceae family (Itokawa et al., 1980; Xu et al., 1996; Weyerstahl et al., 1995) and compound **3** was first isolated from the fruits of *Aframomum sceptrum* which is also the plant in Zingiberaceae family (Duker-Eshun et al., 2002). Compound **2** has never been reported for its biological activity whereas **3** had been reported only its moderate inhibition of growth of *Plasmodium falciparum* strain 3D7 (Duker-Eshun et al., 2002). Therefore, this is the first report

on biological study of compounds **2** and **3** against NO production. Moreover, compounds **2** and **3** were first isolated from *C. mangga* rhizomes from the present study.

3.2.2 Effect of isolated compounds on cell viability

The effect of compounds on RAW264.7 cell viability were determined by MTT assay. The survival of cells was not significantly affected by treatment with compounds **1**, **2, 3** and **4** at concentrations ranging from 3 to 30 μM. However, higher doses of the compounds **1**, **3** and **4** (100 μM) except that of compound **2** decreased cell survival (< 80%).

3.2.3 Effect of isolated compounds on prostaglandin E_2 production

The amounts of PGE_2 in the culture supernatants were determined by ELISA assay. RAW 264.7 cells were stimulated with 75 μg/ml of LPS and the production of PGE_2 was increased by the enzymatic reaction of COX-2. When compounds **1**-**4** were added to the culture media at the time of stimulation of cells, they inhibited the production of PGE_2 in dose-dependent manners. Inhibitory potency against PGE_2 production by **1** was the strongest, followed by **4, 3** and **2**, whose IC_{50} values were found to be 4.5, 5.6, 35.3 and 42.5 μM, respectively. Indomethacin, a positive control, was found to possess an IC_{50} value of 0.4 μM (Table 9). Therefore compounds **1**-**4** may inhibit NO synthase and COX enzymes production.

Table 7 Inhibition on NO production[a] of fractions from *C. mangga* rhizomes.

Sample	% inhibition at various concentrations (μg/ml)					IC_{50} (μg/ml)
	0	3	10	30	100	
EtOH extract	0.0 ± 3.5	-15.0 ± 3.7	40.3 ± 10.7	93.6 ± 3.7**	-	11.8
Hexane fraction	0.0 ± 3.6	26.1 ± 2.4	65.1 ± 2.8**	89.5 ± 1.6**	-	3.8
Chloroform fraction	0.0 ± 3.6	34.2 ± 2.4**	84.0 ± 1.6**	100.7 ± 2.3**	-	2.1
EtOAc fraction	0.0 ± 3.0	17.4 ± 3.6	27.1 ± 2.8	60.6 ± 1.7**	-	23.5
Water fraction	0.0 ± 3.0	-	-	-	40.0 ± 1.5**	>100
L-Nitroarginine (L-NA)	0.0 ± 9.9	11.7 ± 4.6	20.2 ± 5.9	34.7 ± 1.8**	71.6 ± 2.6**	61.8 (13.5)[c]
Caffeic acid phenethylester (CAPE)	0.0 ± 9.9	30.7 ± 3.2*	68.6 ± 3.4**	98.7 ± 1.2[b]**	98.9 ± 2.1[b]**	5.6 (1.4)[c]

Statistical significance, *p<0.05, **p<0.01

[a]Each value represents mean ± S.E.M. of four determinations.

[b]Cytotoxic effect was observed.

[c]Values in parenthesis are IC_{50} (μg/ml)

Table 8 Inhibition on NO production[a] of compounds isolated from *C. mangga* rhizomes.

Compound	% inhibition at various concentrations (μM)					IC_{50} (μM)
	0	3	10	30	100	
Demethoxycurcumin (**1**)	0.0 ± 4.9	9.2 ± 5.7	31.7 ± 4.4**	93.3 ± 4.9**	110.0 ± 3.6[b]**	12.1
15,16 bisnorlabda-8(17), 11 dien-13-one (**2**)	0.0 ± 4.9	16.7 ± 3.9	39.2 ± 5.5**	49.2 ± 3.7**	65.0 ± 1.0**	30.3
(*E*)-15,15-diethoxylabda-8(17),12-dien-16-al (**3**)	0.0 ± 4.9	37.8 ± 1.3**	41.9 ± 2.9**	67.0 ± 3.0**	93.1 ± 4.5[b]**	9.4
Bisdemethoxycurcumin (**4**)	0.0 ± 4.9	1.7 ± 3.4	20.0 ± 2.4**	73.3 ± 1.4**	107.5 ± 3.5[b]**	16.9
Indomethacin	0.0 ± 3.6	14.5 ± 2.7	30.2 ± 1.6**	47.6 ± 2.3**	80.3 ± 1.5**	14.5
L-Nitroarginine (L-NA)	0.0 ± 3.9	-	24.1 ± 2.1	29.9 ± 1.8*	70.4 ± 2.5**	62.7
Caffeic acid phenethylester (CAPE)	0.0 ± 3.9	26.1 ± 2.9	85.6 ± 2.1**	88.7 ± 1.6[b]**	93.8 ± 3.0[b]**	5.2

Statistical significance, *p<0.05, **p<0.01

[a]Each value represents mene ± S.E.M. of four determinations.

[b]Cytotoxic effect was observed.

Table 9 PGE_2 inhibitory effects of compounds[a] from *C. mangga* rhizomes.

Compounds	% inhibition at various concentrations (μM)								IC_{50} (μM)
	0	0.1	0.3	1	3	10	30	100	
Demethoxycurcumin (**1**)	0.0 ± 2.0	-	-	23.4 ± 1.1**	31.3 ± 0.8**	71.5 ± 0.5**	74.6 ± 0.2**	75.5 ± 0.3**	4.5
15,16 bisnorlabda-8(17), 11 dien-13-one (**2**)	0.0 ± 2.0	-	-	-	-	19.5 ± 2.3**	46.8 ± 1.0**	65.1 ± 0.3**	42.5
(*E*)-15,15-diethoxylab- da-8(17),12-dien-16-al (**3**)	0.0 ± 2.0	-	-	-	38.6 ± 1.5 **	41.75 ± 2.5**	42.87 ± 4.3**	60.36 ± 0.5**	35.3
Bisdemethoxycurcumin (**4**)	0.0 ± 2.0	-	-	30.5 ± 0.5**	34.6 ± 0.2 **	68.8 ± 0.2**	77.0 ± 0.2**	79.5 ± 0.6 **	5.6
Indomethacin	0.0 ± 2.0	38.4 ±0.8**	48.7 ±0.4**	52.7 ± 0.7**	74.6 ± 0.1**	76.9 ± 0.3**	77.2 ± 0.1**	78.1 ± 0.2**	0.4

Statistical significance, $^{**}p<0.01$

[a]Each value represents mean ± S.E.M. of four determinations.

3.2.4 Effect of isolated compounds on the level of mRNA expression of iNOS and COX-2

In order to know the anti-inflammatory mechanism of compounds **1**-**4** on the gene expression of proinflammatory enzymes, the mRNA expression of iNOS and COX-2 was determined by RT-PCR. RAW 264.7 cells treated with LPS (75 μg/ml) induced the iNOS and COX-2 mRNA expression while their mRNA was not detectable in unstimulated macrophages. RT-PCR analysis showed that demethoxycurcumin (**1**), (*E*)-15,15-diethoxylabda-8(17),12-dien-16-al (**3**) and bisdemethoxycurcumin (**4**) inhibited LPS-induced iNOS and COX-2 mRNA expression while 15,16 bisnorlabda-8(17), 11 dien-13-one (**2**) specially inhibited iNOS mRNA expression (Figure 19-22). Furthermore, demethoxycurcumin and bisdemethoxycurcumin showed cytotoxic effects at the concentration of 100 μM which could be observed from the DNA fragments of β-actin of these two compounds that were less than those of other concentrations (Figure 19, 22). Therefore, the suitable concentrations of compounds **1** and **4** should be concerned for pharmaceutical preparation for treatment of inflammatory-related diseases. For indomethacin, a clinically used drug, it mainly inhibited both iNOS and COX-2 mRNA expression (Figure 23).

It has been reported that not only proinflammatory cytokines but also proinflammatory mediators, such as PGE_2 and NO generated largely by overexpression of COX-2 and iNOS mRNA, respectively and also play pivotal roles in tissue injuries (Jin et al., 2007; Vane et al., 1994; Tetsuka et al., 1994). The gene expression of these proinflammatory enzymes and cytokines have been shown to be regulated by nuclear factor kappa B (NF-κB) (Nanji et al., 2003; Kabouridis et al., 2002; Farombi et al., 2009).

Activation of a transcription factor NF-κB is associated with inflammation, increasing cellular proliferation and increasing programmed cell death. Moreover, there is an evidence for the role of NF-κB activation leading cell to apoptosis and activating a rapid progression of gene expression (Ghosh and Karin, 2002; Li et al., 1999; Aggarwal et al., 2003). Thus the blockage of the transcriptional activity of NF-κB in the microglial nucleus can suppress the expression of iNOS, COX-2 and pro-inflammatory cytokines that offers a potentially effective therapeutic approach to mitigate the progression of tissue inflammatory diseases (Petrova et al.,

1999; Ye and Johnson, 2001; Roshak et al., 1996; Schmedtje et al., 1997; Xie et al., 1994). Recent studies have also shown that NO generated by iNOS stimulates the synthesis of inflammatory prostaglandins by activating COX-2 (Thomas and Ramwell, 1998; Lowenstein et al., 1992). Thus the inhibition of NO pathway and/or the suppression of the overexpression of iNOS and COX-2 mRNA may offer a potentially effective therapeutic approach to mitigate the progression of tissue inflammatory diseases.

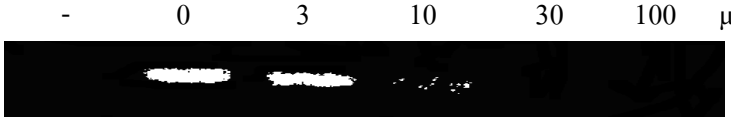

Figure 19 Effect of demethoxycurcumin (**1**) at various concentrations (0, 3, 10, 30, 100 μM) on mRNA expression of iNOS, COX-2 and β-actin by LPS-induced NO and PGE_2 production in RAW 264.7 cells.

RAW 264.7 cells were cultured in the presence of LPS (75 μg/ml) with or without demethoxycurcumin for 20 h. At the end of the incubation time, cells were lysed and total RNA was prepared for the RT-PCR analysis of mRNA expression. iNOS (580bp) and COX-2 (860bp) were detected by agarose gel electrophoresis. PCR of β-actin was performed to control similar initial cDNA content of samples.

(-) = LPS (-), sample (-)

(0) = LPS (+), sample (-)

3-100 = LPS (+), sample (+)

Figure 20 Effect of 15,16 bisnorlabda-8(17), 11 dien-13-one (**2**) at various concentrations (0, 3, 10, 30, 100 μM) on mRNA expression of iNOS, COX-2 and β-actin by LPS-induced NO and PGE_2 production in RAW 264.7 cells.

RAW 264.7 cells were cultured in the presence of LPS (75 μg/ml) with or without 15,16 bisnorlabda-8(17), 11 dien-13-one for 20 h. At the end of the incubation time, cells were lysed and total RNA was prepared for the RT-PCR analysis of mRNA expression. iNOS (580bp) and COX-2 (860bp) were detected by agarose gel electrophoresis. PCR of β-actin was performed to control similar initial cDNA content of samples.

(-) = LPS (-), sample (-)

(0) = LPS (+), sample (-)

3-100 = LPS (+), sample (+)

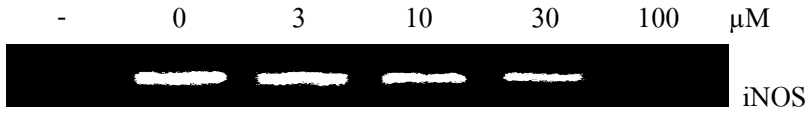

Figure 21 Effect of (*E*)-15,15-diethoxylabda-8(17),12-dien-16-al (**3**) at various concentrations (0, 3, 10, 30, 100 μM) on mRNA expression of iNOS, COX-2 and β-actin by LPS-induced NO and PGE_2 production in RAW 264.7 cells.

RAW 264.7 cells were cultured in the presence of LPS (75 μg/ml) with or without (*E*)-15,15-diethoxylabda-8(17),12-dien-16-al for 20 h. At the end of the incubation time, cells were lysed and total RNA was prepared for the RT-PCR analysis of mRNA expression. iNOS (580bp) and COX-2 (860bp) were detected by agarose gel electrophoresis. PCR of β-actin was performed to control similar initial cDNA content of samples.

(-) = LPS (-), sample (-)

(0) = LPS (+), sample (-)

3-100 = LPS (+), sample (+)

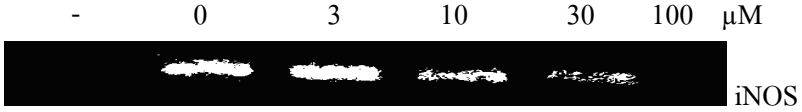

Figure 22 Effect of bisdemethoxycurcumin (**4**) at various concentrations (0, 3, 10, 30, 100 μM) on mRNA expression of iNOS, COX-2 and β-actin by LPS-induced NO and PGE_2 production in RAW 264.7 cells.

RAW 264.7 cells were cultured in the presence of LPS (75 μg/ml) with or without bisdemethoxycurcumin for 20 h. At the end of the incubation time, cells were lysed and total RNA was prepared for the RT-PCR analysis of mRNA expression. iNOS (580bp) and COX-2 (860bp) were detected by agarose gel electrophoresis. PCR of β-actin was performed to control similar initial cDNA content of samples.

(-) = LPS (-), sample (-)

(0) = LPS (+), sample (-)

3-100 = LPS (+), sample (+)

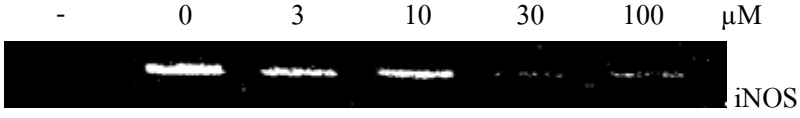

Figure 23 Effect of indomethacin at various concentrations (0, 3, 10, 30, 100 μM) on mRNA expression of iNOS, COX-2 and β-actin by LPS-induced NO and PGE_2 production in RAW 264.7 cells.

RAW 264.7 cells were cultured in the presence of LPS (75 μg/ml) with or without indomethacin for 20 h. At the end of the incubation time, cells were lysed and total RNA was prepared for the RT-PCR analysis of mRNA expression. iNOS (580bp) and COX-2 (860bp) were detected by agarose gel electrophoresis. PCR of β-actin was performed to control similar initial cDNA content of samples.

(-) = LPS (-), sample (-)

(0) = LPS (+), sample (-)

3-100 = LPS (+), sample (+)

CHAPTER 4

CONCLUSIONS

Chemical investigation of the *Curcuma mangga* rhizomes, led to the isolation of three active compounds including demethoxycurcumin (**1**), 15,16 bisnorlabda-8(17), 11 dien-13-one (**2**) and (*E*)-15,15-diethoxylabda-8(17),12-dien-16-al (**3**) whereas bisdemethoxycurcumin (**4**) was isolated from ethanol extract of *Curcuma longa* rhizomes. The structure elucidations were confirmed by spectroscopic techniques, physical properties and comparing with the reported literatures. This is the first report of compounds **2** and **3** that were isolated from *C. mangga* rhizomes. These two compounds have never been reported for their biological activity against inflammation. Therefore, this is also the first report on the anti-inflammatory properties of compounds **2** and **3** against NO and PGE_2 production as well as mRNA expression of iNOS and COX-2 genes.

The investigation of anti-inflammatory activity of various extracts from *C. mangga* rhizomes against LPS-induced NO production in RAW 264.7 cell lines was found that the chloroform fraction exhibited the most potent inhibitory activity, followed by the hexane, EtOAc and water fractions, respectively.

The investigation of anti-inflammatory activity of isolated compounds showed that compound **3** exhibited the highest activity against NO production, followed by compounds **1** and **2**, respectively. Compound **4**, also possessed marked NO inhibitory activity. Compounds **1** and **3** exhibited higher effect than indomethacin and L-NA, positive controls, whereas compound **4** possessed comparable activity to that of indomethacin and higher effect than that of L-NA but lower than that of CAPE. The inhibitory effect of compounds **1**-**4** on LPS-induced PGE_2 production, showed that compound **1** exerted the strongest inhibitory efficacy, followed by compounds **4, 3** and **2**, respectively. The mechanism in transcriptional level revealed that compounds **1**, **3** and **4** down-regulated the mRNA expressions of iNOS and COX-2 genes in dose-dependent manners, whereas compound **2** down-regulated only the expression of iNOS mRNA. Furthermore, demethoxycurcumin and bisdemethoxycurcumin showed cytotoxic effects

at 100 μM which could be observed from the DNA fragments of β-actin of these two compounds.

These results suggest that *C. mangga* and its compounds exert anti-inflammatory activity and has potential to be developed as a pharmaceutical preparation for treatment of inflammatory-related diseases in an appropriate concentrations. The main anti-inflammatory mechanism of the active compounds from *C. mangga* rhizomes was found to inhibit NO and PGE_2 production through the inhibition of iNOS and COX-2 genes. The present study also supports the traditional use of *C. mangga* rhizomes for treatment of inflammatory-related diseases.

REFERENCES

Abas, F., Lajis, N.H., Shaari, K., Israf, D.A., Stanslas, J., Yusuf, U.K. and Raoft, S.M., 2005. A labdane diterpene glucoside from the rhizomes of *Curcuma mangga*. Journal of Natural Products. 68: 1090-1093.

Abas, F., Lajis, N.H., Israf, D.A., Khozirah, S. and UmiKalsom, Y. 2006. Antioxidant and nitric oxide inhibition activities of selected Malay traditional vegetables. Food Chemistry. 95: 566-573.

Aggarwal, B.B., Kumar, A. and Bharti, A.C. 2003. Anticancer potential of curcumin: preclinical and clinical studies. Anticancer Research. 23: 363-398.

Baldwin, A.S., Jr. 1996. The NF-κB and IκB Proteins: new discoveries and insights. Annual Review of Immunology. 14: 649-681.

Bredt, D.S. and Snyder, S.H. 1990. Isolation of nitric oxide synthetase, a calmodulin-requiring enzyme. Proceedings of the National Academy of Sciences. 87: 682-685.

Brouet, I. and Ohshima, H. 1995. Curcumin, an anti-tumour promoter and anti-inflammatory agent, inhibits induction of nitric oxide synthase in activated macrophages. Biochemical and Biophysical Research Communications. 206: 533-540.

Chainani-Wu, N. 2003. Safety and anti-inflammatory activity of curcumin: a component of tumeric (*Curcuma longa*). Journal of Alternative and Complementary Medicine. 9:161-168.

Chan, E.W.C., Lim, Y.Y.,Wong, L.F., Lianto, F.S., Wong, S.K., Lim, K.K., Joe, C.E. and Lim, T.Y. 2008. Antioxidant and tyrosinase inhibition properties of leaves and rhizomes of ginger species. Food Chemistry. 109: 477-483.

Cho, Y-C., Kim, H.J., Kim Y-J., Lee, K.Y., Choi, H.J., Lee, I-S. and Kang, B.Y. 2008. Differential anti-inflammatory pathway by xanthohumol in IFN-γ and LPS-activated macrophages. International Immunopharmacology. 8: 567-573.

Chung, J.W., Noh, E.j., Zhao, H.L., Sim, J-S., Ha, Y.W., Shin, E.M., Lee, E.B., Cheong, C.S. and Kim, Y.S. 2008. Anti-inflammatory activity of prosapogenin methyl ester of platycodin D via nuclear factor-kappa B pathway inhibition. Biological and Pharmaceutical Bulletin. 31: 2114-2120.

Cobb, J.P., Buchman, T.G., Karl, I.E. and Hotchkiss R.S. 2000. Molecular biology of multiple organ dysfunction syndrome: injury, adaptation, and apoptosis. Surgical Infections. 1: 207-215.

Coleman, J.W. 2001. Nitric oxide in immunity and inflammation. International Immunopharmacology. 1: 1397-1406.

Cother, E. J. 1987. A note on the use of Merckoquant test strips for detection of nitrate reduction in plant pathogenic bacteria. Plant Pathology. 36: 374-376.

Crawford, N. M. 2006. Mechanisms for nitric oxide synthesis in plants. Journal of Experimental Botany. 57: 471-478.

Cummings, K. L. and Tarleton, R. L. 2004. Inducible nitric oxide synthase is not essential for control of *Trypanosoma cruzi* infection in mice. Infection and Immunity. 72: 4081-4089.

Du, Z-Y., Liu, R-R., Shao, W-Y., Mao, X-P., Ma, L., Gu, L-Q., Huang, Z-S. and Chan, A.S.C. 2006. α-Glucosidase inhibition of natural curcuminoids and curcumin analogs. European Journal of Medicinal Chemistry. 41: 213-218.

Duker-Eshun, G., Jaroszewski, J.W., Asomaning, W.A., Oppong-Boachie, F., Olsen, C.E. and Christensen, S.B. 2002. Anti-plasmodial activity of labdanes from *Aframomum latiflolium* and *Aframomum sceptum*. Planta Medica. 68: 642-644.

Eun-Kyoung, S., Cho, H., Jeong-Sik, K., Na-Young, K., Nyeon-Hyeong, A., Jeong-Ah, k., Seung-Ho, L. and Youn-Chul, K. 2001. Diarylheptanoids with free radical scavenging and hepatoprotective activity *in vitro* from *Curcuma longa.* Planta medica. 67; 876-877.

Farah, M.H. and Samuelsson, G. 1991. Pharmacologically active phenylpropanoids from *Senra incana*. Planta Medica. 58: 14-18.

Farombi, E.O., Shrotriya, S. and Surh, Y-J. 2009. Kolaviron inhibits dimethyl nitrosamine-induced liver injury by suppressing COX-2 and iNOS expression via NF-κB and AP-1. Life Sciences. 84: 149-155.

Feghali, C.A. and Wright, T.M. 1997. Cytokine in acute and chronic inflammation. Frontiers in Bioscience. 2: 12-26.

Foegh, M.L., Hecker, M. and Ramwell, P.W. 1998. The eicosanoids: prostaglandins, thromboxanes, leukotrienes, and related compounds. Katzung, B.G. (ed) Basic and clinical pharmacology (7th ed), Stamford, USA. Appleton and lange. 304-318.

Gafner, S., Lee, S-K., Cuendet, M., Barthélémy, S., Vergnes, L., Labidalle, S., Mehta, R.G., Boone, C.W. and Pezzuto, J.M. 2004. Biologic evaluation of curcumin and structural derivatives in cancer chemoprevention model systems. Phytochemistry. 65: 2849-2859.

Ghosh, S. and Karin, M. 2002. Missing pieces in the NF-κB puzzle. Cell. 109: 81-96.

Guevara, I., Iwanejko, J.,Dembin´ska-Kiec, A., Pankiewicz, J., Wanat, A., Anna, P., Gołąbek, I., Bartus, S., Malczewska-Malec, M. and Szczudlik, A. 1998. Determination of nitrite / nitrate in human biological material by the simple Griess reaction. Clinica Chimica Acta. 274: 177-188.

Guo, L.Y., Cai, X.F., Lee, J.J., Kang, S.S., Shin, E.M., Zhou, H.Y., Jung, J.W. and Kim, Y.S. 2008. Comparison of suppressive effects of demethoxycurcumin and bisdemethoxycurcumin on expressions of inflammatory mediators *in vitro* and *in vivo.* Archives of Pharmacal Research. 31: 490-496.

Gupta, A. P., Gupta, M. M. and Kumar, S. 1999. Simultaneous determination of curcuminoids in *Curcuma* samples using high performance thin layer chromatography. Journal of Liquid Chromatography and Related Technologies. 22: 1561-1569.

Gould, B.E. 2002. Inflammation and healing. Gould B.E. (ed.). Pathophysiology of the health professions (2nd ed), Philadelphia, USA. W.B. Saunders Company. 12-33.

Han, S-S., Keum, Y-S., Seo, H-J. and Surh, Y-J. 2002. Curcumin suppresses activation of NF-κB and AP-1 induced by phorbol ester in cultured human promyelocytic leukemia cells. Journal of Biochemistry and Molecular Biology. 35: 337-342.

Inoue, K., Nomura, C., Ito, S., Nagatsu, A., Hino, T. And Oka, H. 2008. Purification of curcumin, demethoxycurcumin, and bisdemethoxycurcumin by high-speed countercurrent chromatography. Journal of Agricultural and Food Chemistry. 56: 9328–9336.

Itokawa, H., Morita, M. and Mihashi, S. 1980. Labdane and bisnorlabdane type diterpenes from *Alpinia speciosa* K. Schum. Chemical and Pharmaceutical Bulletin. 28: 3452-3454.

Jayaprakasha, G.K., Jagan, L., Rao, M. and Sakariah, K.K. 2002. Improved HPLC method for the determination of curcumin, demethoxycurcumin and bisdemethoxycurcumin. Journal of Agricultural and Food Chemistry. 50: 3668-3672.

Jin, C-Y., Lee, J-D., Park, C., Choi, Y.H. and Kim, G-Y. 2007. Curcumin attenuates the release of pro-inflammatory cytokines in lipopolysaccharide-stimulated BV2 microglia. Acta Pharmacologica Sinica. 10: 1645-1651.

Kabouridis, P.S., Hasan, M., Newson, J., Gilroy, D.W. and Lawrence, T. 2002. Inhibition of NF-κB activity by a membrane-transducing mutant of IκBα. The Journal of Immunology. 169: 2587-2593.

Kiat, T.S. and Pippen, R. 2006. Screening of selected Zingiberaceae extracts for dengue-2 virus protease inhibitory activities. Sunway Academic Journal. 3: 1-7.

Kim, J.H., Shim, J.S., Lee, S-K., Kim, K-W., Rha, S.Y., Chung, H.C. and Kwon, H.J. 2002. Microarray-based analysis of anti-angiogenic activity of demethoxycurcumin on human umbilical vein endothelial cells: crucial involvement of the down-regulation of matrix metalloproteinase. Japanese Journal of Cancer Research. 93: 1378-1385.

Kim, S.S., Oh, O-J., Min, H-Y., Park, E-J., Kim, Y., Park, H.J., Han, Y.N. and Lee, S.K. 2003. Eugenol suppresses cyclooxygenase-2 expression in lipopolysaccharide-stimulated mouse macrophage RAW264.7 cells. Life Sciences. 73: 337-348.

Kiuchi, F., Goto, Y., Sugimoto, N., Konda, K. And Tsuda, T. 1993. Nematocidal activity of turmeric: synergistic action of curcuminoids. Chemical and Pharmaceutical Bulletin. 41: 1640-1643.

Kone, B.C., Kuncewicz, T., Zhang, W and Yu, Z-Y. 2003. Protein interactions with nitric oxide synthases: controlling the right time, the right place, and the right amount of nitric oxide. American Journal of Physiology Renal Physiology. 285: 178-190.

Kosuge, T., Ishida, H. and Yamazaki, H. 1985. Studies on active substances in the herbs used for oketsu ("Stagnant Blood") in Chinese medicine. III. On the anticoagulative

principles in Curcumae rhizome. Chemical and Pharmaceutical Bulletin. 33: 1499-1502.

Kumar, V. 2005. Robbins and cotran pathologic basis of disease http:// www.mdconsult.com/ das/book/body/156276671-4/0/2060/24.html (Accessed: 2008, July 29).

Kumar, V., Abbas, A.S., Fausto, N. and Mitchell, R.N. 2007. Acute and chronic inflammation. Kumar, V., Abbas, A.S., Fausto, N. And Mitchell, R.N. (eds). Robbins basic pathology (8^{th} ed), Philadelphia, USA. Elsevier Saunders. 31-58.

Lantz, R.C., Chen, G.J., Sólyom, A.M., Jolad, S.D. and Timmewmann, B.N. 2005. The effect of turmeric extracts on inflammatory mediator production. Phytomedicine. 12: 445-452.

Lantz, R.C., Chen, G.J., Sarihan, M., Sólyom, A.M., Jolad, S.D. and Timmewmann, B.N. 2007. The effect of extracts from ginger rhizome on inflammatory mediator production. Phytomedicine. 14: 123-128.

Lestariana, W., Mubarika, S. and Sismindari. 2003. Identification and test of active protein resemble Ribosome-inactivating proteins (RIPS) on *Kaempferia rotunda* Linn. Berkala llmu Kedokteran. 35: 189-196.

Li, Z. and Nabel, G.J. 1997. A new member of the IκB protein family, IκBε, inhibits RelA (p65)-mediated NF-κB transcription. Molecular and Cellular Biology. 17: 6184-6190.

Li, Z-W., Chu, W., Hu, y., Delhase, M., Deerinck, T., Ellisman, M., Johnson, R. and Karin, M. 1999. The IKKβ subunit of IκB kinase (IKK) is essential for nuclear factor κB activation and prevention of apoptosis. The Journal of Experimental Medicine. 189: 1839-1845.

Lowenstein, C.J., Glatt, C.S., Bredt, D.D. and Snyder, S.H. 1992. Cloned and expressed macrophage nitric oxide synthase contrasts with the brain enzyme. Proceedings of the National Academy of Sciences. 89: 6711-6715.

Makboon, K., Likhitwitayawuid, K. and Ruangrungsi, N. 2000. Chemical constituents of *Curcuma mangga* rhizome. Available: http://dcms.thailis.or.th/ dcmsn /browse. php?option=show& Browse_type=subject &subjid=56146 (Accessed: 2007, July 8).

Margaros, I. and Vassilikogiannakis, G. 2008. Synthesis of (+)-Zerumin B using a regioselective singlet oxygen furan oxidation. Journal of Organic Chemistry. 73: 2021-2023.

Nakao, S., Ogtata, y., Shimizu, E., Yamazaki, M., Furuyama, S. and Sugiya, S. 2002. Tumor necrosis factor α (TNF-α)-induced prostaglandin E_2 release is mediated by the activation of cyclooxygenase-2 (COX-2) transcription via NFκB in human gingival fibroblasts. Molecular and Cellular Biochemistry. 238: 11-18.

Nanji, A.A., Jokelainen, K., Tipoe, G.L., Rahemtulia, A., Thomas, P. and Dannenberg, A.J. 2003. Curcumin prevents alcohol-induced liver disease in rats by inhibiting the expression of NF-κB-dependent genes. Physiology Gastrointestinal and Liver Physiology. 284: 321-327.

Natarajan, K., Singh, S., Burke, T.R., Jr, Grunberger, D. and Aggarwal, B.B. 1996. Caffeic acid phenethyl ester is a potent and specific inhibitor of activation of nuclear transcription factor NF-kappa B. Proceedings of the National Academy of Sciences. 93: 9090-9095.

Naumann, M. 2000. Nuclear factor-κB activation and innate immune response in microbial pathogen infection. Biochemical Pharmacology. 60: 1109-1114.

Newton, D.C., Bevan, S.C., Choi, S., Robb, G.B., Millar, A., Wang, Y. and Marsden, P.A. 2003. Translational regulation of human neuronal nitric oxide synthase by an alternatively spliced 5'-untranslated region leader exon. The Journal of Biological Chemistry. 278: 636-644.

Pahl, H.L. 1999. Activators and target genes of Rel/NF-κB transcription factors. Oncogene. 18: 6853-6866.

Pan, C-H., Kim, E.S., Jung, S.H., Nho, C.W. and Lee, J.K. 2008. Tectorigenin inhibits IFN-γ/LPS induced inflammatory responses in murine macrophage RAW 264.7 cells. Archives of Pharmacal Research. 31: 1447-1456.

Paramasivam, M., Poi, R., Banerjee, H. and Bandyopadhyay, A. 2009. High-performance thin layer chromatographic method for quantitative determination of curcuminoids in *Curcuma longa* germplasm. Food Chemistry. 113: 640-644.

Péret-Almeida, L., Cherubino, A.P.F., Alves, R.J., Dufossé, L. and Glória, M.B.A. 2005. Separation and determination of the physico-chemical characteristics of

curcumin, demethoxycurcumin and bisdemethoxycurcumin. Food Research International. 38: 1039-1044.

Petrova, T.V., Akama, K.T. and Eldik, L.J.V. 1999. Cyclopentenone prostaglandins suppress activation of microglia: down-regulation of inducible nitric-oxide synthase by 15-deoxy-$D^{12,14}$-prostaglandin. Proceedings of the National Academy of Sciences. 96: 4668-4673.

Riedemann, N.C., Guo, R-F. and Ward, P.A. 2003. Novel strategies for the treatment of sepsis. Nature Medicine. 9: 517-524.

Rioja, I., Terencio, M.C., Ubeda, A., Riguera, R., Quintela, J.M. and Alcaraz, M.J. 2002. A new ditriazine inhibitor of NF-κB modulates chronic inflammation and angiogenesis. Naunyn-Schmiedeberg's Arch Pharmacol. 365: 357-364.

Rollinger, J.M., Hornick, A., Langer, T., Stuppner, H. and Prast, H. 2004. Acetylcholinesterase inhibitory activity of scopolin and scopoletin discovered by virtual screening of natural products. Journal of Medicinal Chemistry. 47: 6248-6254.

Roshak, A.K., Jackson, J.R., McGough, K., Chabot-Fletcher, M., Mochan, E., and Marshall§, L.A. 1996. Manipulation of distinct NFκB proteins alters interleukin-1β induced human rheumatoid synovial fibroblast prostaglandin E_2 formation. The Journal of Biological Chemistry. 271: 31496-31501.

Rote, N.S. 2002. Inflammation. McCance, K.L. and Huether, S.E. (eds). The biologic basis for disease in adults and children (4^{th} ed), Missouri, USA. Mosby. 197-226.

Sakurai, H., Kohsaka, H., Liu, M-F., Higashiyama, H., Hirata, Y., Kanno, K., Saito, I. and Miyasaka, N. 1995. Nitric oxide production and inducible nitric oxide synthase expression in inflammatory arthritides. Journal of Clinical Investigation. 96: 2357-2363.

Salvemini, D., Seibert, K., Masferrer, J.L., Misko, T.P., Currie, M.G. and Needleman, P. 1994. Endogenous nitric oxide enhances prostaglandin production in a model of renal inflammation. The Journal of Clinical Investigation. 93: 1940-1947.

Schmedtje, Jr, J.F., Ji, Y-S., Liu, W.-L., DuBois§, R.N. and Runge, M.S. 1997. Hypoxia induces cyclooxygenase-2 via the NF-κB p65 transcription factor in human vascular endothelial cells. The Journal of Biological Chemistry. 272: 601-608.

Schroder, K, Sweet, M.J. and Hume, D.A. 2006. Signal integration between IFNγ and TLR signalling pathways in macrophages. Immunobiology. 211: 511–524.

Scotter, M.J. 2009. Synthesis and chemical characterisation of curcuminoid colouring principles for their potential use as HPLC standards for the determination of curcumin colour in foods. Food Science and Technology. 42: 1345-1351.

Scudiere, D.A., Shoemaker, R.H., Paul!, K.D., Monks, A., Tierney, S., Nofziger, T.H., Currens, M.J., Seniff, D. and Boyd, M.R. 1988. Evaluation of a soluble tetrazolium/formazan assay for cell growth and drug sensitivity in culture using human and other tumor cell lines. Cancer Research. 48: 4827-4833.

Serhan, C.N. and Savill, J. 2005. Resolution of inflammation: the beginning programs the end. Nature Immunology. 6: 1991-1997.

Shishodia, S., Majumdar, S., Banerjee, S. and Aggarwal, B.B. 2003. Ursolic acid inhibits nuclear factor-κB activation induced by carcinogenic agents through suppression of IκBα kinase and p65 phosphorylation: correlation with down-regulation of cyclooxygenase 2, matrix metalloproteinase 9, and cyclin D1. Cancer Research. 63: 4375-4383.

Singh, S. and Aggarwal, B.B. 1995. Activation of transcription factor NF-κB is suppressed by curcumin (diferulolylmethane). The Journal of Biological Chemistry. 270: 24995-25000.

Singh, M. and Singh, N. 2009. Molecular mechanism of curcumin induced cytotoxicity in human cervical carcinoma cells. Molecular and Cellular Biochemistry. 325: 107-119.

Song, M-Y., Kim, E-K., Moon, W-S., Park, J-W., Kim, H-J., So, H-S., Park, R., Kwon, K-B., Park, B-H. 2009. Sulforaphane protects against cytokine and streptozotocin-induced β-cell damage by suppressing the NF-κB pathway. Toxicology and Applied Pharmacology. 235: 57–67.

Stuehr, D.J. 2004. Enzymes of the L-arginine to nitric oxide pathway. The Journal of Nutrition. 134: 2748-2751.

Sugiatno, E., Samsudin, A.R., Ibrahim, M.F. and Sosroseno, W. 2006. The effect of nitric oxide on the production of prostaglandin E_2 by hydroxyapatite-stimulated a human osteoblast (HOS) cell line. Biomedicine and Pharmacotherapy. 60: 147-151.

Sun, j., Zhang, X., Broderick, m. and Fein, H. 2003. Measurement of nitric oxide production in biological systems by using Griess reaction assay. Sensors. 3: 276-284.

Surh, Y-J., Chun, K-S., Cha, H-H., Han, S-S., Keum, Y-S., Park, K-K. and Lee, S.S. 2001. Molecular mechanisms underlying chemopreventive activities of anti-inflammatory phytochemicals: down-regulation of COX-2 and iNOS through suppression of NF-ΚB activation. Mutation Research. 480–481: 243–268.

Tetsuka, T., Daphna-Iken, D., Srivastava, S.K., Baier, L.D., Dumaine, J. and Morrison, A.R. 1994. Cross-talk between cyclooxygenase and nitric oxide pathways: Prostaglandin E_2 negatively modulates induction of nitric oxide synthase by interleukin 1. Proceedings of the National Academy of Sciences. 91: 12168-12172.

Tewtrakul, S. and Subhadhirasakul, S. 2007. Anti-allergic activity of some selected plants in the Zingiberaceae family. Journal of Ethnopharmacology. 109: 535-538.

Tewtrakul, S. and Subhadhirasakul, S. 2008. Effects of compounds from *Kaempferia parviflora* on nitric oxide, prostaglandin E_2 and tumor necrosis factor-alpha productions in RAW264.7 macrophage cells. Journal of Ethnopharmacology. 120: 81-84.

Thomas, G. and Ramwell, P.W. 1998. Nitric oxide, donors and inhibitors. Katzung, B.G. Basic and clinical pharmacology (7^{th} ed), Stamford, USA. Appleton and lange. 319-324.

Tsikas, D. 2007. Analysis of nitrite and nitrate in biological fluids by assays based on the Griess reaction: Appraisal of the Griess reaction in the L-arginine/nitric oxide area of research. Journal of Chromatography B. 851: 51–70.

Vane, J. R., Mitchell, J. A., Appleton, I., Tomlinson, A., Bishop-Bailey, D., Croxtall, J. and Willoughby, D.A. 1994. Inducible isoforms of cyclooxygenase and nitric-oxide synthase in inflammation. Proceedings of the National Academy of Sciences. 91: 2046-2050.

Wake forest university health sciences. 2009. Available: http://www.mydietaryfats.org/index.php/site/content/C33/ (Accessed: 2008, May 26).

Wattanapitayakul, S.K., Suwatronnakorn, M., Chularojmontri, L., Herunsalee, A., Niumsakul, S., Charuchongkolwongse, S. and Chansuvanich, N. 2007. *Kaempferia parviflora*

ethanolic extract promoted nitric oxide production in human umbilical vein endothelial cells. Journal of Ethnopharmacology. 110: 559–562.

Weyerstahl. P., Schwieger, R., Schwope, I. and Hashem, Md. A. 1995. Synthesis of some naturally occurring drimane and dinorlabdane derivatives. Liebigs Annalen. 7: 1389-1392.

Xie, Q-w., Kashiwabara, Y. and Nathan, C. 1994. Role of transcription factor NF-κB/Rel in induction of nitric oxide synthase. The Journal of Biological Chemistry. 269: 4705-4708.

Xu, H-X., Dong, H. and Sims, K-Y. 1996. Labdane diterpenes from *Alpinia zerumbet*. Phytochemistry. 42: 149-151.

Yamamoto, Y. and Gaynor, R.B. 2001. Therapeutic potential of inhibition of the NF-κB pathway in the treatment of inflammation and cancer. Journal of Clinical. 107: 135-142.

Ye, S-M and Johnson, R.W. 2001. Regulation of interleukin-6 gene expression in brain of aged mice by nuclear factor κB. Journal of Neuroimmunology. 117: 87–96.

Yodkeeree, S., Chaiwangyen, W., Garbisa, S.and Limtrakul, P. 2008. Curcumin, demethoxycurcumin and bisdemethoxycurcumin differentially inhibit cancer cell invasion through the down-regulation of MMPs and uPA. Journal of Nutritional Biochemistry. 20: 87-95.

Zeng, Y-C., Qui, F., Takahashi, K., Liang, J., Qu, G-X. and Yao, X-S. 2007. New sesquiterpenes and calebin derivatives from *Curcuma longa.* Chemical and Pharmaceutical Bulletin. 55: 940-943.

APPENDIX

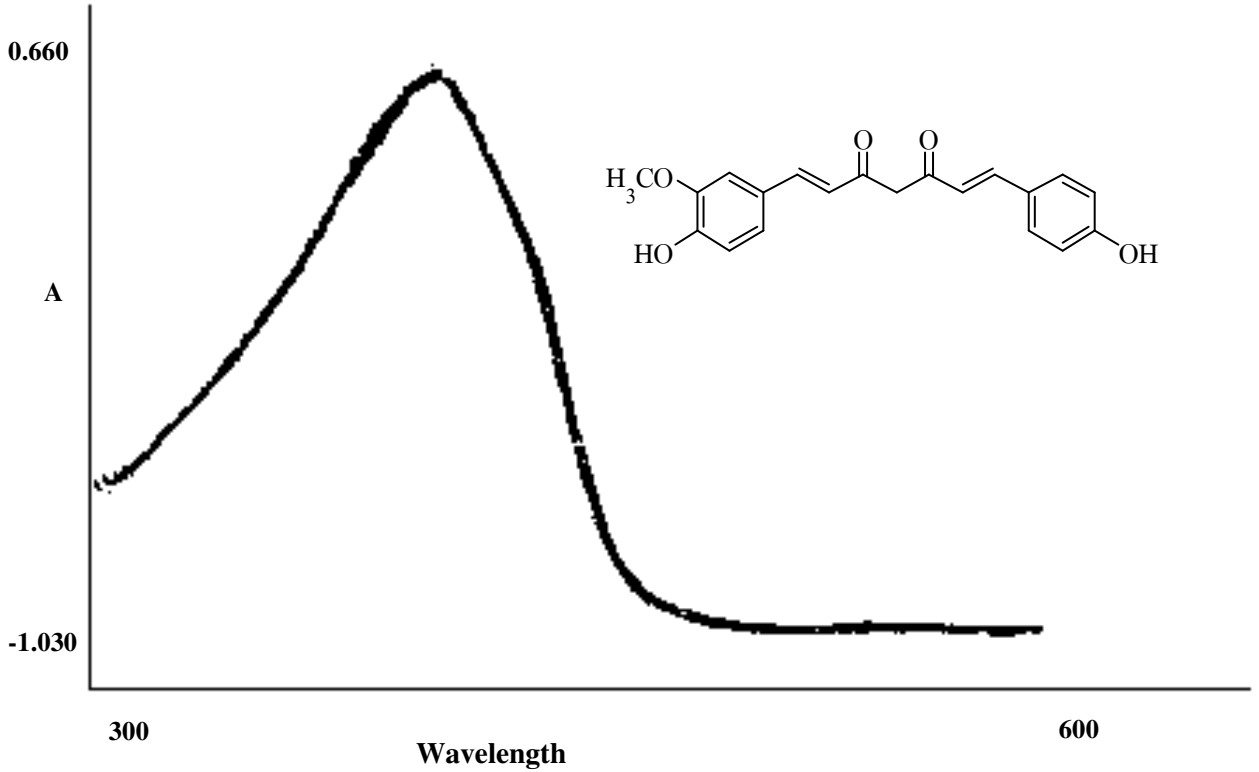

UV spectrum of compound **1** ($CHCl_3$)

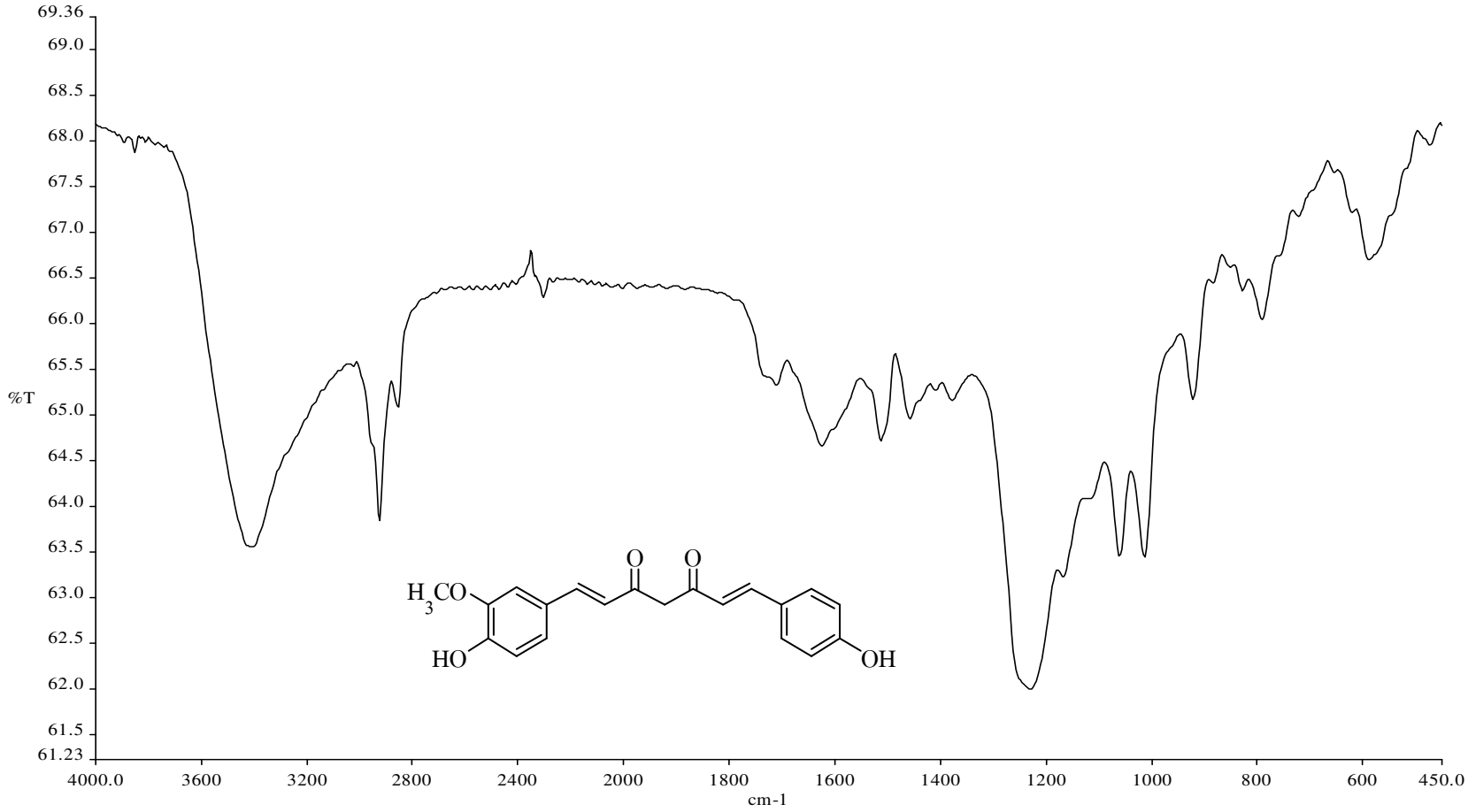

IR spectrum of compound **1** (KBr)

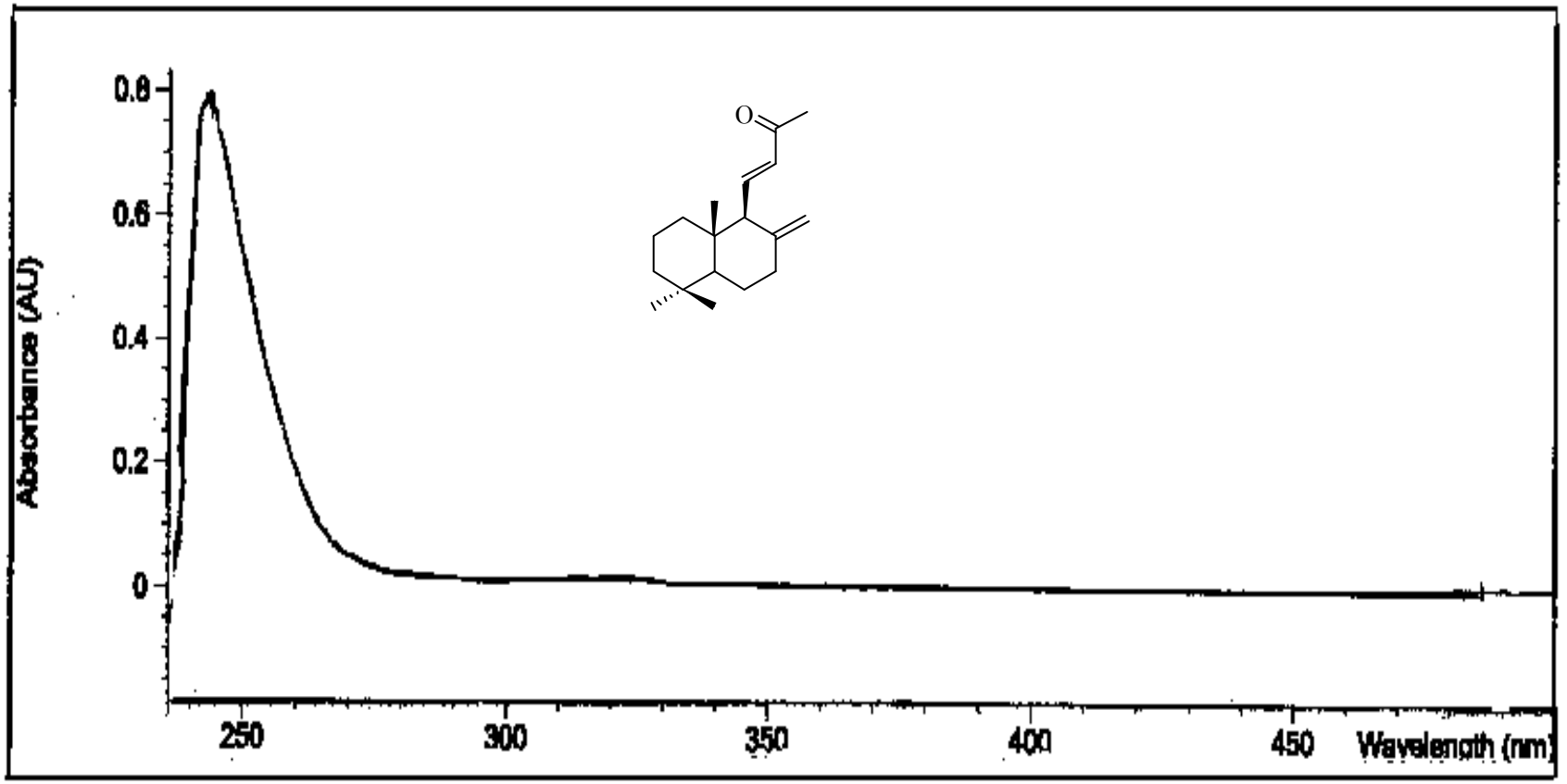

UV spectrum of compound **2** ($CHCl_3$)

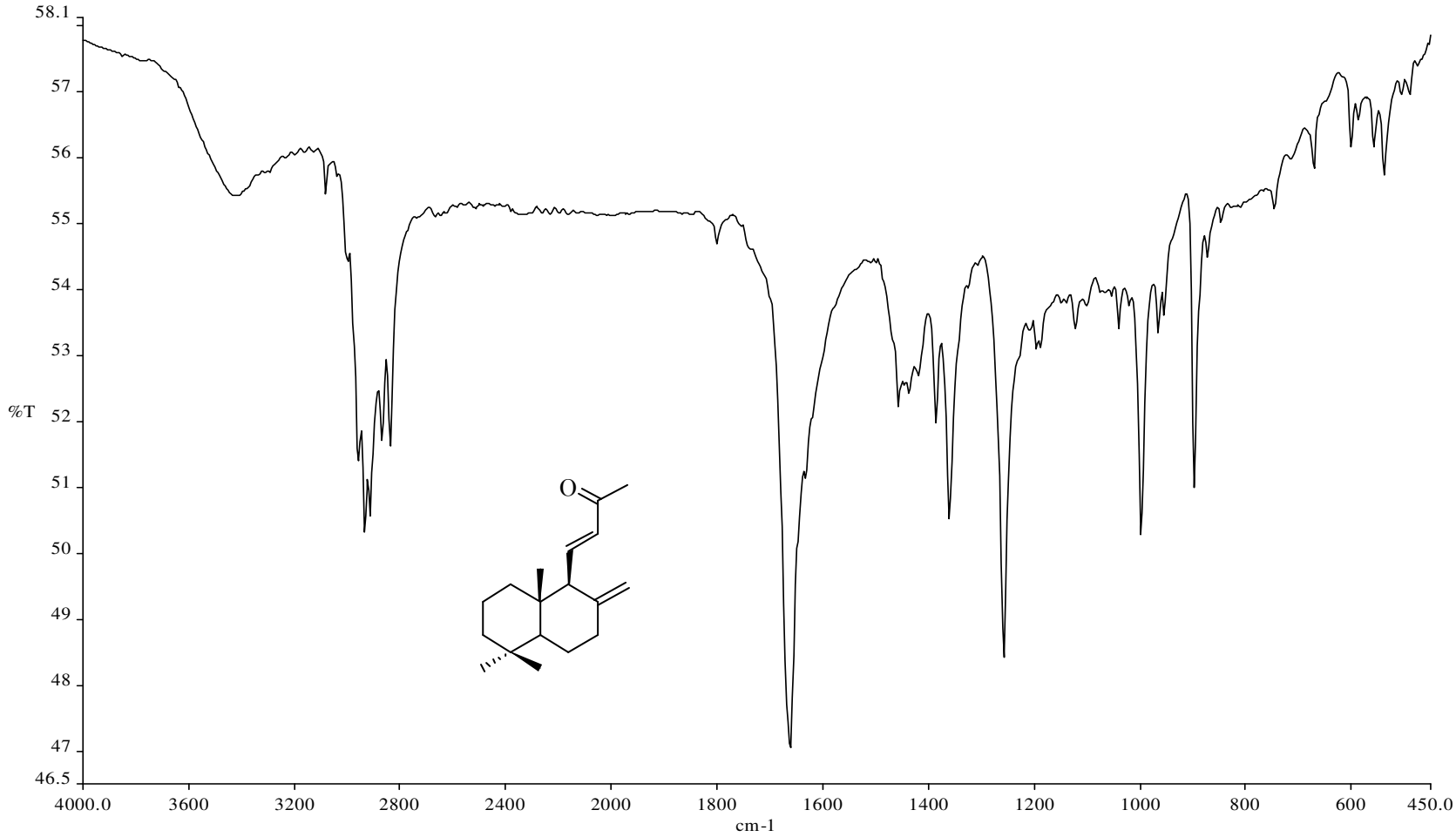

IR spectrum of compound **2** (KBr)

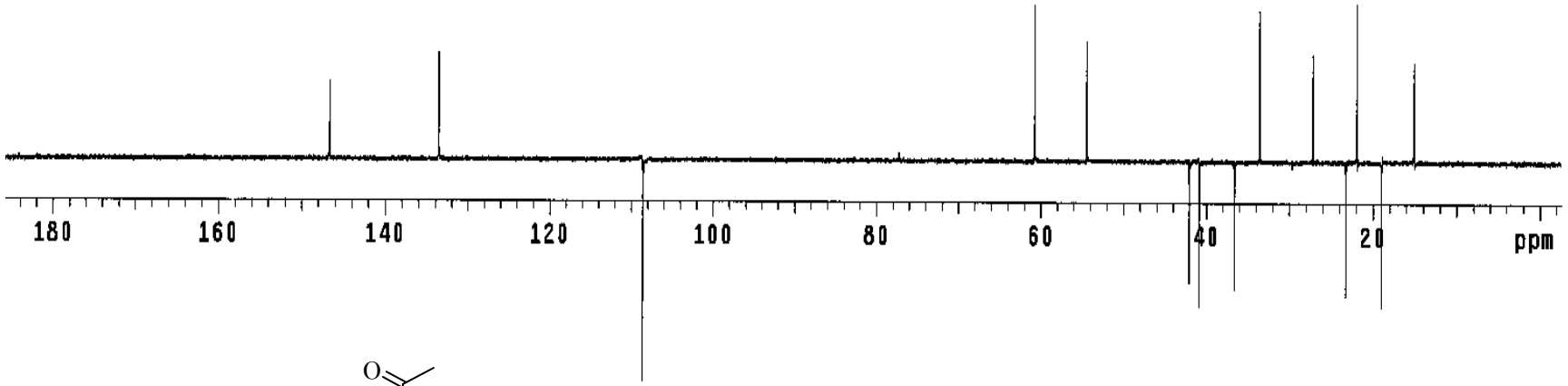

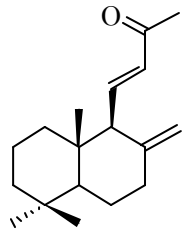

DEPT 135° spectrum of compound **2** ($CDCl_3$)

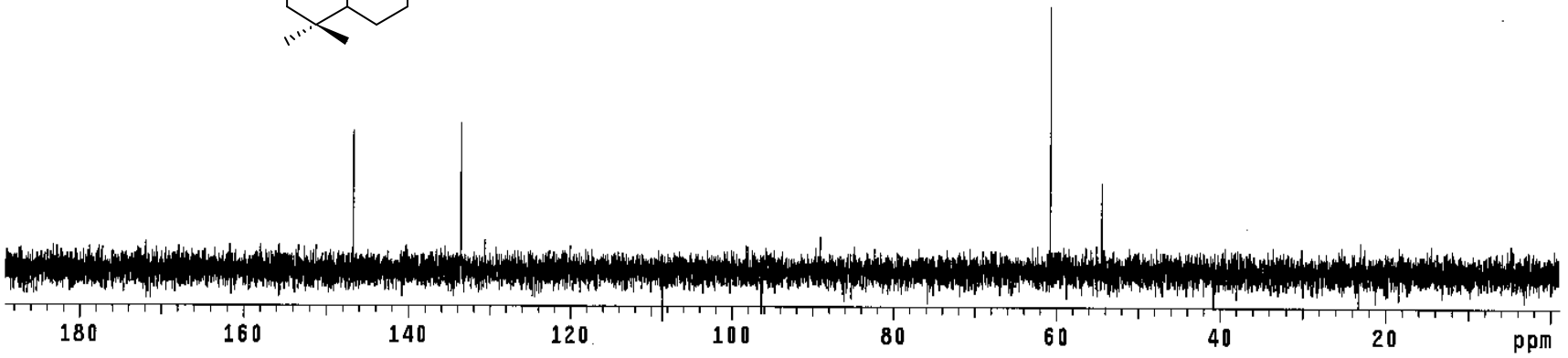

DEPT 90° spectrum of compound **2** ($CDCl_3$)

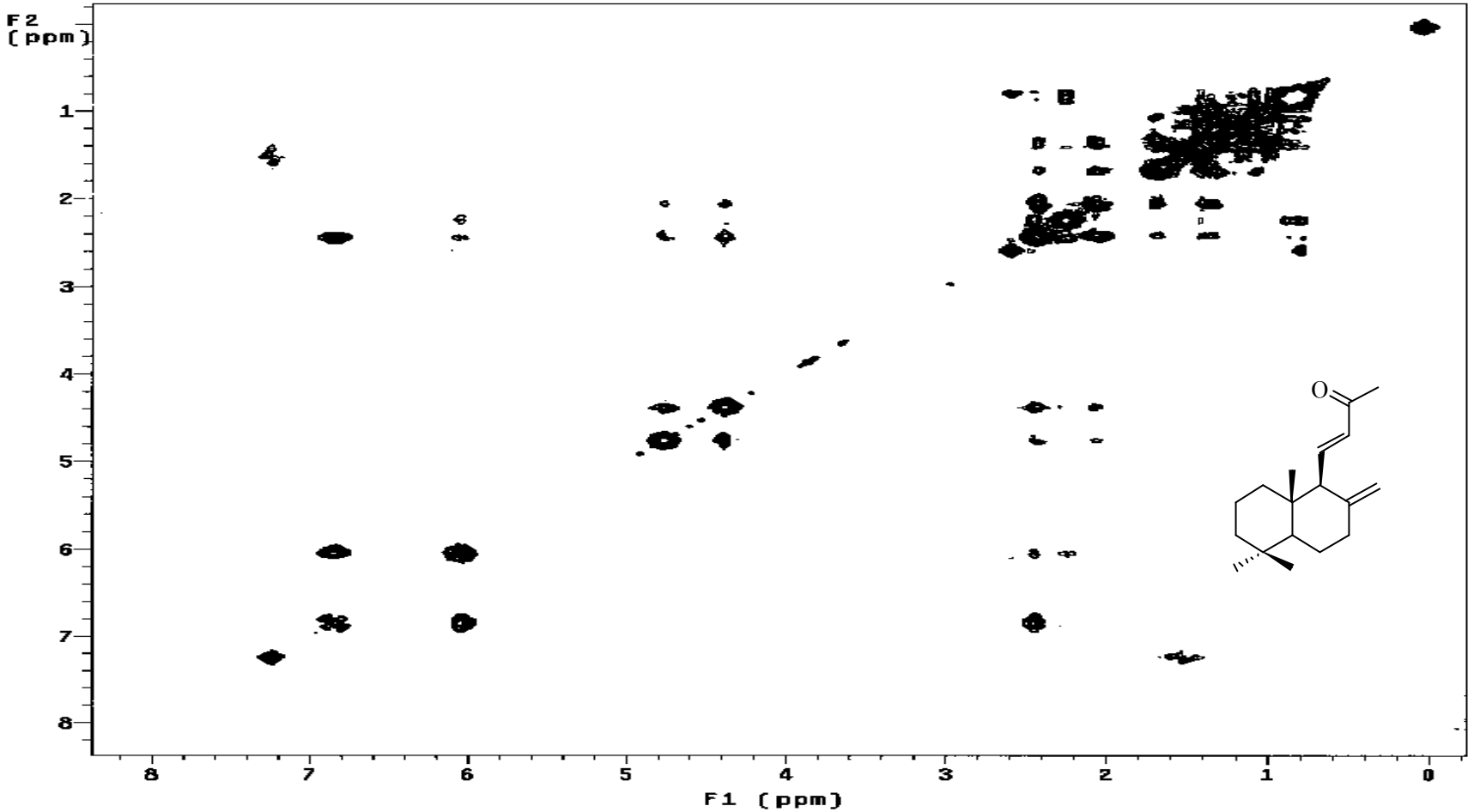

^{1}H-^{1}H COSY spectrum of compound **2** ($CDCl_3$)

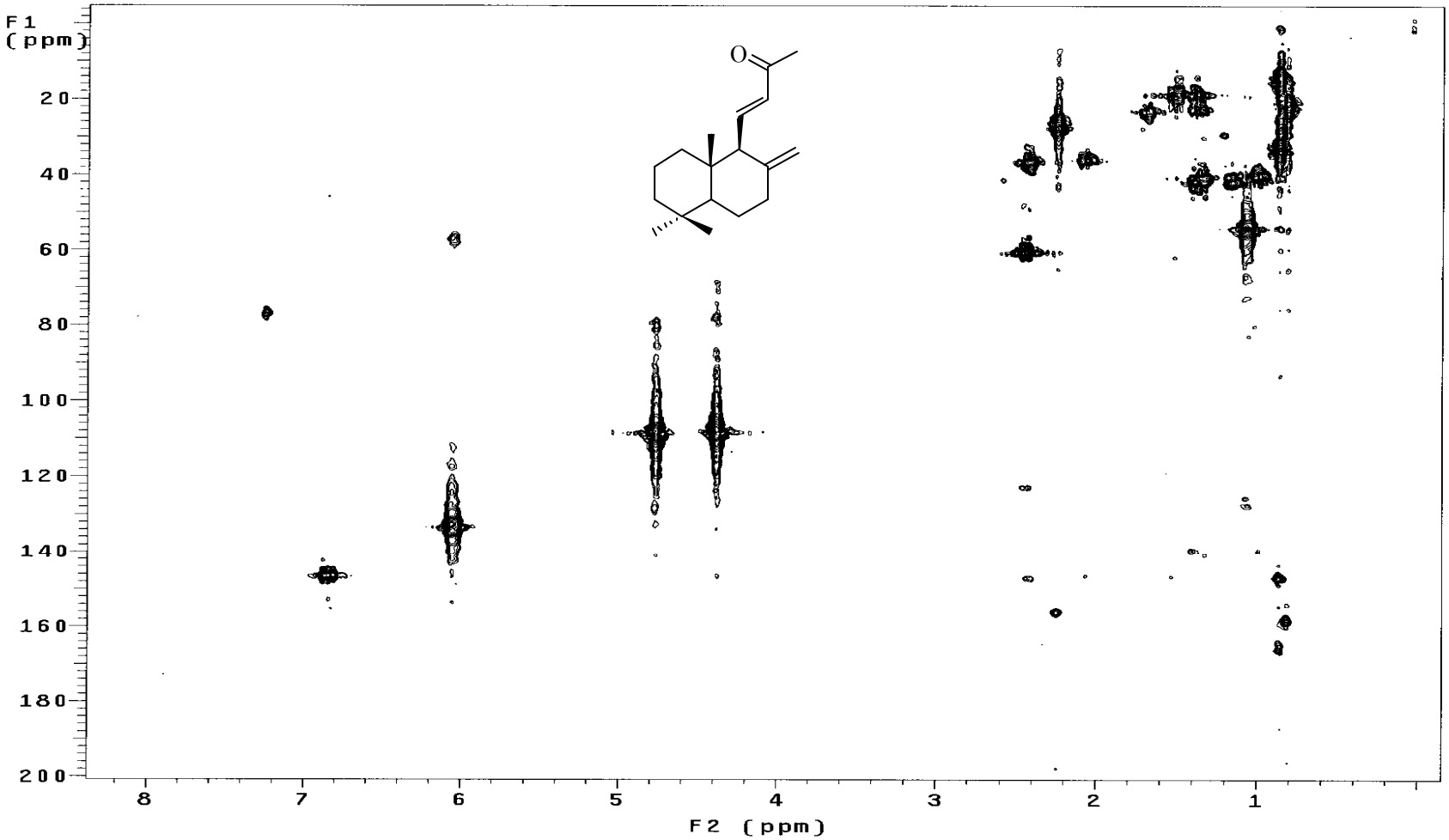

HMQC spectrum of compound **2** ($CDCl_3$)

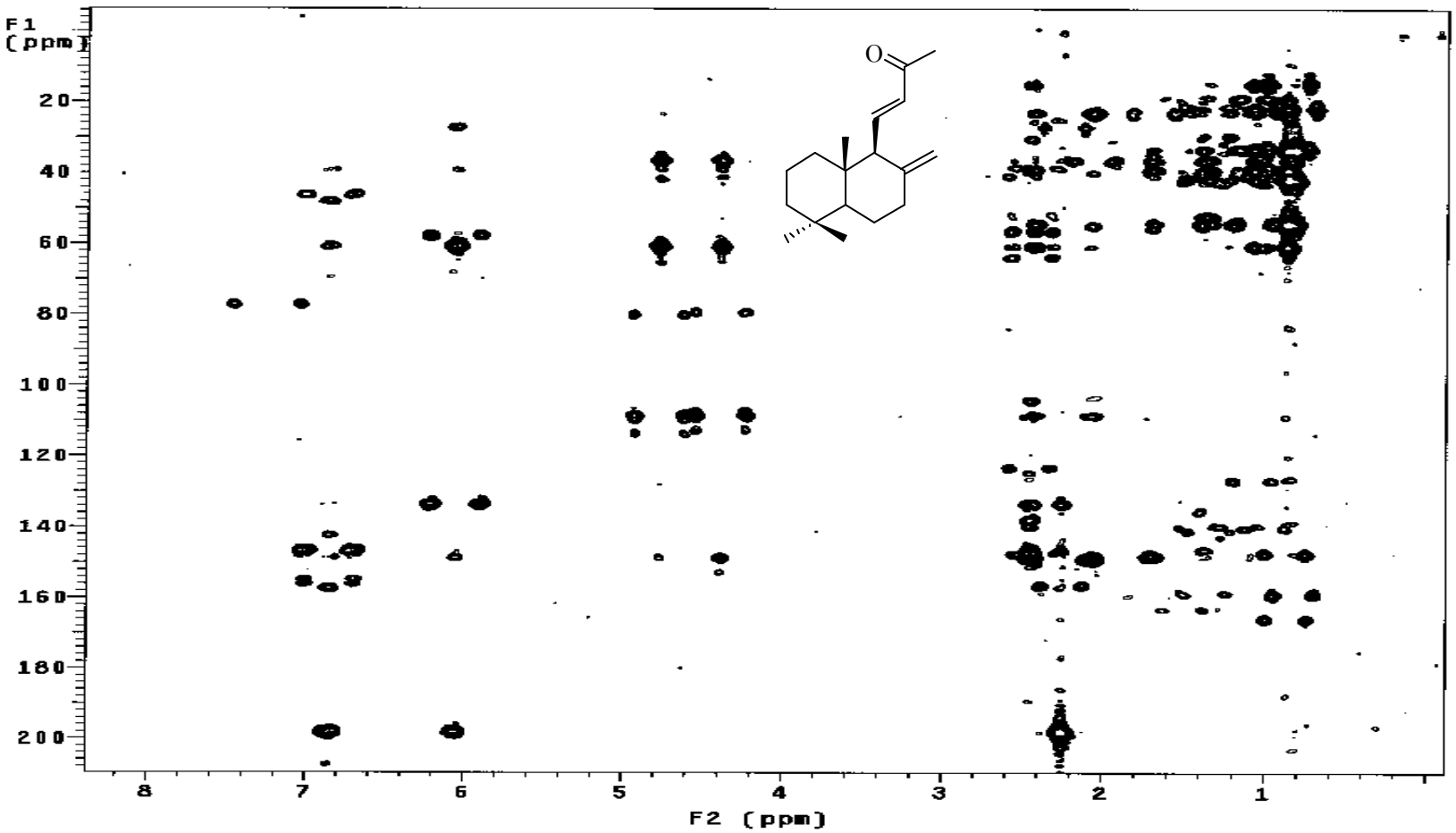

HMBC spectrum of compound **2** ($CDCl_3$)

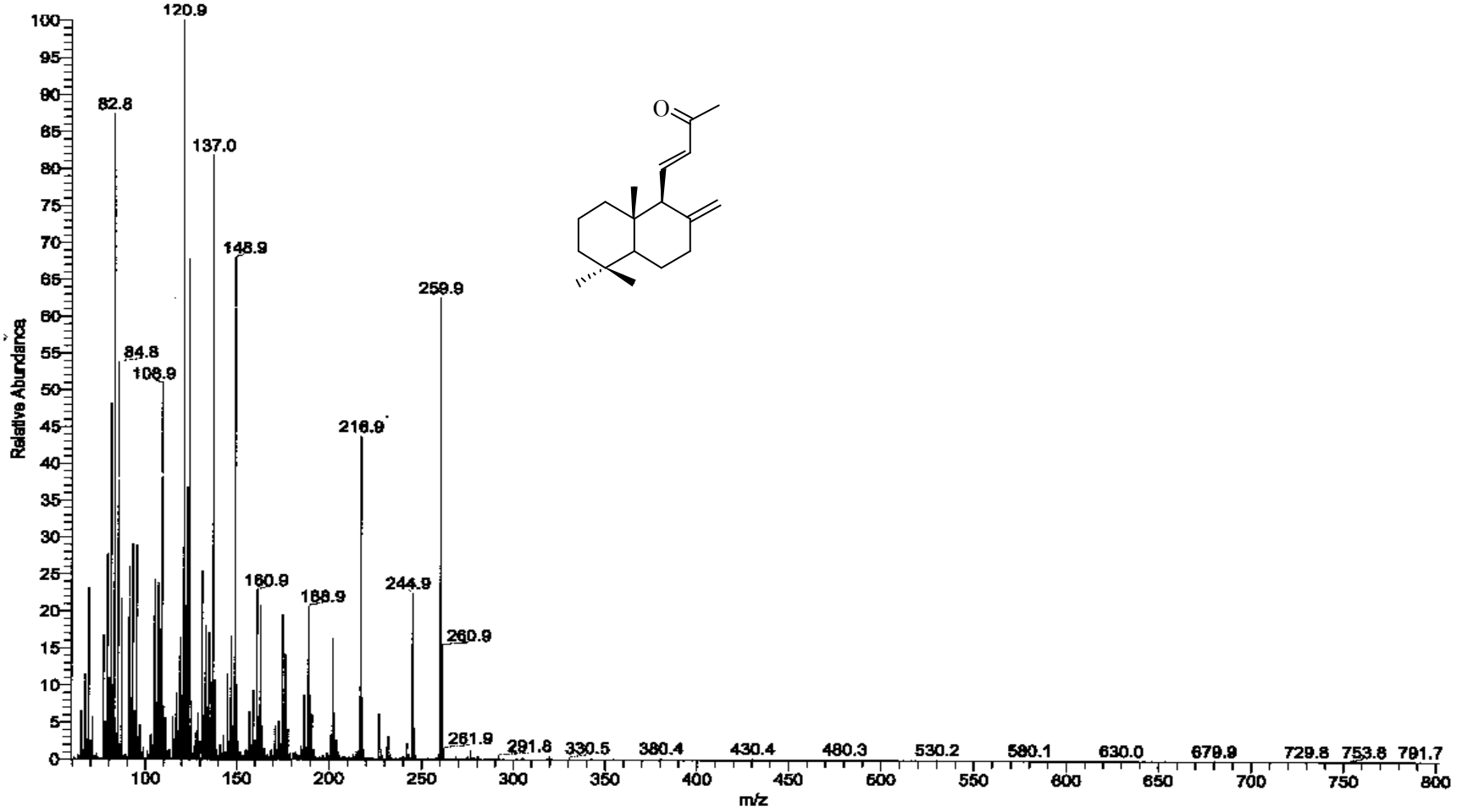

EI mass spectrum of compound **2**

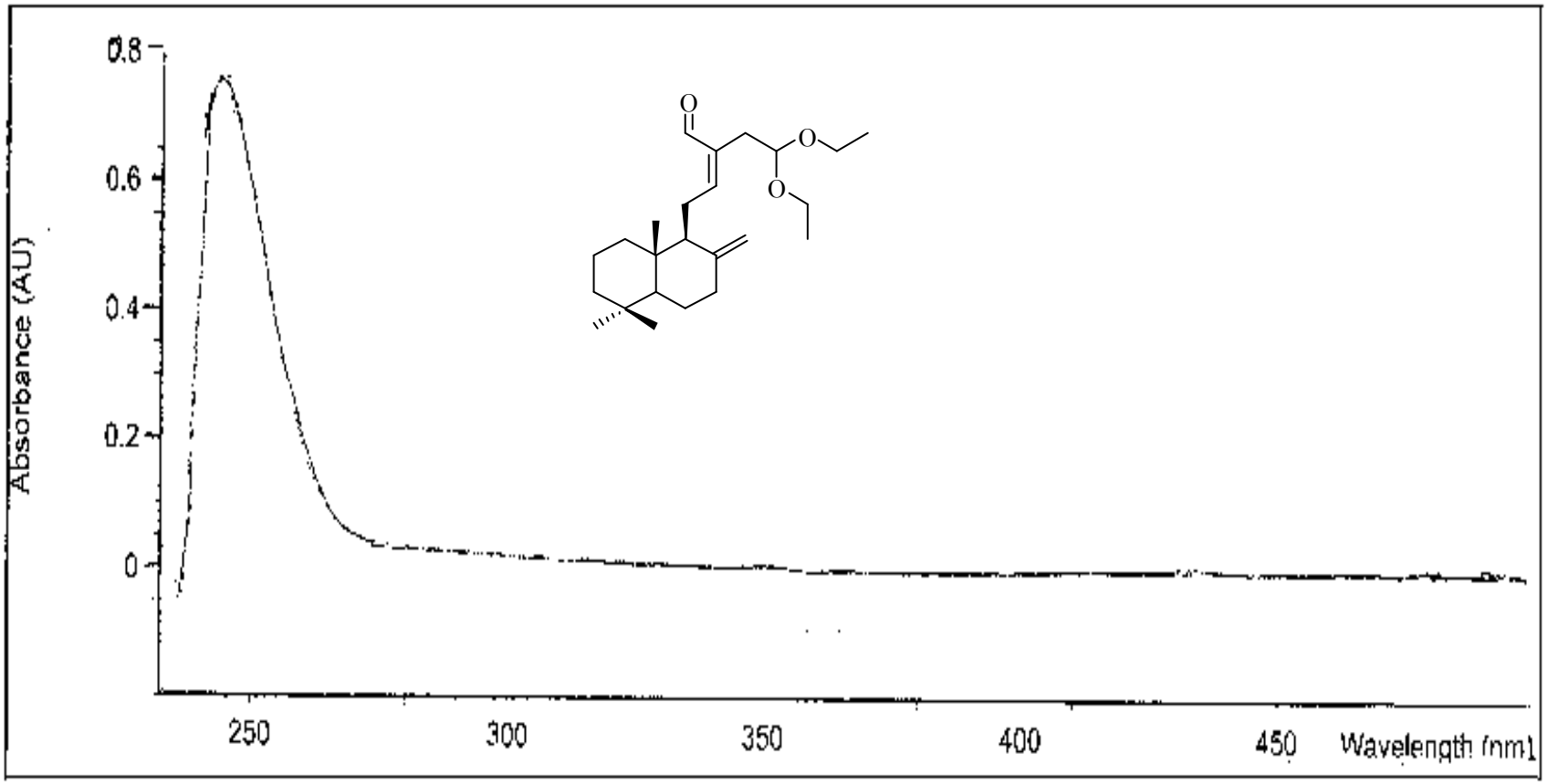

UV spectrum of compound **3** ($CHCl_3$)

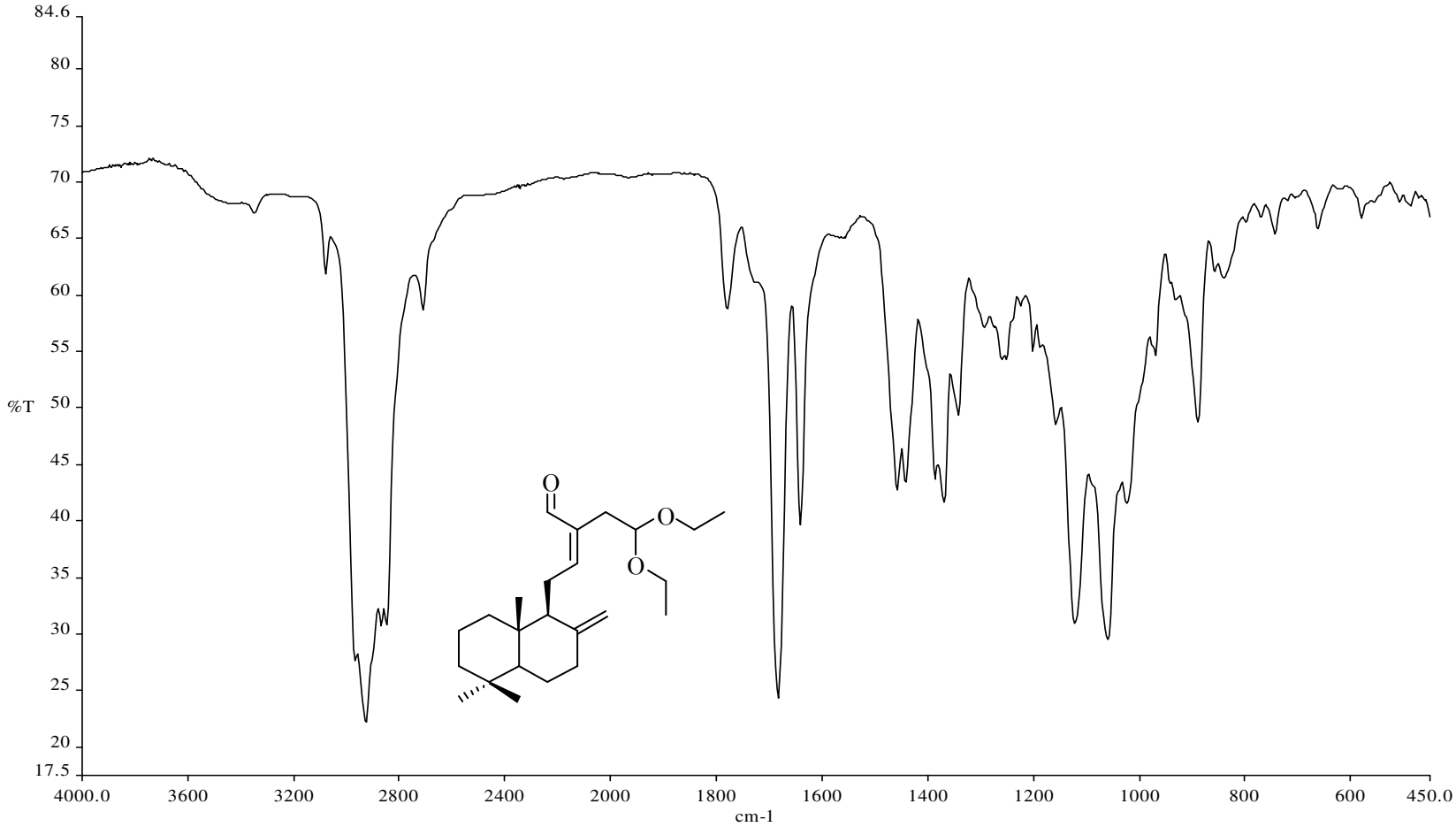

IR spectrum of compound **3** (KBr)

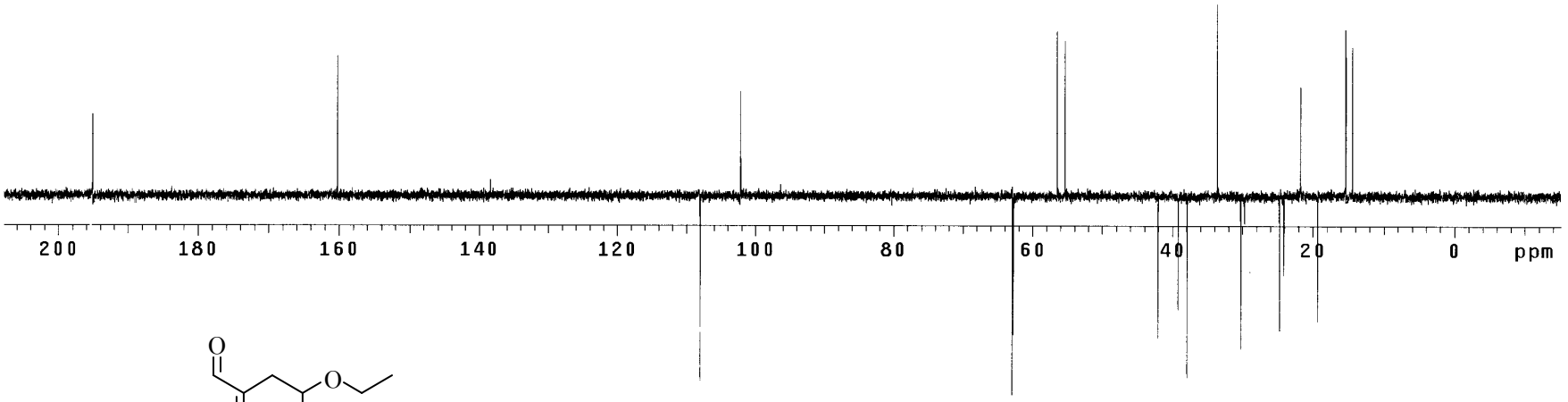

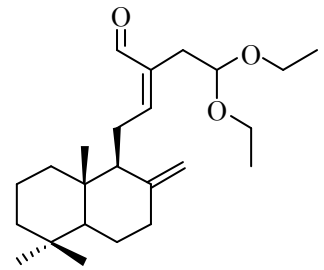

DEPT 135° spectrum of compound **3** ($CDCl_3$)

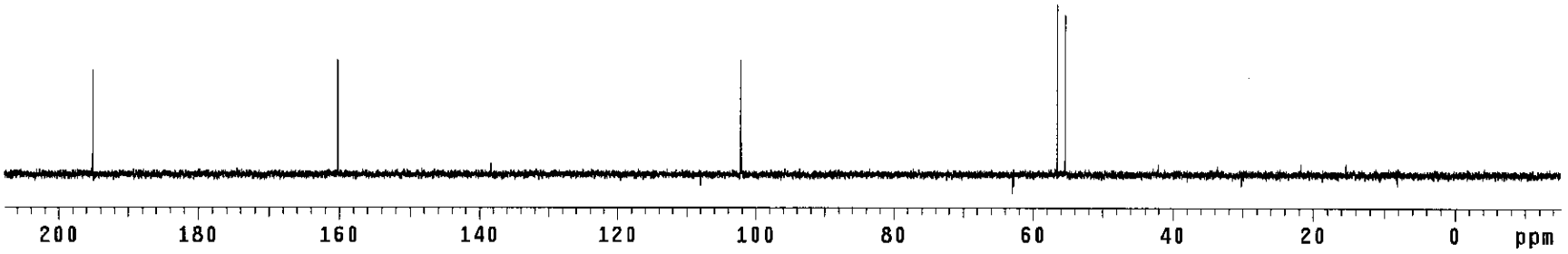

DEPT 90° spectrum of compound **3** ($CDCl_3$)

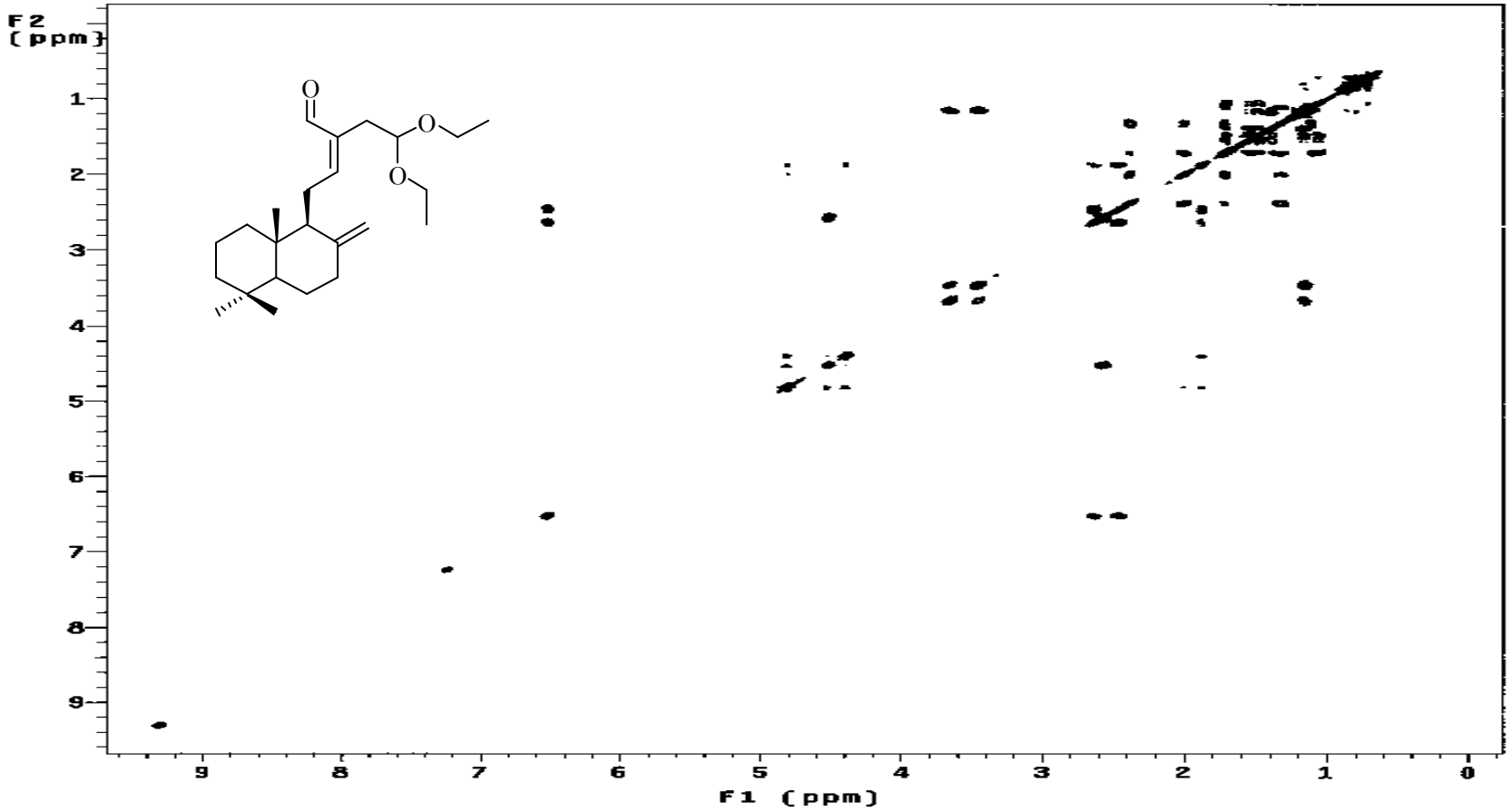

^{1}H-^{1}H COSY spectrum of compound **3** ($CDCl_3$)

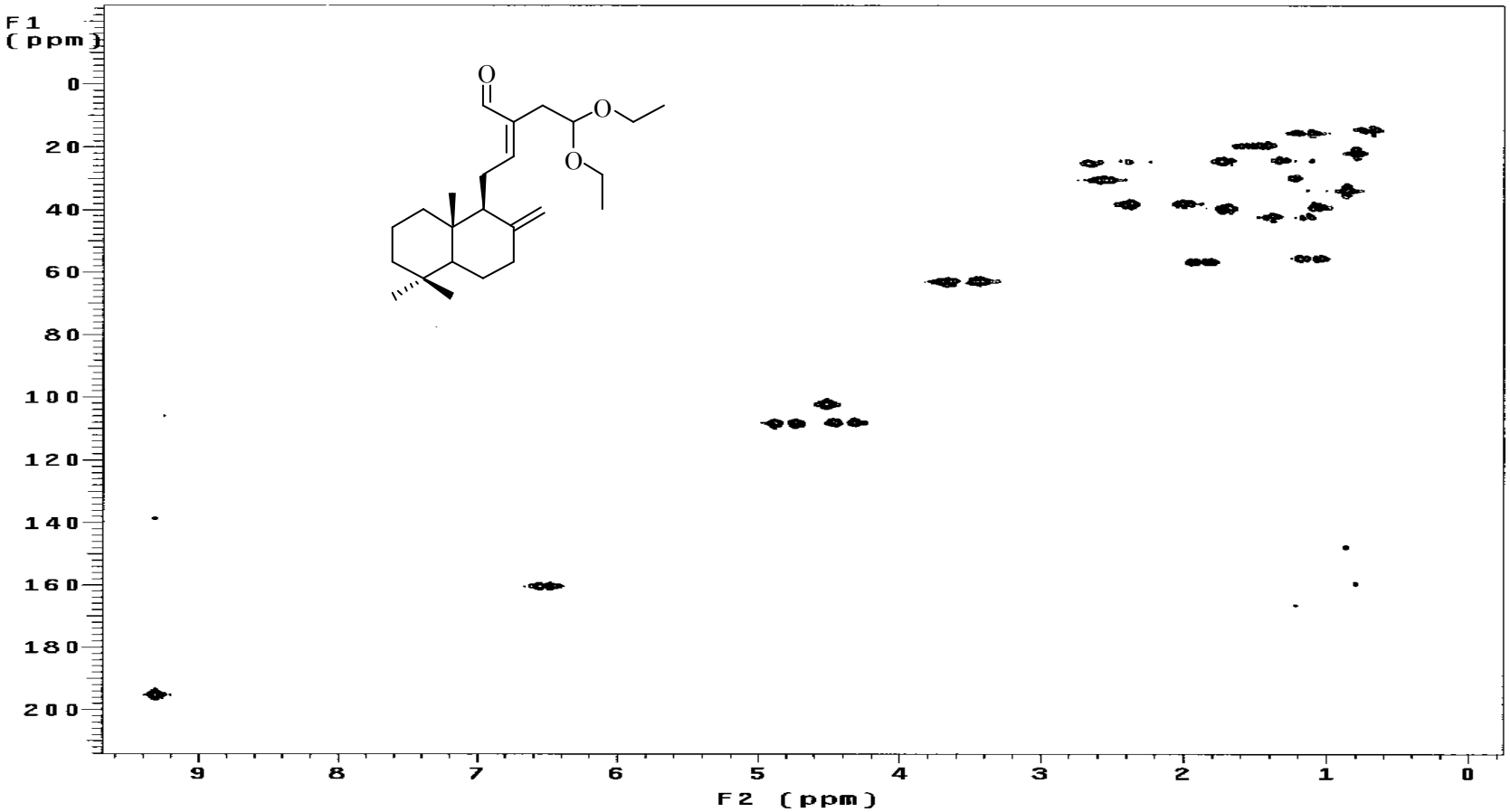

HMQC spectrum of compound **3** ($CDCl_3$)

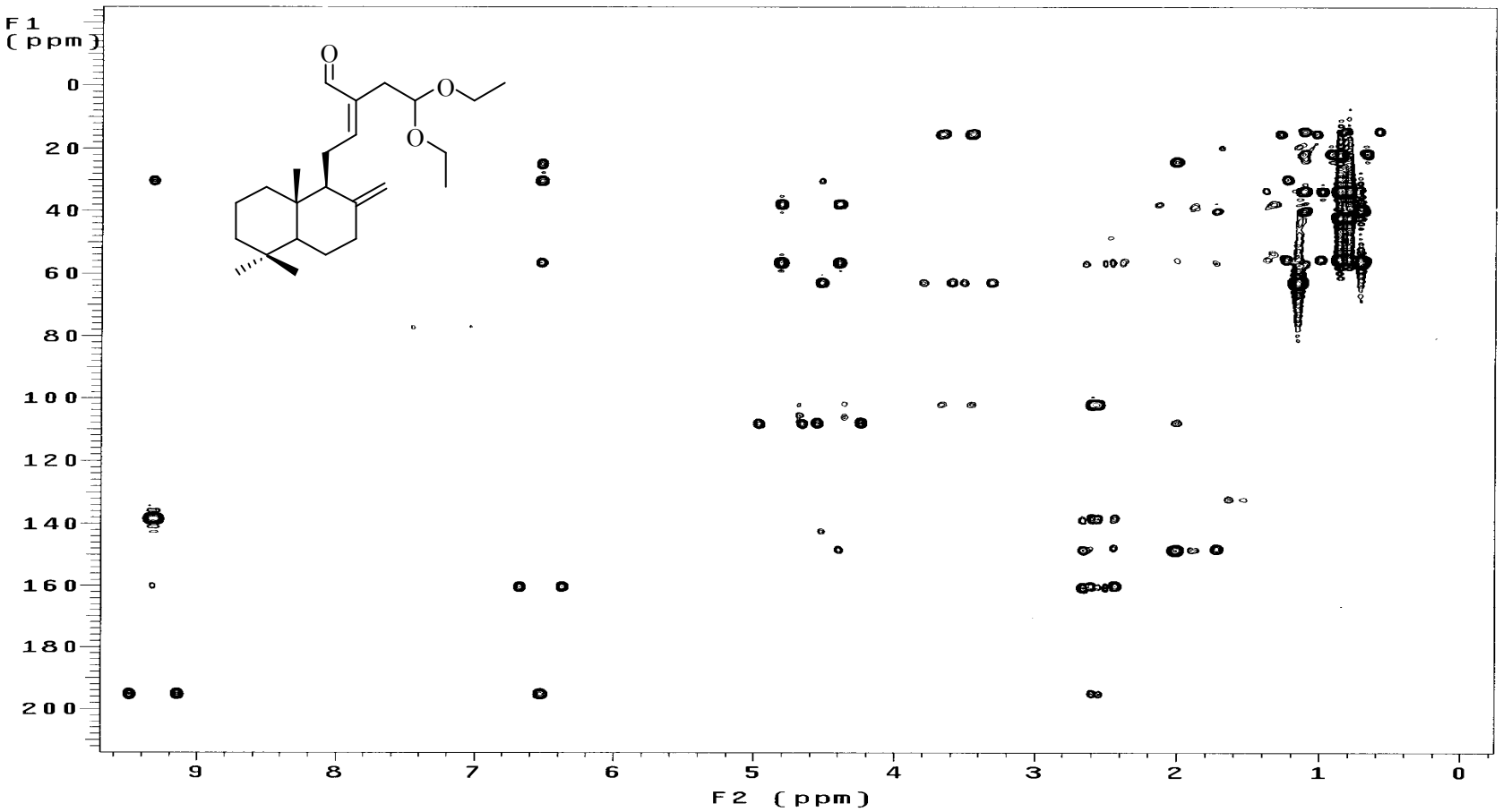

HMBC spectrum of compound **3** ($CDCl_3$)

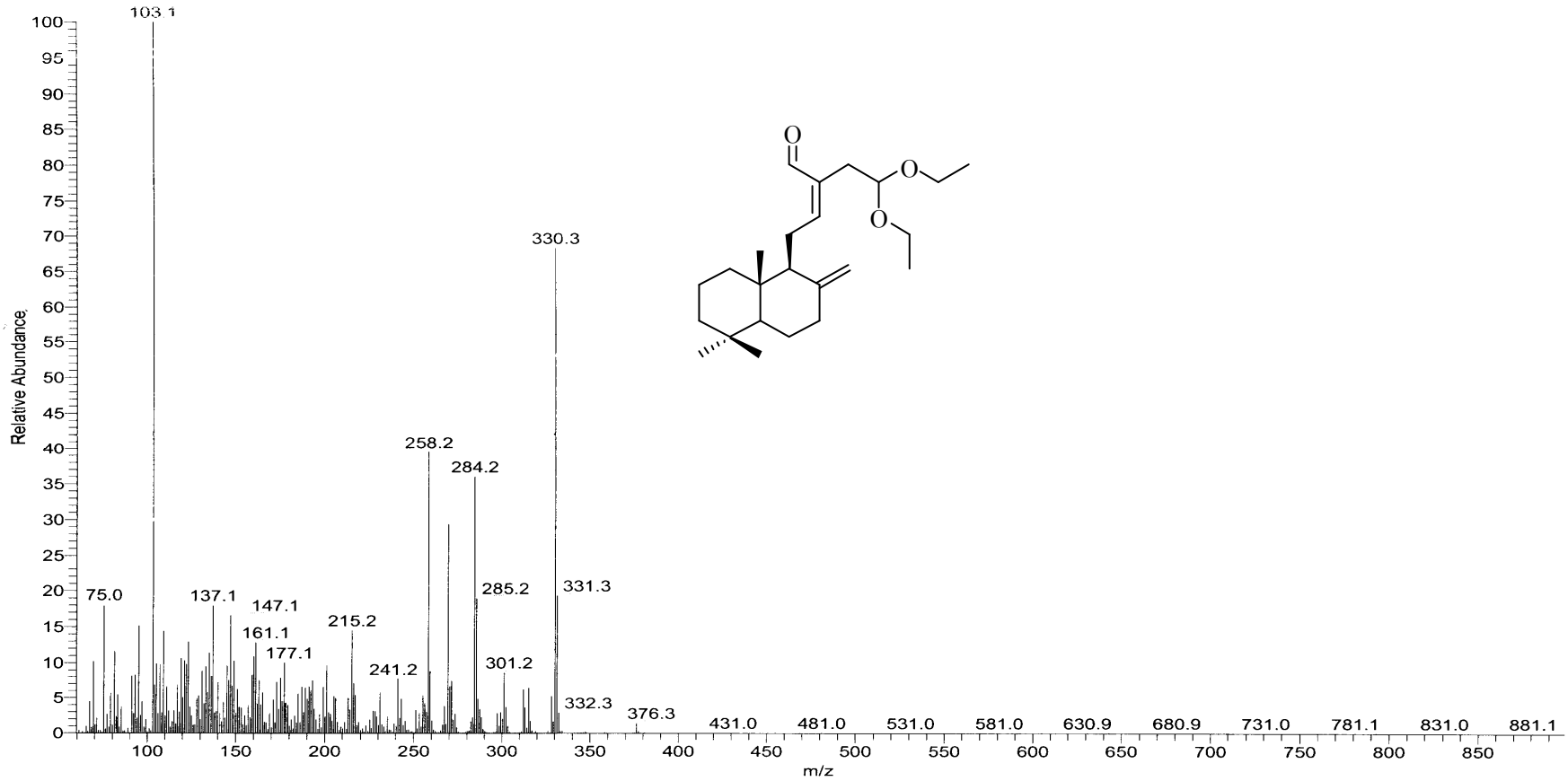

EI mass spectrum of compound **3**

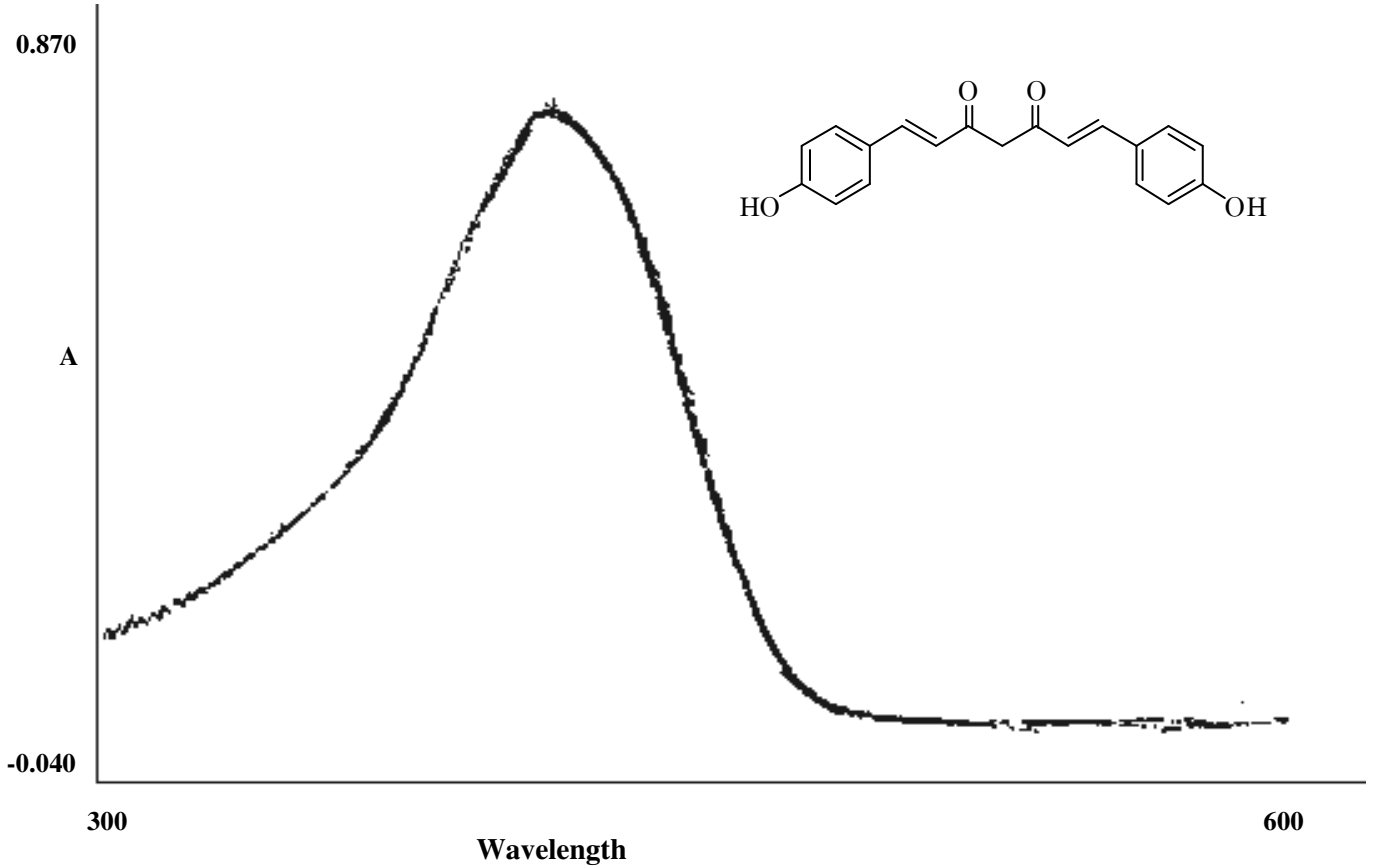

UV spectrum of compound **4** (CH_3OH)

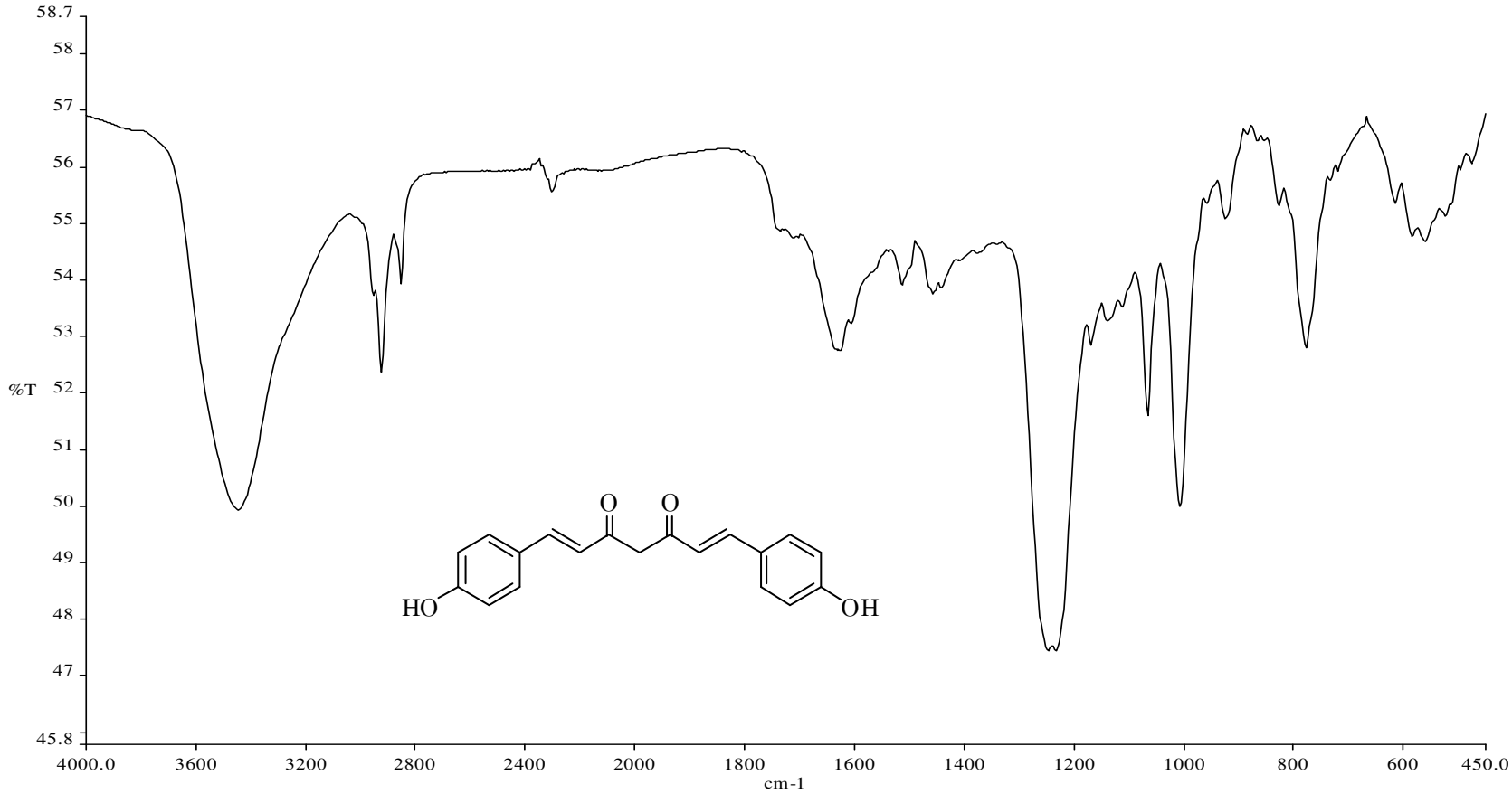

IR spectrum of compound **4** (KBr)

conc. (μM)	cpd **1**	cpd **2**	cpd **3**	cpd **4**	Indo	L-NA	CAPE
3	9.2	16.7	37.8	1.7	15.5	-	26.1
10	31.7	39.2	41.9	20	36.4	24.1	85.6
30	93.3	49.2	67	73.3	60.9	29.9	88.7
100	110	65	93.1	107.5	104.5	70.4	-

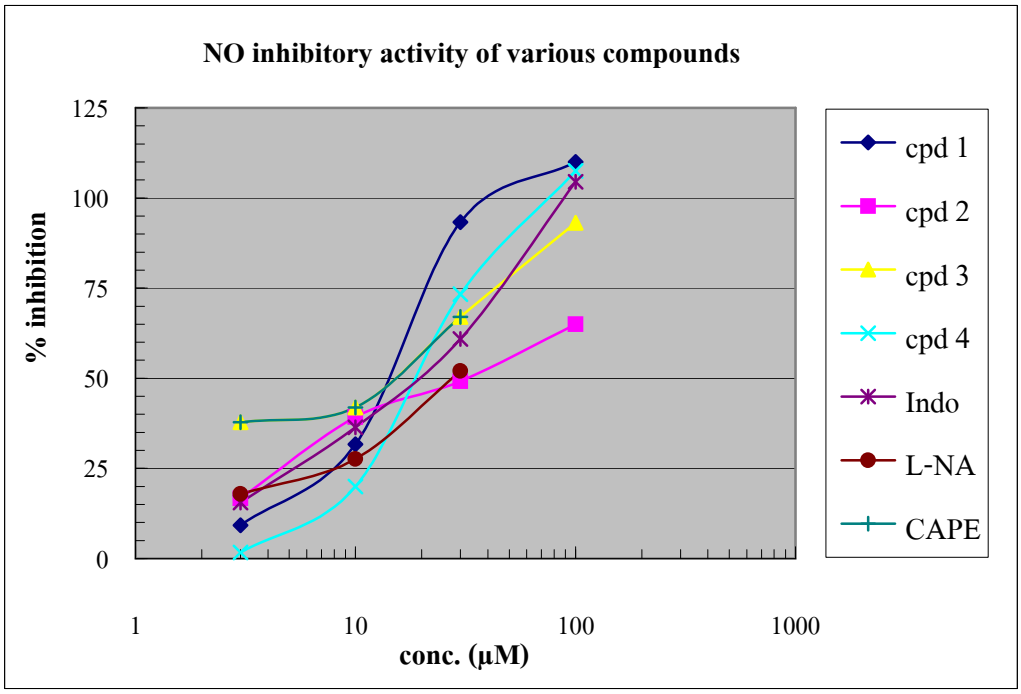

compound **1**	y = 31.189 Ln (x) - 27.896,	r^2 = 0.9401
compound **2**	y = 13.357 Ln (x) + 4.4334,	r^2 = 0.9811
compound **3**	y = 16.403 Ln (x) + 13.17,	r^2 = 0.9244
compound **4**	y = 31.812 Ln (x) - 40.098,	r^2 = 0.965
Indomethacin	y = 25.106 Ln (x) - 17.274,	r^2 = 0.969
L-NA	y = 0.5312x + 16.678,	r^2 = 0.9904
CAPE	y = 27.541Ln(x) + 4.3513,	r^2 = 0.8083

VITAE

Name Miss Kanidta Kaewkroek

Student ID 4910720031

Education Attainment

Degree	Name of Institution	Year of Graduation
Bachelor of Science (Chemistry)	Prince of Songkla University	2005

List of Publication and Proceedings

Kaewkroek, K., Wattanapiromsakul, C. and Tewtrakul, S. 2009. Nitric oxide inhibitory substances from *Curcuma mangga* rhizomes. Songklanakarin Journal of Science and Technology. 31: 293-297.

Kaewkroek, K., Wattanapiromsakul, C. and Tewtrakul, S., 2009. Effects of compounds isolated from *Curcuma mangga* on nitric oxide production in RAW264.7 macrophage cells. Proceeding of The 12th Nationnal Graduate Research Conference, Khon Kaen University, Thailand. 1174-1181.